TITLE:

CRITICAL BEHAVIOR AND PHYSICOCHEMICAL PROPERTIES OF HYDROPHILIC POLYMER GELS(Dissertation_全文)

AUTHOR(S):

Takigawa, Toshikazu

CITATION:

Takigawa, Toshikazu. CRITICAL BEHAVIOR AND PHYSICOCHEMICAL PROPERTIES OF HYDROPHILIC POLYMER GELS. 京都大学, 1995, 博士(工学)

ISSUE DATE:

1995-07-24

URL:

https://doi.org/10.11501/3105609

RIGHT:

京都大学学術情報リポジトリ
KURENAI 紅
Kyoto University Research Information Repository

新 制
工
1005
京大附図

CRITICAL BEHAVIOR AND PHYSICOCHEMICAL PROPERTIES OF HYDROPHILIC POLYMER GELS

TOSHIKAZU TAKIGAWA

1995

CRITICAL BEHAVIOR AND PHYSICOCHEMICAL PROPERTIES OF HYDROPHILIC POLYMER GELS

Toshikazu Takigawa

1995

CONTENTS

Chapter 1

General Introduction

Gels are popular materials in our life. For example, there are various kind of gel-like materials in foods.[1,2] Most of soft tissues in human body are also considered as polymer gels.[3] The applications of synthetic polymer gels have been made extensively and various types of gels have been produced in industries. Historically speaking, studies on gels were carried out chiefly by chemists and they still proceed their work intensively. Current developments in polymer physics[4,5] have attracted physicists to the studies on polymer gels, and now polymer gels are studied as a part of physics of complex fluids, or physics of soft materials.[6,7] The physics of the complex fluids is developing rapidly and providing new and interesting aspects of polymer gels, such as volume transition.[8,9]

A polymer gel is defined as a three-dimensional (3d) network with infinite molecular weight, swollen in solvent, and is classified into two categories, dependently of the type of crosslink region; one is so-called "chemical gel" where covalent bonds act as crosslinks, and the other "physical gel".[4] There are various kinds of crosslinks in physical gels;[4] for instance, helical domains act as crosslinks in gelatin gel. The physical gels are in solid state at certain temperatures (usually, around room temperature) but change to liquids by raising (or lowering) temperature, and the liquids (polymer solutions) are sometimes called sols. The change between the two states is

called sol-gel transition and occurs thermoreversibly, although hysteresis behavior is often observed for the transition. The transition temperature is close to the temperature at which conformational change of polymer chains occurs, and the change causes the formation (or annihilation) of crosslink regions. Phase diagrams have been obtained for several physical gel systems.[10] They show that there exists a critical polymer concentration. The system shows the sol-gel transition when the polymer concentration is higher than the critical concentration, but sol-gel transition is not observed when the concentration is lower than the critical concentration. In the latter case, only the cluster formation (or annihilation) is observed around the temperature for the conformational change. The system composed of the clusters is viscous but is still in liquid state, and is also called sol.

Gelation process must be clarified for understanding of physicochemical as well as mechanical properties of polymer gels, since the process determines the properties through the structure. Full description of the gelation process is very difficult because various factors affect the process, but studies on how physical quantities change with extent of reaction will give us useful information on the gelation process. Gelation was first treated as a sequential reaction of multi-functional monomers, and the critical concentration for gelation and the dependence of physical quantities on the extent of reaction have been widely studied.[4,11] Recent studies have paid much attention to the critical behavior of physical quantities (i.e., how they

converge to zero or diverge to the infinity, as a system approaches the gelation point). Using a quantity called relative distance from the gelation point (ε), the critical behavior of physical quantity (here, symbolized by Q) is assumed to be expressed by

$$Q \sim \varepsilon^{p} \qquad (1\text{-}1)$$

where p is called the critical exponent for Q. The exponent p is negative when Q diverges to the infinity, or is positive when converges to 0, as ε approaches zero. The theory based on Bethe lattice, which inherently has the infinite space dimension (d), has been now called as a classical (or mean-field) theory for the gelation.[4,11,12] The theory neglects the effects of excluded volume and closed ring formation.[4,12] Although the gelation threshold obtained by the classical theory has been shown to agree fairly well with those obtained by experiments, the critical behavior is quite different between the theory and experiments.[4,12,13]

A percolation theory[4,12-15] has been highlighted as useful tool for describing the critical behavior for gelation. The percolation theory is, in principle, based on modeling of the cluster formation in the lattice with finite space dimension, and takes the effects of excluded volume and closed ring formation into account.[4,12] Based on the percolation, gelation can be regarded as a critical phenomenon such that occurs around thermodynamical critical point,[12,15,16] and sol-gel transition is

analogized with the thermodynamical second-order transition. The order parameter, which is a basic quantity for describing the critical phenomenon, for the sol-gel transition is a gel fraction and the high symmetry phase is assigned to the sol phase.[12,13,15] There are several types of models for percolation;[12,13,15] site-percolation and bond-percolation are typical among them. Several types of lattices are employed for the analytical and numerical studies on percolation. The analytical and numerical studies have provided important and interesting predictions that the critical exponents, which determines the critical behavior of the physical quantities, depend only on d, although the threshold value depends on the types of models and lattices used.[4,12,13,15] There exists a critical dimension for the percolation. At and above the critical dimension, the critical exponents obtained by the percolation agree with those obtained by the classical (mean-field) theory. The critical dimension for the percolation is six and this value is often used as d for the Bethe lattice. We can think that the percolation involves the classical theory for gelation as a special case for d=6.[12] There are several equalities among the critical exponents, which are called scaling relations, and the scaling relation containing d is called especially the hyperscaling relations.[12,13,15] The scaling relations including hyperscaling relations hold for both the percolation and classical theories, but d=6 must be used for the hyperscaling in the classical theory.[12] The concept of fractality[17-20] becomes very important in studies on critical

phenomena. The fractal objects have no characteristic length and show the self-similarity over all the scale length.[17-20] It has been found that there are many fractal objects in the field of chemistry as well as physics; a polymer gel at the gelation point, for example, has been considered as a fractal with fractal dimension (d_f) of 2.5.[12,13,15,17-20]

Physical quantities treated with the percolation theory can be divided into two groups;[15,18-20] one is called static quantities, and the other the dynamic ones; for example, the molecular weight and the correlation length belong to the former group, and the modulus and the viscosity to the latter. The critical behavior of the dynamic quantities have been less understood compared with that of the static ones. For understanding of the critical behavior of the dynamic quantities, the idea of multi-fractal[18-20] (i.e., nested fractal) for the fractal objects has become more important. Related to the critical behavior, attention has been paid to crossover behavior at present.[19]

As reviewed above, theoretical studies provide a lot of information on the critical behavior of polymer gels. Numerical simulations have also been made to check the theoretical predictions to large extent.[21] Polymer systems showing sol-gel transition have been now re-recognized as good systems to check the theoretical predictions by experiments in the percolation theory. Experimental studies on the critical behavior of polymer gels have increased at present. The critical behavior of the dynamic quantities of polymer gels has also been studied

experimentally by many researchers, but the studies have focused mainly on modulus[22-26]. This originates from the experimental difficulty for the other quantities. The value of the critical exponent for modulus still remains scattered at present.[24,25] Studies are only a few for the crossover of elasticity. Thus, the critical behavior of dynamic quantities for polymer gels is still uncertain.

Polymer gels far from the gelation point have enough crosslink points, and then physicochemical properties of polymer gels can be treated by usual physical chemistry of polymers. Starting point for describing physicochemical properties of polymer gels will be free energy (F). Among the physicochemical properties, free swelling is one of the most important properties of the polymer gels. The system to be considered comprises polymer network of flexible polymer chains and solvent molecules. Since the volume (V) change of the gel specimen in usual experiments will occur isothermally at a constant pressure, it is convenient to use the Gibbs free energy. Hereafter, we regard F as the Gibbs free energy. Basically, for electrically neutral gels, F consists of three components.[4,8,9,11]

$$F=F_0+F_m+F_e \qquad (1\text{-}2)$$

Here, F_0 is the free energy of polymer chains and solvent molecules. F_m is the mixing free energy of chains and solvent molecules and F_e being the elastic free energy of the polymer network. Since solvent molecules can move through the gel-solvent

interface, the system considered is an open (exactly speaking, semi-open) system in a thermodynamical sense. Using osmotic pressure (Π) defined by[8,9,11]

$$\Pi=-(\delta F/\delta V)_T \tag{1-3}$$

the equilibrium condition is given by

$$\Pi=0 \tag{1-4}$$

The quantity Π comprises two terms.

$$\Pi=\Pi_m+\Pi_e \tag{1-5}$$

Π_m originates from F_m and Π_e from F_e. The detailed expressions for Π_m and Π_e (or, F_m and F_e) depend on the theory used. The Flory-type classical theory provides Π_m and Π_e as[8,9,11]

$$\Pi_m=-(k_BT/v_s)[\ln(1-\phi)+\phi+\chi\phi^2] \tag{1-6}$$

$$\Pi_e=N_ck_BT[(\phi/2\phi_0)-(\phi/\phi_0)^{1/3}] \tag{1-7}$$

Here, v_s, k_B, T, ϕ, χ and N_c are respectively the volume of a solvent molecule, the Boltzmann constant, the absolute temperature, the volume fraction of polymer network, the interaction parameter between polymer and solvent, and the number of active chains in unit volume. The quantity ϕ_0 is the value of

ϕ before swelling. Using the value of V before swelling (V_0), $\phi_0/\phi=V/V_0$. On the other hand, the scaling theory[4,5] for polymers have shown that[8,27]

$$\Pi_m=A\phi^n \qquad (1\text{-}8)$$

$$\Pi_e=B\phi^m \qquad (1\text{-}9)$$

Here, A and B are constants, and m=1/3 and n=9/4 for good solvent. Time (t) evolution for small volume element of polymer gels in the course of swelling can be described by the following equation.[8,28,29]

$$\rho(\delta^2\mathbf{v}/\delta t^2)=\mathrm{div}\sigma-\zeta(\delta\mathbf{v}/\delta t) \qquad (1\text{-}10)$$

Here, ρ, $\mathbf{v}$, σ and ζ are the density, displacement vector, stress tensor and the friction coefficient between network and solvent molecules, respectively. In most cases, the acceleration term is neglected because the motion is slow enough.[8,28,29]

Experimental studies on equilibrium swelling behavior and swelling dynamics of polymer gels have been carried out intensively, and the results have been analyzed by the theory reviewed above.[8,9,24,27-37] The studies, however, have dealt almost with the free swelling. It is very important to investigate anisotropic swelling behavior, which will occur for gels under constraints, for further understanding of physicochemical properties of polymer gels.

The aim of this study is to investigate properties of

hydrophilic polymer gel systems near as well as far from the gelation points by focusing on the critical behavior of the dynamic quantities near the gelation point, and on swelling and stress relaxation for non-critical (i.e., well-crosslinked) gels.

This dissertation consists of six chapters. Structure and mechanical properties of poly(vinyl alcohol) (PVA) gels swollen in various solvents are discussed in Chapter 2. Chapters 3 describes the critical behavior of the specific viscosity and intrinsic viscosity. Critical and crossover behavior of Young's modulus are shown in Chapter 4. Chapters 5 deals theoretically with the swelling and stress relaxation of polymer gels after uniaxial deformation is applied to the gels. In Chapter 6, experimental results of the swelling and stress relaxation for uniaxially stretched poly(acrylamide) (PAAm) gels are shown and are compared with the theoretical predictions.

References and Notes

1. A. H. Clark and S. B. Ross-Murphy, *Adv. Polym. Sci.*, **83**, 57 (1987)
2. K. Nishinari, *J. Soc. Rheol. Jpn.*, **17**, 100 (1989)
3. "*Hydrogels for Medical and related Applications*", J. D. Andrade, Ed., American Chemical Society, Washington D. C., 1976
4. P. G. de Gennes, "*Scaling Concept in Polymer Physics*", Cornell University Press, Ithaca and London, 1979
5. M. Doi and S. F. Edwards, "*The Theory of Polymer Dynamics*", Clarendon Press, Oxford, 1986
6. "*Space-Time Organization in Macromolecular Fluids*", F. Tanaka, M. Doi and T. Ohta, Eds., Springer Verlag, Berlin and Heidelberg, 1989
7. "*Dynamics and Patterns in Complex Fluids*", A. Onuki and K. Kawasaki, Eds., Springer-Verlag, Berlin and Heidelberg, 1990
8. "*Adv. Polym. Sci., Vol. 109*", K. Dusek, Ed., Springer-Verlag, Berlin and Heidelberg, 1993
9. "*Adv. Polym. Sci., Vol. 110*", K. Dusek, Ed., Springer-Verlag, Berlin and Heidelberg, 1993
10. M. Ohkura, Doctoral Dissertation, Kyoto University, 1992
11. P. J. Flory, "*Principles of Polymer Chemistry*", Cornell University Press, Ithaca, 1971
12. R. Zallen, "*The Physics of Amorphous Solids*", Wiley Interscience, New York, 1983
13. D. Stauffer, A. Coniglio and M. Adam, *Adv. Polym. Sci.*, **44**,

103 (1982)

14. J. M. Hammersley, *oc. Cambridge Phil. Soc.*, **53**, 642 (1957)
15. D. Stauffer, "*Introduction to Percolation Theory*", Taylor and Francis, London and Philadelphia, 1985
16. E. H. Stanley, "*Introduction to Phase Transitions and Critical Phenomena*", Clarendon Press, Oxford, 1971
17. B. B. Mandelbrot, "*Fractal Geometry of Nature*", Freeman, San Francisco, 1977
18. "*On Growth and Form*", H. E. Stanley and N. Ostrowsky, Eds., Martinus Nijhoff, Dordrecht, 1986
19. "*Fractals in Physics*", L. Pietronero and E. Tosatti, Eds., North-Holland, Amsterdam, 1986
20. "*Fractals and Disordered Systems*", A. Bunde and S. Halvin, Eds., Springer-Verlag, Berlin and Heidelberg, 1991
21. see, for example, S. Kirkpatrick, *Rev. Mod. Phys.*, **45**, 574 (1973), and also articles in refs. 18, 19 and 20
22. B. Gauthier-Manuel and E. Guyon, *J. Phys. (Paris)*, **41**, L503 (1980)
23. M. Adam, M. Delsanti, D. Durand and G. Hill, *Pure and Appl. Chem.*, **53**, 1489 (1981)
24. M. Tokita, R. Niki and K. Hikichi, *J. Chem. Phys.*, **83**, 2583 (19859
25. M. Tokita and K. Hikichi, *Phys, Rev.*, **A35**, 4329 (1987)
26. M. Adam, M. Delsanti, J. P. Munch and D. Durand, *J. Phys. (Paris)*, **48**, 1809 (1987)
27. E. Geissler, A. M. Hecht, f. Horkay and M. Ziriny, *Macromol.*, **21**, 2594 (1988)

28. T. Tanaka, L. O. Hocker and G. B. Benedek, *J. Chem. Phys.*, **59**, 5151 (1973)

29. T. Tanaka and D. J. Fillmore, *J. Chem. Phys.*, **70**, 1214 (1979)

30. E. Geissler and A. M. Hecht, *Macromol.*, **13**, 1276 (1980)

31. E. Geissler and A. M. Hecht, *Macromol.*, **14**, 185 (1981)

32. A. Peters and S. J. Candau, *Macromol.*, **19**, 1952 (1986)

33. A. Candau and S. J. Candau, *Macromol.*, **21**, 2278 (1988)

34. F. Horkay, *Macromol.*, **22**, 2007 (1989)

35. F. Horkay, A. M. Hecht and E. Geissler, *J. Chem. Phys.*, **91**, 2706 (1989)

36. A. M. Hecht, F. Horkay, E. Geissler and M. Zriyi, *Polym. Comm.*, **31** 53 (1990)

37. Y. Li and T. Tanaka, *J. Chem. Phys.*, **90**, 5161 (1989)

Chapter 2

Structure and Mechanical Properties of Poly(vinyl alcohol) Gels Swollen by Various Solvents

2-1 Introduction

Studies on the preparation and mechanical properties of poly(vinyl alcohol) (PVA) hydrogels have been carried out by many researchers.[1-4] However, the relationship between the structure and mechanical properties of PVA hydrogels remains unclear. According to the preparation method developed by Hyon et al.,[3] currently the best way to obtain highly transparent and strong PVA hydrogels, the hydrogels are prepared in several steps where precursor gels are formed, as is shown in the next section. It is necessary to clarify the structure, swelling and mechanical properties relationship of the precursor gels as well as the hydrogels for designing the PVA hydrogels with desirable mechanical properties. In the present chapter, swelling and mechanical properties of PVA hydrogel and PVA gels obtained by swelling precursors in various solvents are described. The discussions and estimation on the structure of these materials were made, being based on the swelling and mechanical behavior of the gels. Among the precursor gels, the gel swollen in the mixed solvent of dimethyl sulfoxide and water is employed in Chapter 4. The same system at lower concentration is used in Chapter 3. This is because the system shows a unique sol-gel transition behavior. The results shown in this chapter will help to understand the unique characteristics of the system.

2-2 Experimental

PVA used in this study was supplied by Unitika Co., Japan. The degree of polymerization was 1700, and the degree of saponification was 99.5mol%. The preparation process of PVA hydrogel is schematically shown in Figure 2-1, which also contains the sample codes used for the PVA hydrogel and PVA gels obtained by swelling precursors in various solvents. The sample, PVA GEL (DMSO/W), was prepared by dissolving PVA in a mixture of water and dimethyl sulfoxide (DMSO) (1:4 by weight) at 105°C, and then maintaining the sample at -20°C for 24h. The polymer concentration, at which PVA was initially dissolved into the solvent, was designated by c_0. PVA GEL (W), PVA GEL (MeOH), and PVA GEL (EtOH) were obtained from PVA GEL (DMSO/W) by exchanging the mixed solvent with water, methanol and ethanol, respectively. PVA GEL, W and PVA GEL, Solv. were also prepared respectively from PVA GEL (EtOH) by drying in a vacuum oven at 30°C and then swelling in water and the organic solvents. The solvent used and the solubility parameter (δ) obtained from the literature,[5] are listed in Table 2-1. In order to prepare PVA HYDROGEL, PVA GEL (EtOH) was dried in a vacuum oven at 30°C, and then annealed in a oil bath. The annealing temperature is expressed as T_a. The PVA HYDROGEL was finally obtained by swelling the annealed gel in water.

Swelling experiments were carried out at room temperature. The degree of swelling of the gels was measured by weight, and expressed in wt% using either PVA content (W_p) or solvent content (W_s) which is equal to 100-W_p.

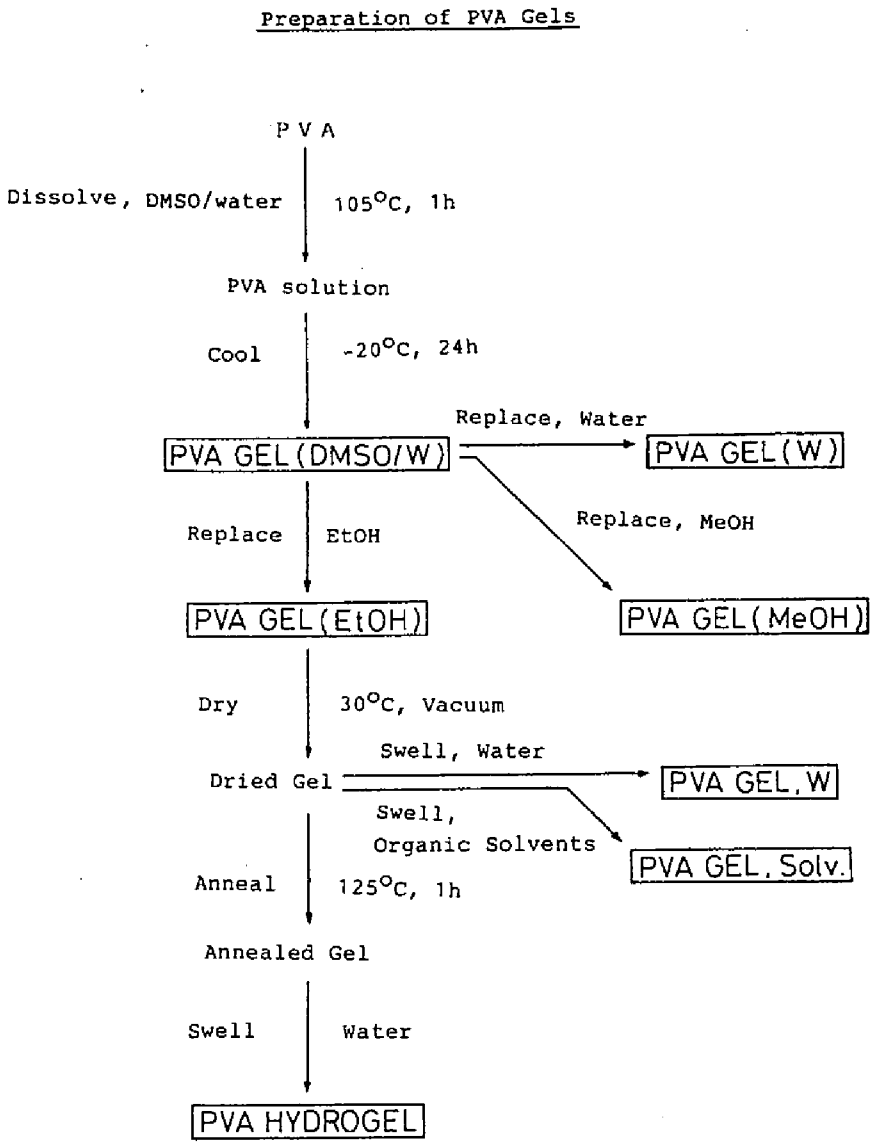

Figure 2-1. Schematic representation of the preparation of PVA hydrogels. Precursor gels at each stage are also shown.

Solvent	$\delta/cal^{1/2}cc^{-1/2}$
water	23.4
formamide	19.2
methanol	14.5
ethanol	12.7
butylolactone	12.6
diethylene glycol	12.1
2-propanol	11.5
2-methyl-1-propanol	10.5
2-methyl-2,4-pentanediol	9.7

Table 2-1. Solubility parameter (δ) of solvents used for swelling dried PVA GEL (EtOH).

The stress-strain curves of PVA gel samples were measured at the room temperature (23-25°C) in solvent by using a Orientec RTM250 Tensile Tester with a specially designed bath. The uniaxial elongation was carried out at a constant crosshead speed (v). Mechanical behavior of PVA gels was described by using stress (σ) and strain (ε) that were defined as follows:[6]

$$\sigma=\sigma_E\lambda \qquad (2\text{-}1)$$

$$\varepsilon=\ln\lambda \qquad (2\text{-}2)$$

where λ is the extension ratio, and σ_E the engineering stress. In obtaining Equation 2-1, we assumed that the volume of a gel was unchanged before and after deformation for all gels.

2-3 Results

Figure 2-2 shows the double-logarithmic plots of σ vs. ε of PVA GEL (DMSO/W). In the low ε region, each curve can be approximated by a line with the slope of unity. The curves start to deviate upwards from the straight line at an intermediate ε. The initial Young's modulus E_0 for each gel can be obtained from the low ε region in Figure 2-2. The value of E_0 increases with increasing W_p of the gels.

In Figure 2-3, similar plots for PVA GEL (W), PVA GEL (MeOH), and PVA GEL (EtOH) are shown. The value of W_p is also shown in the figure. For these gels, c_0 was fixed at 10wt%. The value W_p of PVA GEL (W) was 17.4wt%; W_p increased by the

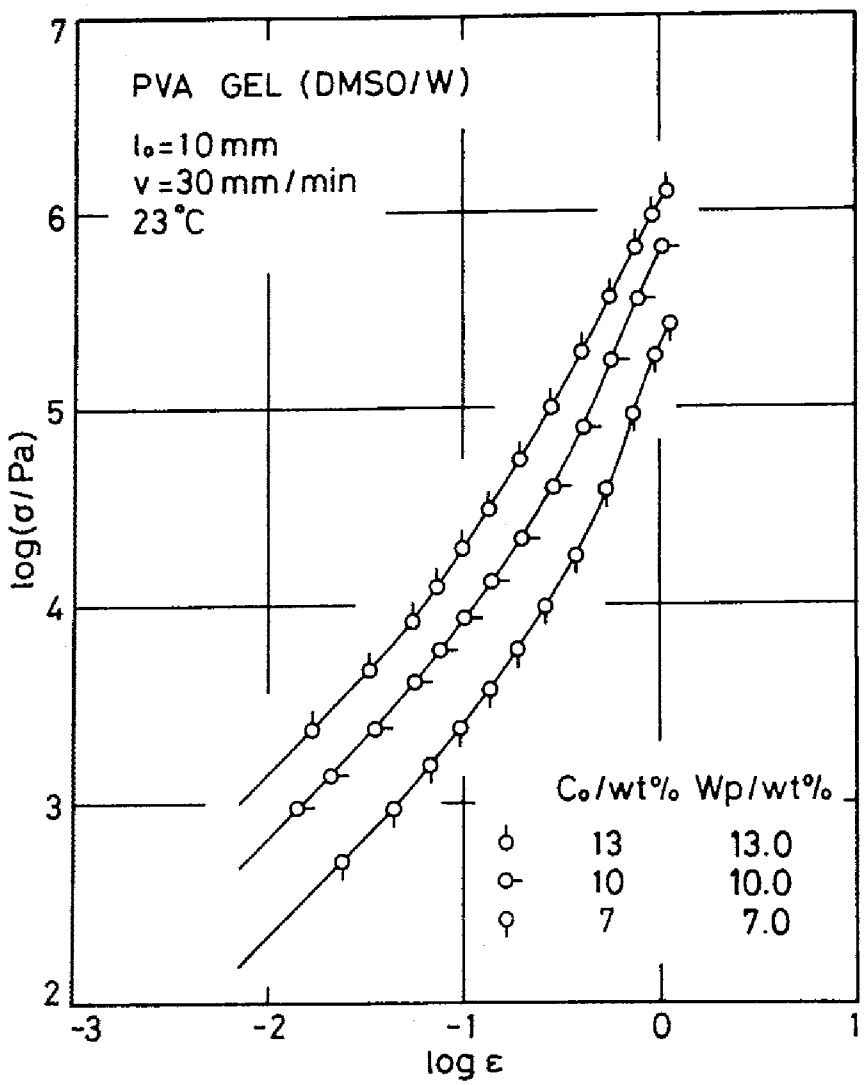

Figure 2-2. Double-logarithmic plots of stress (σ) against strain (ε) for PVA GEL (DMSO/W).

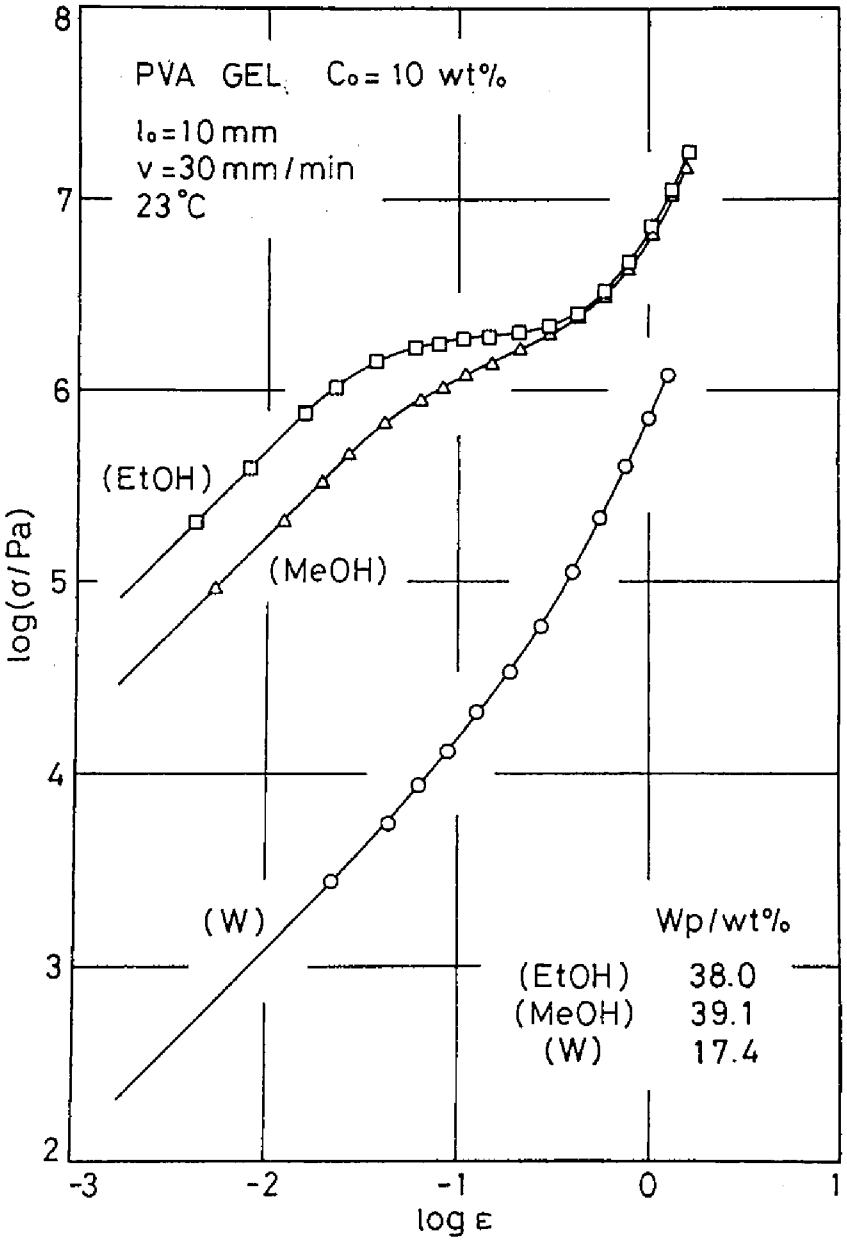

Figure 2-3. Double-logarithmic plots of stress (σ) against strain (ε) for PVA GEL (EtOH), PVA GEL (MeOH) and PVA GEL (W).

exchange of DMSO/W with water. W_p is also increased by organic solvent exchange as shown for PVA GEL (MeOH) and PVA GEL (EtOH), which were a little opaque. The W_p values for the gels are high compared with that for PVA GEL (W), but there is no difference between W_p's of PVA GEL (MeOH) and PVA GEL (EtOH). The stress-strain curve of PVA GEL (W) is very similar to that of PVA GEL (DMSO/W) (Figure 2-2). The curves for PVA GEL (MeOH) and PVA GEL (EtOH) can be approximated by a line with the slope of unity in the low ε region, but shoulders are observed in the middle region.

The solvent contents (W_s) in wt% of the gels prepared by drying PVA GEL (EtOH) and then immersing them in various solvents listed in Table 2-1, are plotted in Figure 2-4 as a function of δ of the solvent. The initial polymer concentration c_0 of the specimens was 10wt% for all cases. These gels are designated by PVA GEL, W and PVA GEL, Solv.. Here, W stands for water, and Solv. refers to each of the organic solvents used for swelling; for example, MeOH (methanol), EtOH (ethanol). As can be seen from this figure, the solvents except water, formamide and methanol do not swell the dried gel. The value W_s increases with increasing δ for methanol, formamide, and water.

Figure 2-5 shows plots of E_0 against polymer concentration (c) in kg/m^3 for PVA GEL, W and PVA GEL, Solv.. The values of E_0 for gels swollen in water, formamide and methanol fall on a line of the slope of 4.7. The value E_0 for the non-swollen PVA gels in the solvents with $\delta \leq 12.7 cal^{1/2} cc^{-1/2}$ shows upward deviation from the line.

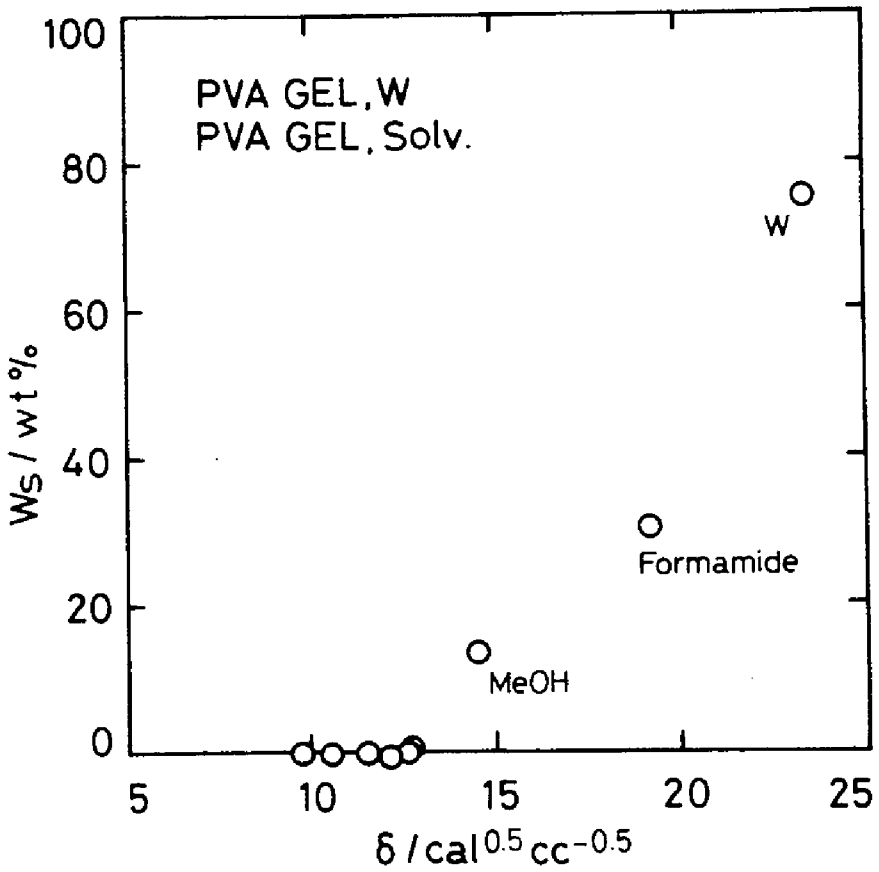

Figure 2-4. Solvent content (W_S) plotted against solubility parameter (δ) for PVA GEL, W and PVA GEL, Solv.

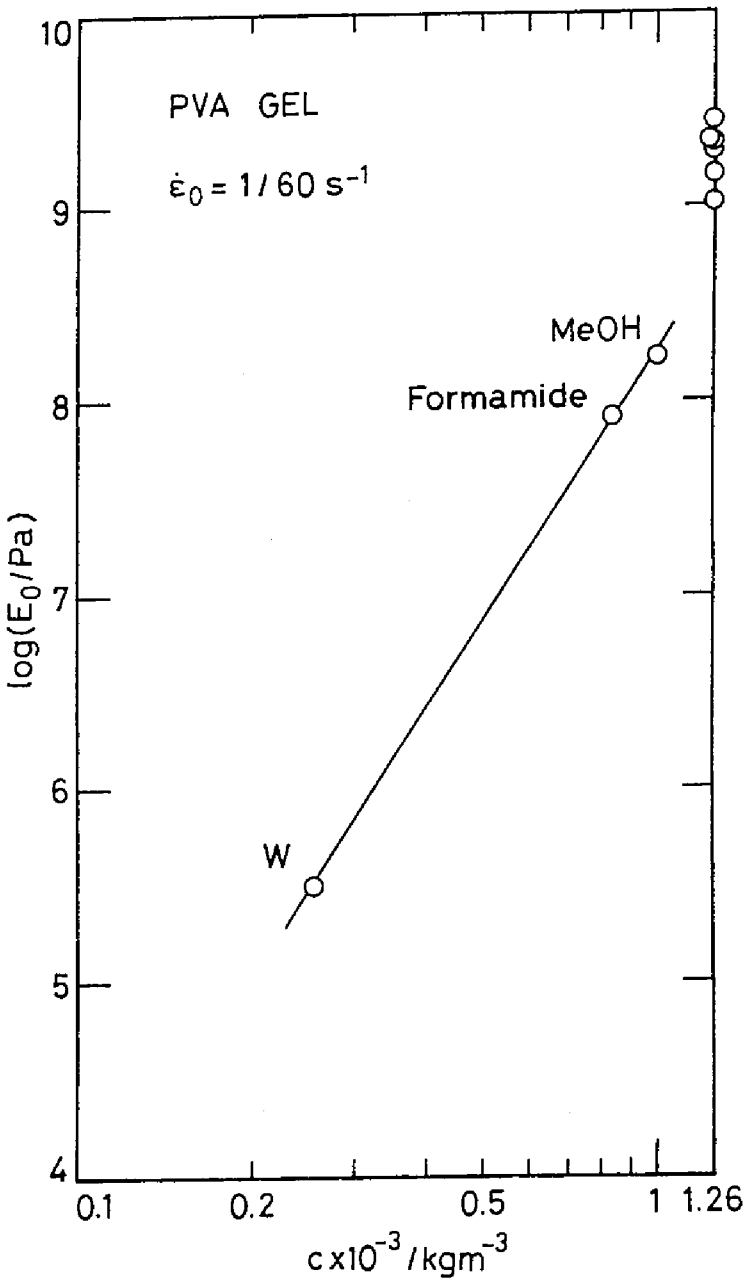

Figure 2-5. Double-logarithmic plots of Young's modulus (E_0) against polymer concentration (c) for PVA GEL, W and PVA GEL, Solv.

In Figure 2-6, W_s of PVA HYDROGEL is plotted against c_0. Except the hydrogel at c_0=7wt% and T_a=125°C, W_s of the gels at the same T_a appears to be independent of c_0. On the other hand, W_s for the hydrogels at the same c_0 decreases with increasing T_a.

Figure 2-7 shows plots of log σ vs. log ε for PVA HYDROGEL at c_0=13wt%. Data for each gel in the low ε region can be expressed by a line of slope one. As T_a increases, the value of E_0 increases and a shoulder in the middle ε range also becomes more pronounced.

In Figure 2-8, similar plots for PVA HYDROGEL annealed at 134°C are shown. As can be seen from this figure, stress-strain curves for the three specimens agree well. The value of E_0 is almost identical for the three samples with different c_0.

The effects of v on the stress-strain behavior was examined for PVA HYDROGEL. The results are shown in Figure 2-9. The curves are shifted vertically in order that they do not overlap each other. In the middle ε region, the shape of the curves changes depending on v. The curve at v=1mm/min clearly exhibits a minimum in the middle ε region. As v increases, the shape of the curves changes to one with inflection-point from its original plateau-like shape.

In Figure 2-10, double-logarithmic plots of σ against ε for PVA HYDROGEL are shown. The maximum strain magnitude imposed on the sample was 1.1×10^{-1} in the first run, and was within the elastic limit. After the strain was recovered by moving the cross-head of the testing machine in the reverse direction to the zero-force point, the stress-strain curves were again measured

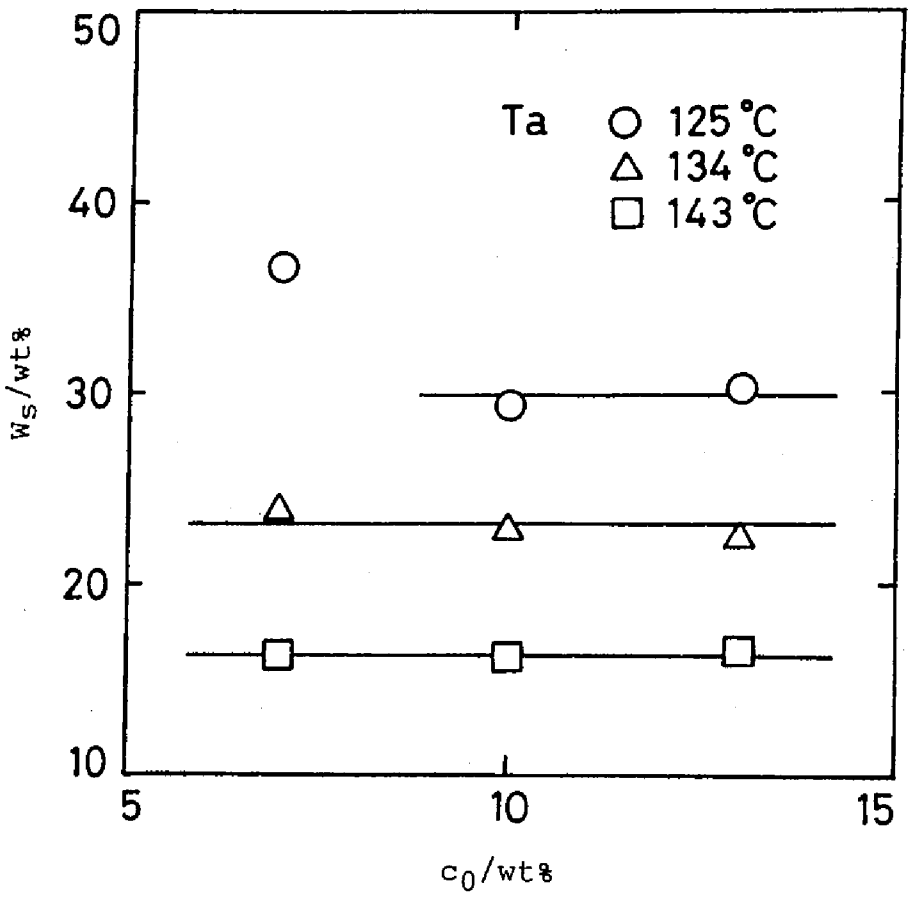

Figure 2-6. Water content plotted vs. initial polymer concentration (c_0) for PVA hydrogels.

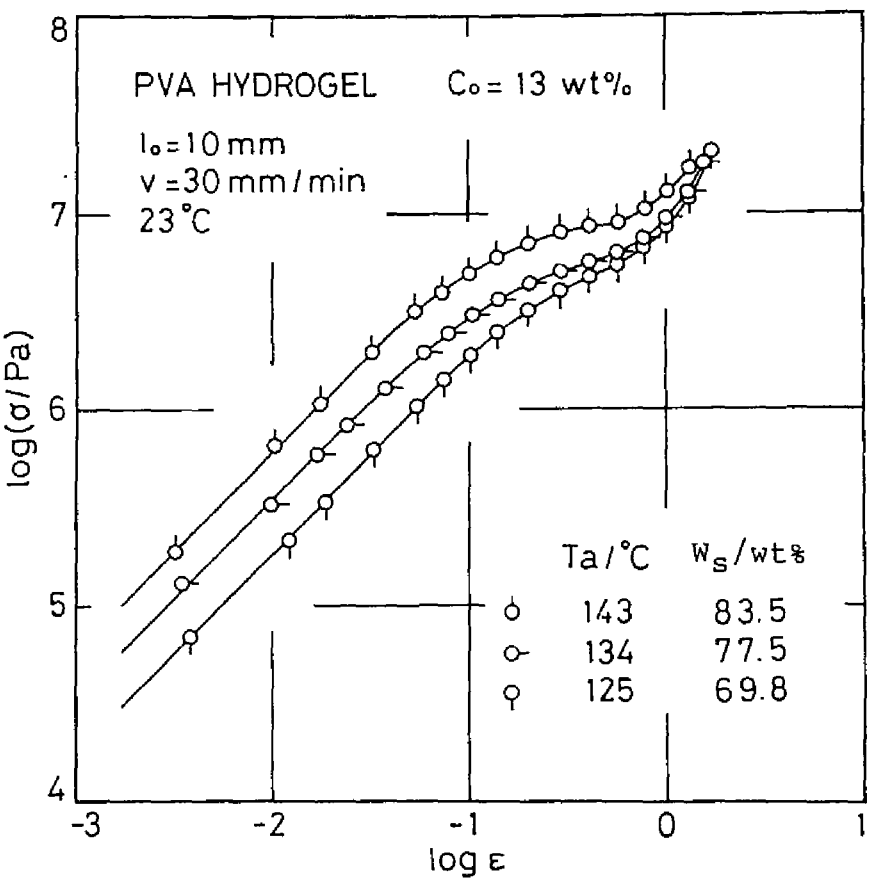

Figure 2-7. Double-logarithmic plots of stress (σ) vs. strain (ε) for PVA hydrogels at initial polymer concentration, (c_0), of 13wt%.

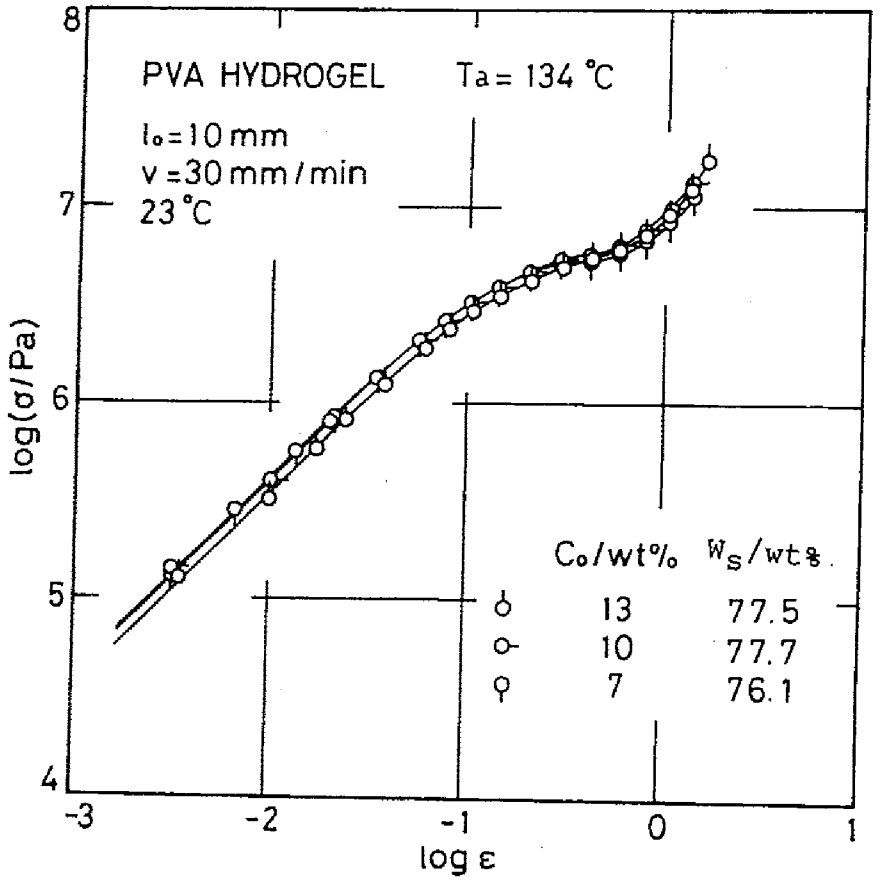

Figure 2-8. Double-logarithmic plots of stress (σ) vs. strain (ε) for PVA hydrogels annealed at 134°C.

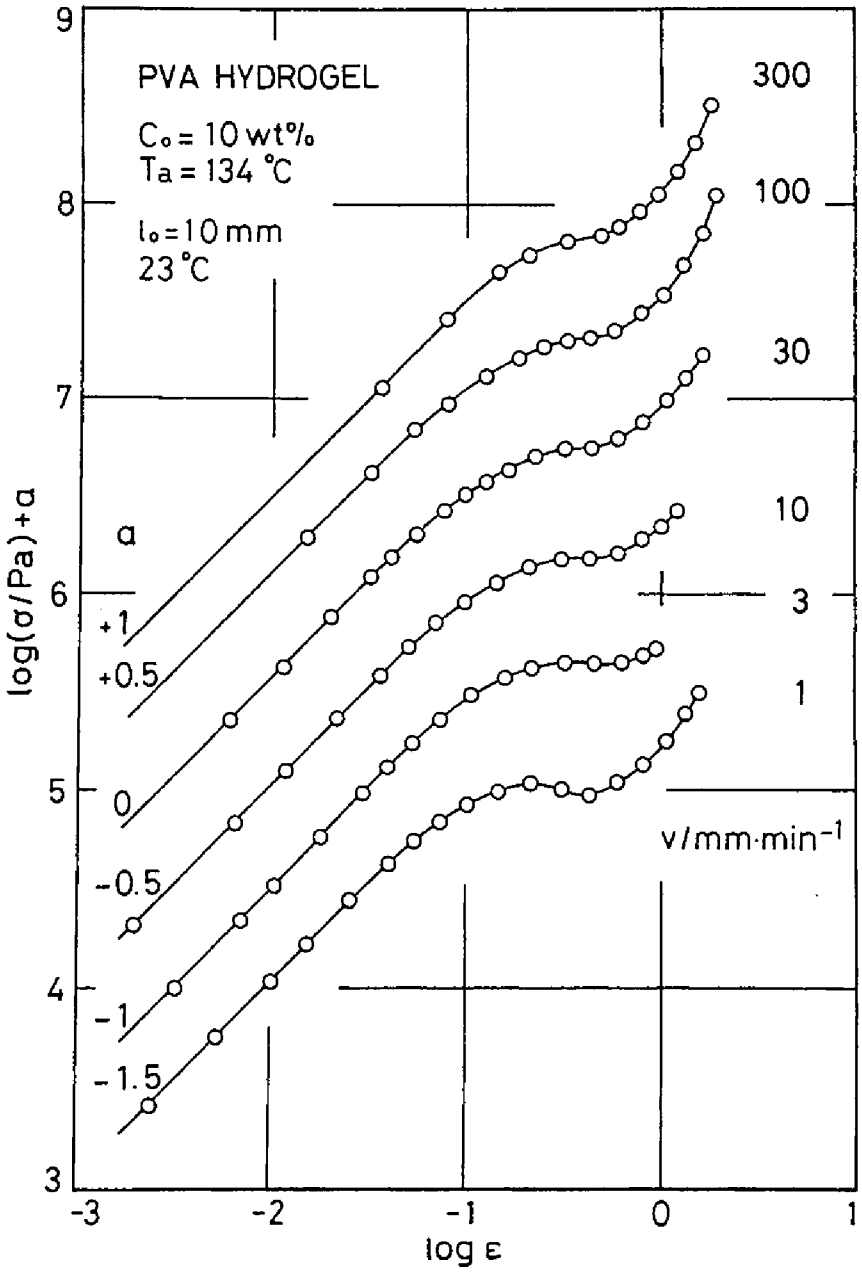

Figure 2-9. Double-logarithmic plots of stress (σ) vs. strain (ε) of PVA hydrogels. Numerals in the figure indicate crosshead speed (v).

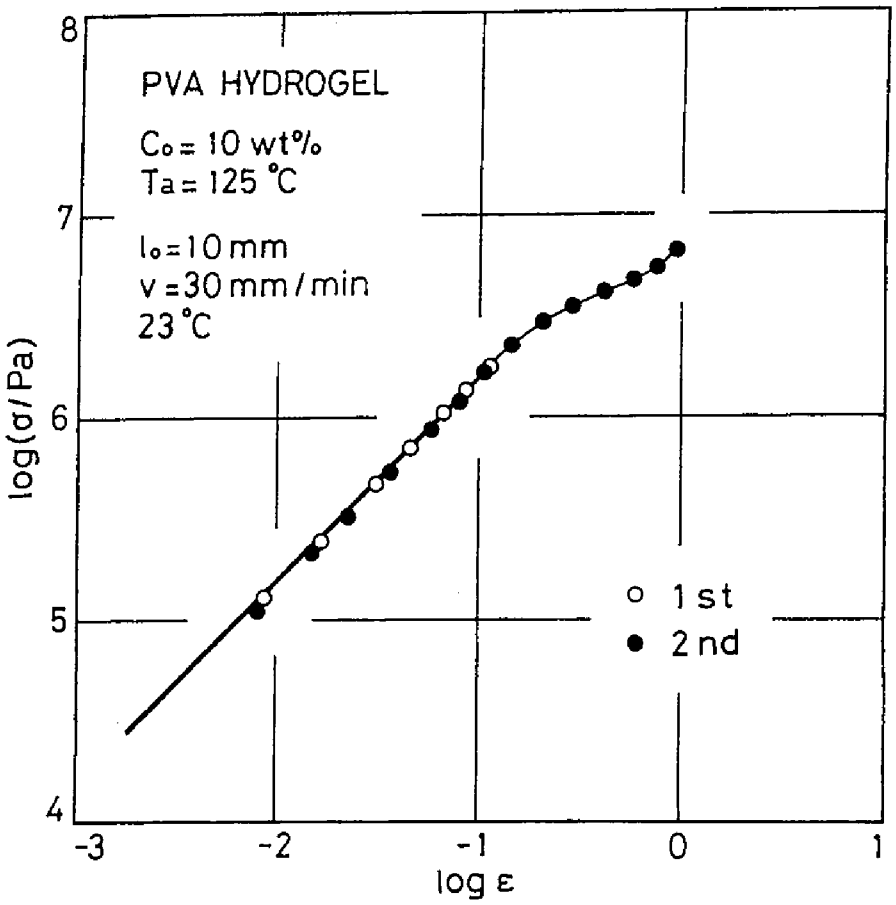

Figure 2-10. Double-logarithmic plots of stress (σ) vs. strain (ε) for PVA hydrogel of c_0=10wt% and T_a=125^{o}C. Open circles indicate the data of the first run, filled circles for the second run. The maximum strain magnitude in the first run experiment is 1.1×10^{-1}.

(the second run). The data points in the first and second experiments coincide well with each other. Similar plots are shown in Figures 2-11 and 2-12. The maximum strain magnitude applied to the sample in the first run is 2.5×10^{-1} in Figure 2-11 and 4.6×10^{-1} in Figure 2-12. As can be seen from these figures, E_0 at the second run decreases with increasing maximum strain amplitude of the first run.

2-4 Discussion

2-4-1 PVA GEL (DMSO/W)

As reported by Naito,[7] water and DMSO act as solvents for PVA, and DMSO is a better solvent than water. The solubility of PVA in a mixture of DMSO and water depends on the composition. PVA precipitates in the mixtures with DMSO contents of 40-70vol% at 30°C.[8] However, it has been also reported[7] that the mixtures of DMSO and water with DMSO contents higher than 70vol% can dissolve PVA and PVA does not precipitate. The solvent we used in this study has DMSO volume contents of 78%, suggesting that the mixture is a solvent for PVA. This fact means that the network structure is homogeneous and the polymer chain strands between crosslink points are flexible.

PVA hydrogels showed a shoulder on $\log\sigma$-$\log\varepsilon$ curve (see, for example, Figure 2-7), and the shoulder is closely related to a breakdown process of the microcrystalline domains which behave as crosslink points, as will be discussed later. The plots in Figure 2-2, however, do not show the shoulder. This implies that the domains acting as crosslinks are smaller in size for PVA GEL

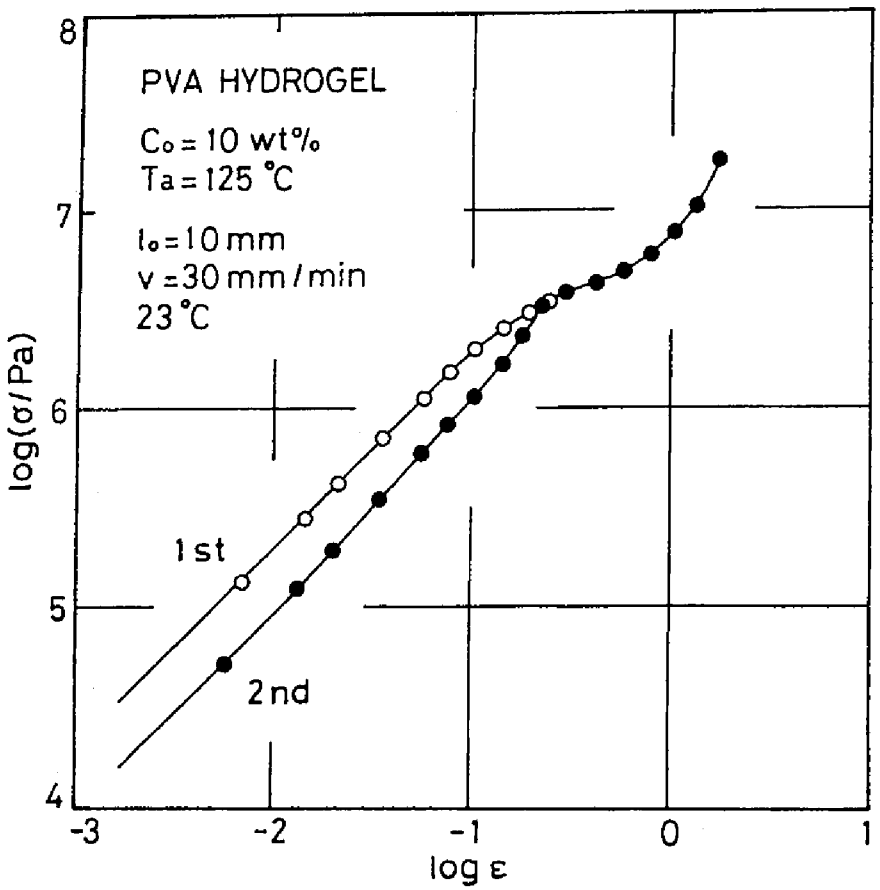

Figure 2-11. Double-logarithmic plots of stress (σ) vs. strain (ε) for PVA hydrogel of c_0=10wt% and T_a=125°C. Symbols are the same as in Figure 2-10. The maximum strain magnitude in the first run experiment is 2.5×10^{-1}.

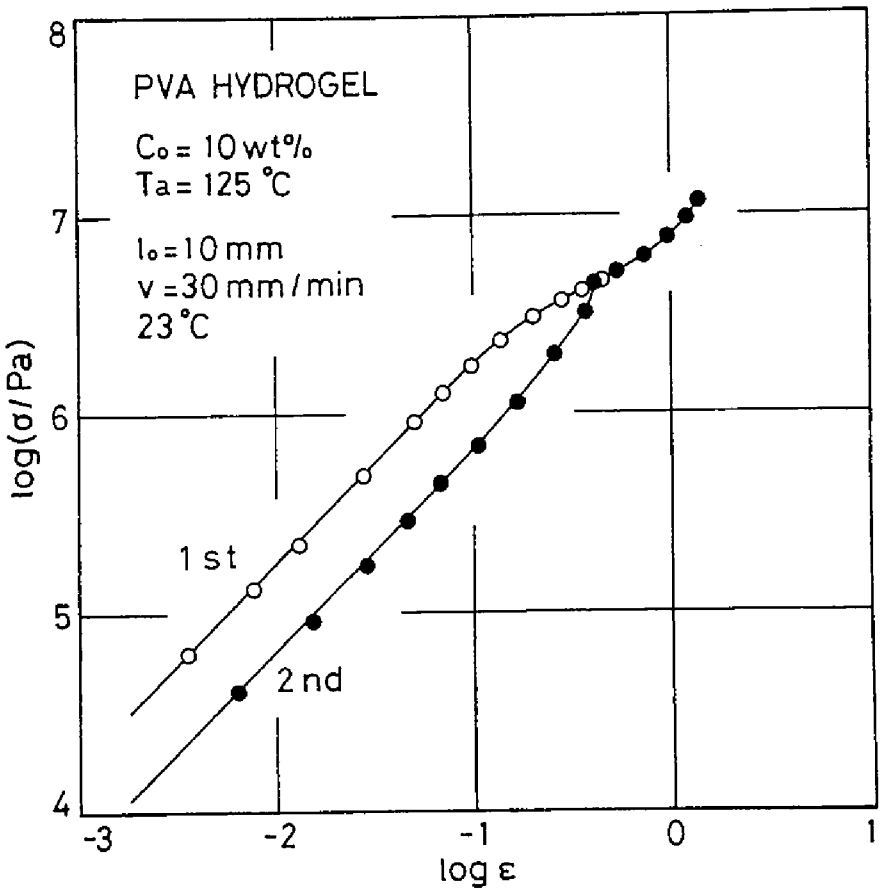

Figure 2-12. Double-logarithmic plots of stress (σ) vs. strain (ε) for PVA hydrogel of c_0=10wt% and T_a=125°C. Symbols are the same as in Figure 2-10. The maximum strain magnitude in the first run experiment is 4.6×10^{-1}.

(DMSO/W) than for PVA HYDROGEL. The domains are composed of several polymer chains, while the microcrystalline domains in PVA HYDROGEL comprise many chains. When strain is applied to the system, stress concentrates on the microcrystalline domains in PVA HYDROGEL and the microcrystalline domains break down at a critical strain, showing a shoulder on log σ-log ε curve. In the case of PVA GEL (DMSO/W), the crosslink domains, to the contrary, are small and uniformly dispersed in the gel, as discussed below. The chains between the domains are also enough flexible. Stress concentrations may not easily occur and the gel behaves like a crosslinked rubber, resulting in no shoulder on log σ-log ε curve.

In the concentrated solutions of PVA where entanglements of PVA chains are already formed uniformly, intermolecular hydrogen bonding rather than intramolecular hydrogen bonding will occur when they are cooled. The crosslinks by the formation of hydrogen bonds between PVA chains start to be formed upon cooling to -20°C. The crosslink points can be considered to occur from entanglement points existing in solution before cooling.[1] A sequence of hydrogen bonds, which are formed at the entanglement points during keeping at -20°C and raising the temperature, can be referred to as a zipper-like domain.[8] The domains caused by this molecular association act as crosslinks in PVA GEL (DMSO/W). In a thermodynamical sense, the zipper-like domains might be regarded as microcrystalline domains because they have a melting point depending on the length.

2-4-2 PVA GEL (W), PVA GEL (MeOH) and PVA GEL (EtOH)

As mentioned previously, W_p of PVA GEL (W) is higher than that of PVA GEL (DMSO/W), suggesting that PVA GEL (W) shrunk during the solvent exchange process. The shrinkage may be because water is a slightly poorer solvent than DMSO/W. However, since the plots of logσ vs. logε for PVA GEL (W) (Figure 2-3) are very similar in the shape to that of PVA GEL (DMSO/W) (Figure 2-2), the structure of the gel is considered to be almost identical to that of PVA GEL (DMSO/W).

The W_p for PVA GEL (MeOH) and PVA GEL (EtOH) are high compared with that for PVA GEL (W). This is because methanol and ethanol are poor solvents for PVA. As mentioned previously, PVA GEL (EtOH) and PVA GEL (MeOH) were slightly opaque, suggesting that phase separation occurs in the gels. The experimental results on the mechanical properties also suggest the phase-separated structure for the gels. The logσ-logε curves of the gels showed a shoulder. The shoulder might be attributed to the formation of large microcrystalline domains or aggregation of microcrystalites, both of which make the gels turbid, during solvent exchange. Such crystalline domains can not be dissolved even though the gels are again immersed in water. Then, we can expect that the gels show a shoulder on the logσ-logε curve as is the case for PVA HYDROGEL. On the other hand, PVA GEL (W), which is prepared through PVA GEL (EtOH), does not show a shoulder. Therefore, we can conclude that PVA GEL (EtOH) and PVA GEL (MeOH) have a two-phase structure. In the course of solvent exchange, the gel size decreases due to the decrease of solvent

power in the gels. The decrease of solvent power also causes the phase separation, which brings a heterogeneity into the gels; it occurs first in the surface area, and then the two phase area diffuses to the central part of the gel. The gels became turbid for initial several days of immersion, but the turbidity did not change during further two weeks. The degree of shrinkage of the gels shows a constant value after about one week, and a phase-separated structure composed of the PVA-rich phase and solvent-rich phase is formed in the gels. The crosslink domains formed initially by the molecular association in PVA GEL (DMSO/W), namely, zipper-like domains, might grow. Most of PVA chains exist in PVA-rich phase where hydrogen bonding between PVA chains also exists. The degree of shrinkage of the gels might be controlled by the type of solvent used for solvent exchange from the mixed solvent. However, W_p of PVA GEL (MeOH) and PVA GEL (EtOH) is almost identical (39.1 and 38.0wt% respectively as shown in Figure 2-3). The reason might be that both the solvents are very poor, and the precipitation and shrinkage of PVA occur too rapidly to reach the equilibrium state.

As can be seen from Figure 2-3, PVA GEL (EtOH) and PVA GEL (MeOH) show high E_0 compared with PVA GEL (W) having a homogeneous structure. The value of E_0 of PVA GEL (EtOH) is higher than that of PVA GEL (MeOH). The values of E_0 of PVA GEL (MeOH) and PVA GEL (EtOH) having two-phase structure are affected by various factors such as morphology, composition of PVA- and solvent-rich phases, as well as PVA content in PVA-rich phase. The morphology of PVA GEL (MeOH) and PVA GEL (EtOH) seems to be

almost identical, because both gels form a bicontinuous structure composed of the PVA- and solvent-rich phases. The difference of E_0 of the gels having two-phase structure is determined by the combination of the PVA content in PVA-rich phase and the composition of the two phases. The higher the concentration in PVA-rich phase becomes, the lower the composition of PVA-rich phase when W_p is kept constant as in the case of PVA GEL (MeOH) and PVA GEL (EtOH). The higher value of E_0 of PVA GEL (EtOH) shows that the effect of concentration of PVA in PVA-rich phase is more dominant than that of the composition. E_0 of PVA-rich phase is affected by the glass transition temperature (T_g) of PVA-rich phase or the crosslink density due to hydrogen bonds in the phase. T_g of PVA has been reported to be 85°C,[5] but T_g of PVA-rich phase is c-dependent; the T_g decreases with decreasing PVA concentration. T_g will be a determining factor of E_0 when T_g of PVA rich phase of both or one of the gels is higher than the room temperature. On the other hand, the crosslink density is a determining factor of E_0 when T_g of PVA-rich phase of both gels is below the room temperature. Although we cannot clarify at present which determines E_0 of PVA-rich phase for the gels, the crosslink density as well as T_g increases with increasing PVA concentration. Independently of which is the determining factor, it is probable that flexibility of chains decreases with increasing PVA concentration, and the flexibility determines E_0. The higher PVA concentration in PVA-rich phase for PVA GEL (EtOH), compared with PVA GEL (MeOH), is because ethanol is poorer solvent than methanol, as can be seen

from the data shown in Figure 2-4. The shoulders on the stress-strain curves for PVA GEL (EtOH) and PVA GEL (MeOH) shown in Figure 2-3 appears to be related to the breakdown process of the PVA-rich phase.

2-4-3 PVA GEL, W and PVA GEL, Solv.

We examined the swelling behavior of dried gels in various solvents. The solubility of polymer with the solubility parameter δ_p in a solvent (δ) should be determined by $|\delta-\delta_p|$. In the particular case in which a single polymer is considered, δ_p is constant and the solubility might be a function of δ of solvents. W_s of the swollen gel was analyzed as a function of δ. Although difference of W_s of PVA-solvent systems can not be completely described by δ because of hydrogen bonding interactions in the systems, δ of solvents will be a crude measure of the extent to which the dried gel absorbs the solvent. The similar case was treated by Dror et al.[9] for polyurethane-solvent systems. Since PVA GEL, Solv. (Solv. refers to the organic solvent with $\delta \leq 12.7 cal^{1/2} cc^{-1/2}$ in Table 2-1) was not swollen in the solvent, PVA GEL, Solv. at $\delta \leq 12.7 cal^{1/2} cc^{-1/2}$ is in glassy state showing high E_0. PVA GEL, W, PVA GEL, Formamide, and PVA GEL, MeOH contained small amount of solvent. The value W_p of PVA GEL, W was slightly higher than that of PVA GEL (W), while PVA GEL, MeOH shows much higher W_p than PVA GEL (MeOH). For the ethanol system, PVA GEL, EtOH do not swell, while PVA GEL (EtOH) contains 62wt% of the solvent. These results suggest that the drying process from PVA GEL (EtOH), through which PVA GEL, W and PVA GEL, Solv.

are prepared, is an important factor for determining W_p of the systems. As stated previously, PVA GEL (EtOH) has a two-phase structure. When PVA GEL (EtOH) is dried, the gel size decreases with increasing time for drying. In this process, however, the phase-separated structure composed of PVA-rich phase and solvent-rich phase, is maintained to a critical polymer concentration where gels become homogeneous. At concentrations higher than the critical concentration, the two phases tend to mix each other thermodynamically, but the existence of hydrogen bonding between PVA chains prevents from mixing. As mentioned previously, hydrogen bonding is formed in PVA rich-phase in PVA GEL (EtOH), and the formation of hydrogen bonding is also enhanced during drying. Hence, it is expected that the degree of phase mixing is very low in the dried gel. This implies that the structure of the dried gel is microporous. PVA GEL, W and PVA GEL, MeOH are prepared by immersing the dried gel into each of the solvents. The W_p of the gel is chiefly determined by what extent of crosslinks by the molecular association as well as hydrogen bonds is broken by swelling; in other words, the degree of breakage depends on the solvent type used. As can be seen from Figures 2-3, 2-4 and 2-5, the small difference in W_p and E_0 between PVA GEL, (W) and PVA GEL, W shows that the structure of these gels is almost identical, suggesting that hydrogen bonds which occur in the solvent exchange process and the drying process, can be easily eliminated by swelling by water, while the crosslinks are maintained. This is because hydrogen bonding between two PVA chains occurring in the solvent exchange and drying stages is

weak compared with the crosslinks formed by the molecular association in PVA GEL (DMSO/W).

When methanol is used as a swelling solvent, the solvent can break only a small amount of the hydrogen bonds, the formation of which is enhanced further by the drying process, resulting in the large difference in W_p between PVA GEL (MeOH) and PVA GEL, MeOH. PVA GEL, MeOH contains most of solvent in porous structure. The structure of PVA GEL, MeOH can be considered to be almost identical to that of PVA GEL (MeOH); both have a phase-separated structure. Formamide is a better solvent than methanol for PVA, but similar structure can also be considered for PVA GEL, Formamide, because E_0 of the gel is comparable with that of PVA GEL (EtOH) with almost the same W_p. On the other hand, as ethanol is a poorer solvent than methanol for PVA, ethanol can not be absorbed by the dry gel.

Dynamic Young's modulus (E') for the PVA GEL (DMSO/W) system is proportional to c^m ($m \simeq 2.3$) in the region of c higher than about 75kg/m^3, as will be shown in Chapter 4. In this system the structure of the gel is unchanged even when c varies. The c dependence of E' of PVA GEL (DMSO/W) was influenced only by the network density. On the other hand, the c dependence of E_0 for the system composed of PVA GEL, W, PVA GEL, Formamide and PVA GEL, MeOH shown in Figure 2-5 is stronger than that for the PVA GEL (DMSO/W) system. The reason of the strong concentration dependence is that the concentration dependence of E_0 in the figure is affected by various factors: the difference of the phase structure, PVA concentration in PVA-rich phase, and so on.

2-4-4 PVA HYDROGEL

The swelling behavior of the hydrogels seems to be strongly affected by the structure of the precursor gels formed in the course of PVA HYDROGEL preparation. PVA HYDROGEL experiences a drying process in the course of the sample preparation. As shrinkage occurs in the drying process, the structure of the dried gels seems to become nearly similar, regardless of c_0. The structural differences of PVA HYDROGEL originating from the difference of c_0 disappeared at this stage, as long as T_a was identical. This will be the reason why PVA HYDROGEL at the same T_a did not show the c_0 dependence of W_s. Crystallization occurs at the annealing process, and crystallinity is determined by T_a. As no structural difference existed for the dried gel at various c_0, the difference in W_s among the hydrogels with different T_a is felt to be determined only by the difference in crystallinity. Microcrystalline domains act as crosslinks in PVA HYDROGEL. The number of crosslinks is independent of c_0 when T_a is identical for the hydrogels; the number of crosslinks in the gel is determined by T_a, and is identical for hydrogels at the same T_a. The number of crosslinks increases with increasing T_a (consequently increasing crystallinity), although the increase of crystallinity also increases the domain size. This causes the decrease of W_s with increasing crystallinity. It is not clear at present why the gel at c_0=7wt%, and T_a=125^{o}C, showed the higher W_s than those for the other gels at the same T_a.

The increase of E_0 shown in Figure 2-7 is due to the decrease of W_s, which originates from the increase of

crystallinity as T_a increases. PVA HYDROGEL contains the microcrystalline domains formed in the annealing process, and also amorphous chains of high mobility because the chains are hydrated. The shoulder in the figure originates from the breakdown of the microcrystalline domains by the deformation imposed. It can be seen from the figure that the shoulder is enhanced with increasing T_a. This is because the microcrystalline domains increase with increasing T_a. The stress-strain curves for the three specimens in Figure 2-8 agreed well. The value of E_0 was almost identical for the three samples with different c_0. This is because the number of crosslinks is almost the same for the hydrogels. The coincidence of the curves for the three specimens in the middle ε region arises because the extent of microcrystalline domain broken down by the deformation applied is the same for the samples.

The v-dependent change in shape of the $\log\sigma$-$\log\varepsilon$ curves (Figure 2-9) appears to be closely related to the stress relaxation in the course of the measurement. At low ε region within the elastic limit, stress relaxation can not occur because the network structure, where microcrystalline domains act as crosslinks, is not broken by the strains. Actually, E_0 of specimens at various v is almost identical, as can be seen from the figure. In the middle ε region, however, the microcrystalline domains are broken down when the deformation is imposed. The breakdown of the domains will originate stress relaxation, and the effect is reflected strongly for the sample at low v, as is observed in the $\log\sigma$-$\log\varepsilon$ curve of v=1mm/min, as

a minimum in the middle σ range.

The data points in the first and second experiments coincided well with each other for the case shown in Figure 2-10. This is because the microcrystalline domains are not broken by the deformation imposed in the first run, since the strain magnitude is small enough. When the applied strain magnitude is larger than that of the linear elasticity limit, however, E_0 at the second run decreases with increasing maximum strain magnitude, compared with E_0 in the first run, as shown in Figures 2-11 and 2-12. This is because the amount of microcrystalline domains, which are broken in the first run, increases as the maximum strain magnitude in the first run increases. On the other hand, the data points obtained by the first and second runs can be smoothly connected by a single curve for each figure, suggesting that in the second run experiment, the maximum strain magnitude in the first run does not affect the stress-strain behavior in the region of ε larger than the maximum strain magnitude in the first run.

2-4-5 Structure of PVA gels

Based on the experimental results, we can estimate the structure of PVA gels. A scheme of the proposed structure for each gel is shown in Figure 2-13. From PVA solutions at c_0 higher than the gelation threshold (C_G), PVA GEL (DMSO/W) with a small crosslink domains (zipper-like domains) and flexible chains, is formed. PVA GEL (W) has almost the same structure as PVA GEL (DMSO/W). On the other hand, PVA GEL (EtOH) and PVA GEL

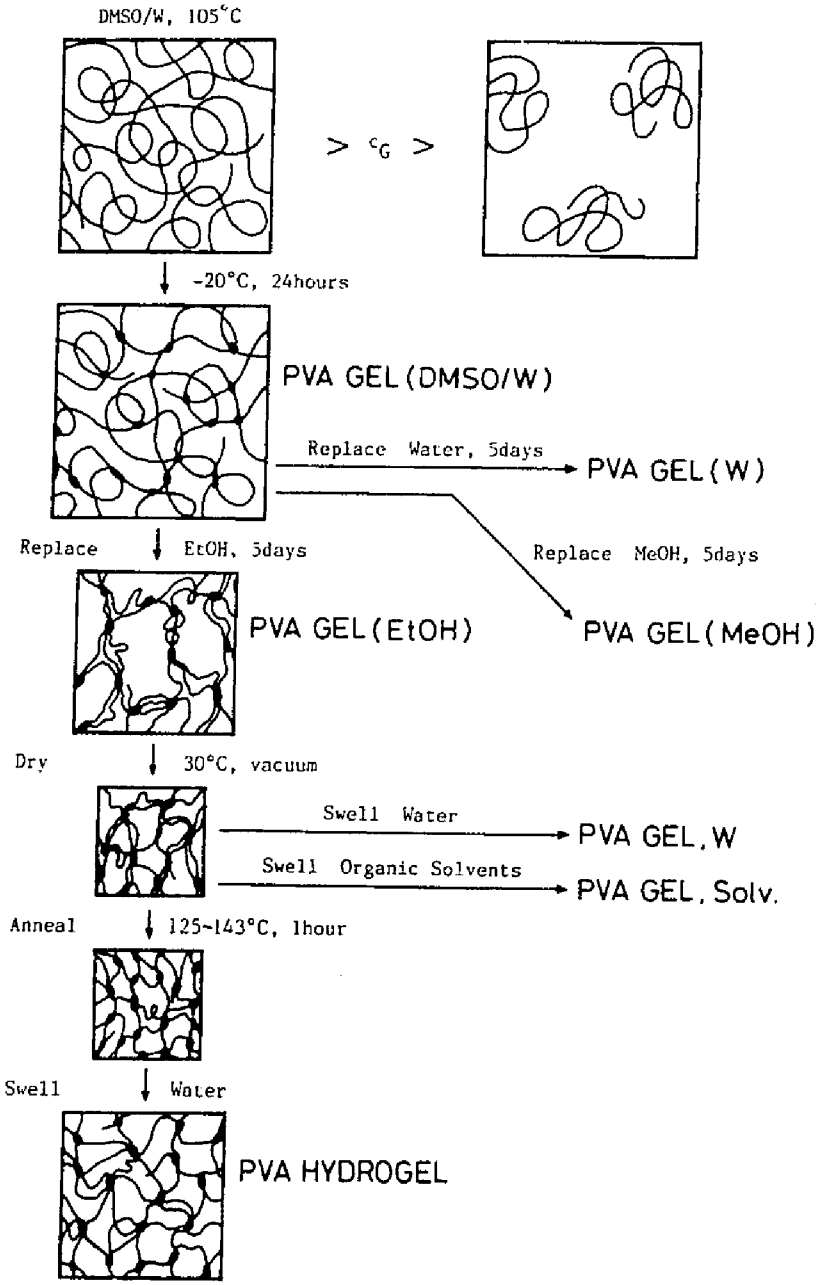

Figure 2-13. Schematic representation of various PVA gels.

(MeOH) have a two-phase structure composed of PVA-rich and solvent-rich phases. The size of the gels is smaller than that of PVA GEL (DMSO/W). The dried gel obtained from PVA GEL (EtOH) shows similar structure to that of PVA GEL (EtOH) and PVA GEL (MeOH), but the size is much reduced. The structure can be considered microporous. PVA GEL, W, which is prepared from the dried PVA GEL (EtOH), has similar structure to PVA GEL (W). PVA GEL, MeOH and PVA GEL, FORMAMIDE have almost the same structure as PVA GEL (EtOH). After annealing the dried gel at high temperatures (T_a), the gels have a structure composed of flexible chain region and microcrystalline domains, because the microporous structure is diminished and crystallinity increases by annealing. The crystallinity increases with increasing annealing temperature. PVA HYDROGEL formed by immersing the annealed gel into water has microcrystalline domains and flexible chains.

2-5 Conclusions

The swelling and mechanical properties of poly(vinyl alcohol) (PVA) hydrogels, and PVA gels obtained by swelling precursors in various solvents were investigated. On the basis of the experimental results, the structure of the gels in various solvents was estimated. PVA gels have a uniform structure with flexible PVA chains in a mixed solvent of dimethylsulfoxide (DMSO) and water. On the other hand, those swollen in methanol, ethanol and formamide have a two-phase structure, which is composed of PVA-rich and solvent rich phases. The PVA chains in

the PVA-rich phase are crosslinked by hydrogen bonding. The degree of swelling of PVA hydrogels depends on annealing temperature, but is almost independent of the initial polymer concentration. Mechanical properties of the hydrogels are also influenced by the degree of swelling. A shoulder is observed in double logarithmic plots of stress vs. strain for the hydrogels, and becomes clearer as annealing temperature increases. This shoulder is closely related to the breakdown of the microcrystalline domains acting as crosslinks. Also, the shape of stress-strain curves plotted double-logarithmically for the hydrogels changes with the extension rate.

References

1. M. Nambu, *Kobunshi Ronbunshu*, **47**, 659 (1990)
2. S.-H. Hyon, W.-I. Cha and Y. Ikada, *Kobunshi Ronbunshu*, **46**, 673 (1989)
3. S.-H. Hyon, W.-I. Cha and Y. Ikada, *Polym. Bull.*, **22**, 119 (1989)
4. M. Watase and K. Nishinari, *Polymer J.*, **21**, 567 (1989)
5. "*Polymer Handbook*", J. Brandrup and E. H. Immergut, eds., Interscience, New York, 1966.
6. E. Kamei and S. Onogi, *Appl. Polym. Symp.*, **27**, 19 (1975)
7. Y. Naito, *Kobunshikagaku*, **15**, 597 (1958)
8. K. Nishinari, S. Koide, P. A. Williams, P. A. and G. O. Phillips, *J. Phys. (Paris)*, **51**, 1759 (1990)
9. M. Dror, M. Z. Elsabee and G. C. Berry, *J. Appl. Polym. Sci.*, **26**, 1741 (1981)

Chapter 3

Divergence of Viscosity of Poly(vinyl alcohol) Solutions near the Gelation Point

3-1 Introduction

Theoretical and experimental studies on the critical behavior of elasticity near the sol-gel transition point, as will be discussed in the next chapter, have been made by several research groups.[1-4] However, studies on the critical behavior of viscosity (η) and intrinsic viscosity ($[\eta]$) are quite few, in spite of its importance.[5-7] The critical behavior of the viscosity and the intrinsic viscosity in the vicinity of the gelation point is described by

$$\eta \sim \varepsilon^{-k} \tag{3-1}$$

$$[\eta] \sim \varepsilon^{-x} \tag{3-2}$$

Here, ε indicates the relative distance from the gelation point. It should be noted that ε in this chapter and Chapter 4 is the relative distance, not the strain. The quantities k and x are the critical exponents for η and $[\eta]$, respectively.

As reviewed by Stauffer et al.,[5] the theoretical value of k obtained from 3-dimensional (3d) percolation theory ranges from 0 to 1.3, depending on the model employed for calculation of the viscosity of a system. Hence, the theoretical value of k is still unclear at present. Among a few experimental studies on k, Adam

et al.[6] have determined experimentally that k=0.76-0.9, depending on polymerizing system where a cluster is formed by the chemical reaction of monomers, and Dumas et al.[7] have reported k=0.95 for a gelatin solution system where the polymer clusters are formed by physical crosslinks. The critical behavior of the viscosity near the sol-gel transition point for physical gel systems other than this gelatin system has not yet been investigated. The situation is similar for the value of x; the value is also still uncertain, although some attempts to estimate the exponent have been reported in the literature.[5,8,9] It is important to examine further in detail whether critical behavior of η and $[\eta]$ for polymer systems can be adequately described by the percolation or classical theory.[5,10] Concentrated solutions of poly(vinyl alcohol) (PVA) form physical gels by cooling the solutions, as shown in the previous chapter. The dilute solutions of PVA are expected to form clusters when they are cooled. The solution is suitable for studies on the physical gelation. In this chapter, the critical behavior of η and $[\eta]$ for the PVA solution systems is described.

3-2 Experimental

PVA employed in this study was kindly supplied by Unitika Co., Japan. The degree of polymerization was 1700 and the degree of saponification was 99.5mol%. A mixture of dimethylsulfoxide (DMSO) and water was used as a solvent. The ratio of DMSO to water was 4:1 by weight. PVA was dissolved in the solvent at 105°C. The viscosity of the samples coded as PVA17U was

measured at 30°C using an Ubbelohde-type capillary viscometer. The elution time of the pure solvent for the viscometer was ca. 350s at 30°C. The solution was also diluted sequentially to the concentration (c) from the original one to extrapolate the viscosity to zero concentration. Separately, PVA solutions, differing in polymer concentration (1.09 to 12.2 kg/m^3) were prepared. They were kept in a freezer at -20°C for 20h, and then at 30°C for 24h. These cooled samples were coded as PVA17UF. For PVA17UF, the initial polymer concentration at which the solutions were prepared and cooled is specified by c_F. The viscosity of these samples was also measured at 30°C using an Ubbelohde-type capillary viscometer. The intrinsic viscosity, $[\eta]$, of the cooled sample (PVA17UF) was also measured but $[\eta]$ for the solution with lowest c_F (c_F=1.09kg/m^3) could not be obtained.

According to the common definition,[11] the relative viscosity, η_r, and the specific viscosity, η_{sp}, are expressed as follows:

$$\eta_r=\eta/\eta_0 \qquad (3\text{-}3)$$

$$\eta_{sp}=(\eta-\eta_0)/\eta_0 \qquad (3\text{-}4)$$

where η and η_0 are the viscosities of the solution and solvent, respectively. Using these quantities and c, the reduced viscosity is defined as η_{sp}/c, and the inherent viscosity as $(\ln\eta_r)/c$. The constant k' of the Huggins equation for η is defined by using following equation.[11]

$$\eta_{sp}/c=[\eta]+k'[\eta]^2c \qquad (3\text{-}5)$$

The constant k' for PVA solutions was estimated by using $[\eta]$ and the slope of plots of (η_{sp}/c) against c.

3-3 Results and Discussion

3-3-1 Divergence of Specific Viscosity

When viscosity measurements for solutions are performed at high shear rates, a system may show non-Newtonian behavior. The critical exponent for the viscosity near the gelation point must be determined using zero-shear viscosity of the system. First the effect of shear rate on the viscosity of PVA17UF solutions was examined. In the present experiments, the shear rate corresponds to the elution time of PVA solutions in a capillary viscometer. For all PVA17UF solutions examined in this study, the viscosity, η_{sp} determined by using a capillary viscometer of the solvent-elution-time of 350s, was almost identical to that determined by using a capillary viscometer of the solvent elution time of 50s. Hence, it is felt that the viscosity data obtained here are those at the zero-shear limit.

Figure 3-1 shows plots of η_{sp} vs. c_F for PVA17UF. The data points are shown in open circles. The quantity η_{sp} for PVA17U is also shown in dashed line as a function of c in this figure. In the region of concentration (c and c_F) lower than ca. $9kgm^{-3}$, PVA17UF shows lower η_{sp} than PVA17U. As will be discussed later, PVA molecules shrink due to the formation of intramolecular

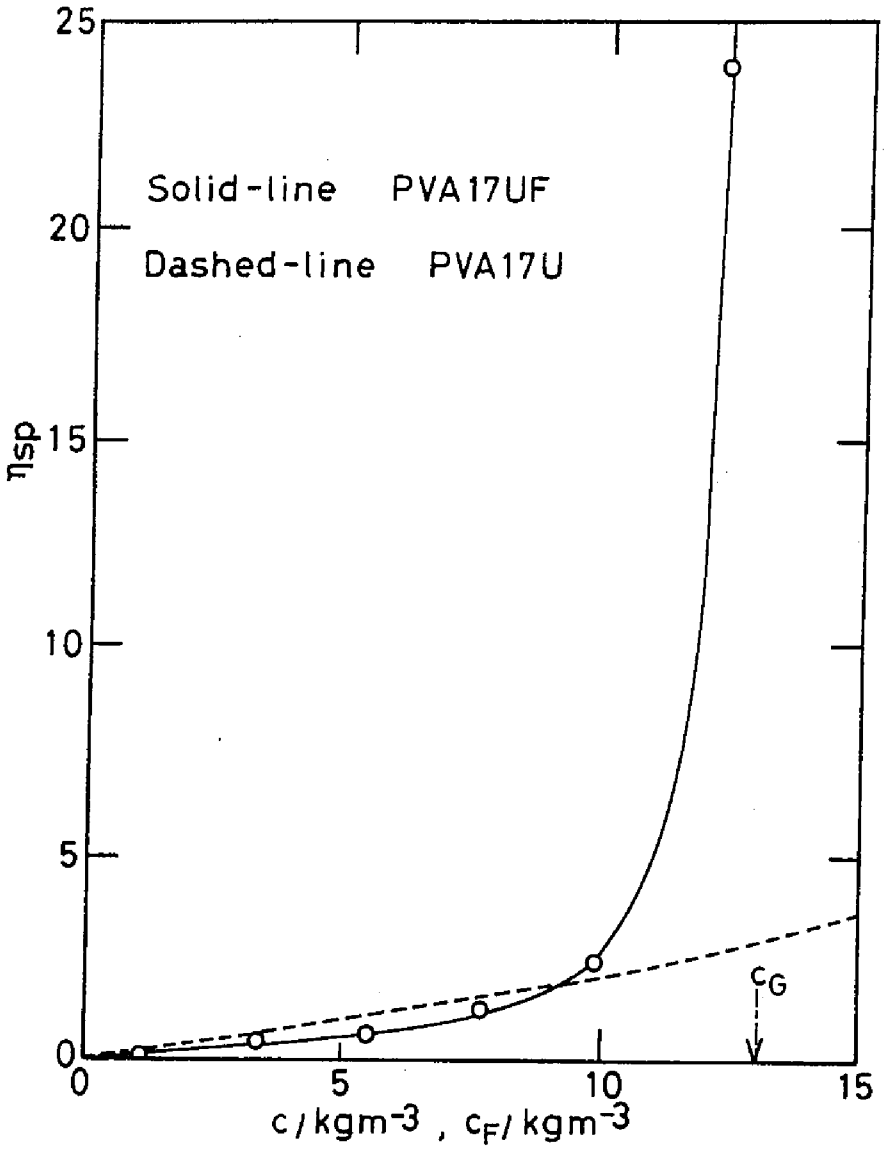

Figure 3-1. Plots of the specific viscosity (η_{sp}) vs. polymer concentration (c_F) for PVAI7UF (solid curve) and η_{sp} vs. concentration (c) for PVA17U (dashed).

hydrogen bonding, and the formation of PVA clusters by intermolecular hydrogen bonding is small in the low concentration region, although actually the formation occurs even at low concentrations. This suggests that the reduced η_{sp} for PVA17UF, compared with PVA17U, in the low concentration region is due to the reduction of the molecular size by intramolecular hydrogen bonding. On the other hand, η_{sp} of PVA17UF increases very rapidly with increasing c_F in the high c_F region. This increase in η_{sp} indicates that cluster formation by intermolecular hydrogen bonding is dominant in this region.

It was assumed that ε was given by

$$\varepsilon=(c_G-c_F)/c_G \qquad (3\text{-}6)$$

The quantity c_G is the concentration at gelation point. Then, the critical behavior of the specific viscosity of PVA17UF can be described by

$$\eta_{sp}\sim(c_G-c_F)^{-k} \qquad (3\text{-}7a)$$

or

$$\eta_{sp}^{-1}\sim(c_G-c_F)^{k} \qquad (3\text{-}7b)$$

The exponent is identical to that of viscosity, because actually the scaled quantity should be $(\eta-\eta_0)$, or η_{sp} instead of η in Equation 3-1. In order to determine the exponent k for PVA17UF,

we plotted η_{sp}^{-1} against c_F. The plots are shown in Figure 3-2. The data in this figure correspond to four data points in the region of c_F higher than 3.3kgm^{-3} in Figure 3-1; the curve shown is obtained by curve fitting for these four data.

By combining Equation 3-7b with its derivative, the following equation is obtained.

$$-\eta_{sp}^{-1}(d\eta_{sp}^{-1}/dc)^{-1}=(c_G-c_F)/k \qquad (3\text{-}8)$$

Using data on the fitted curve in the range of c_F=5.50 to 12.2kgm^{-3}, and their differential values, the quantity in the left hand side of Equation 3-8 was calculated and plotted against c_F. The results are shown in Figure 3-3. From these plots, it was deduced that k=1.67 and c_G=13.1kgm^{-3}. Using this value of c_G, all data for PVA17UF were re-plotted double-logarithmically in order to check the validity of the method used for the determination of k and c_G. The results are shown in Figure 3-4. The line in this figure is of slope -1.67. As can be seen from this figure, the five data points at high c_F side can be well approximated by a line of slope -1.67. Therefore, the five data points are located in the scaling region where η_{sp} is described by Equation 3-7a. Only η_{sp} at the highest (c_G-c_F) deviates from the line, this deviation arising because it is too far from the critical regime.

The value of k obtained here is larger than those reported by both Adam et al.[6] for polymerizing systems, and Dumas et al.[7] for the gelatin system. It is unknown at present exactly why the

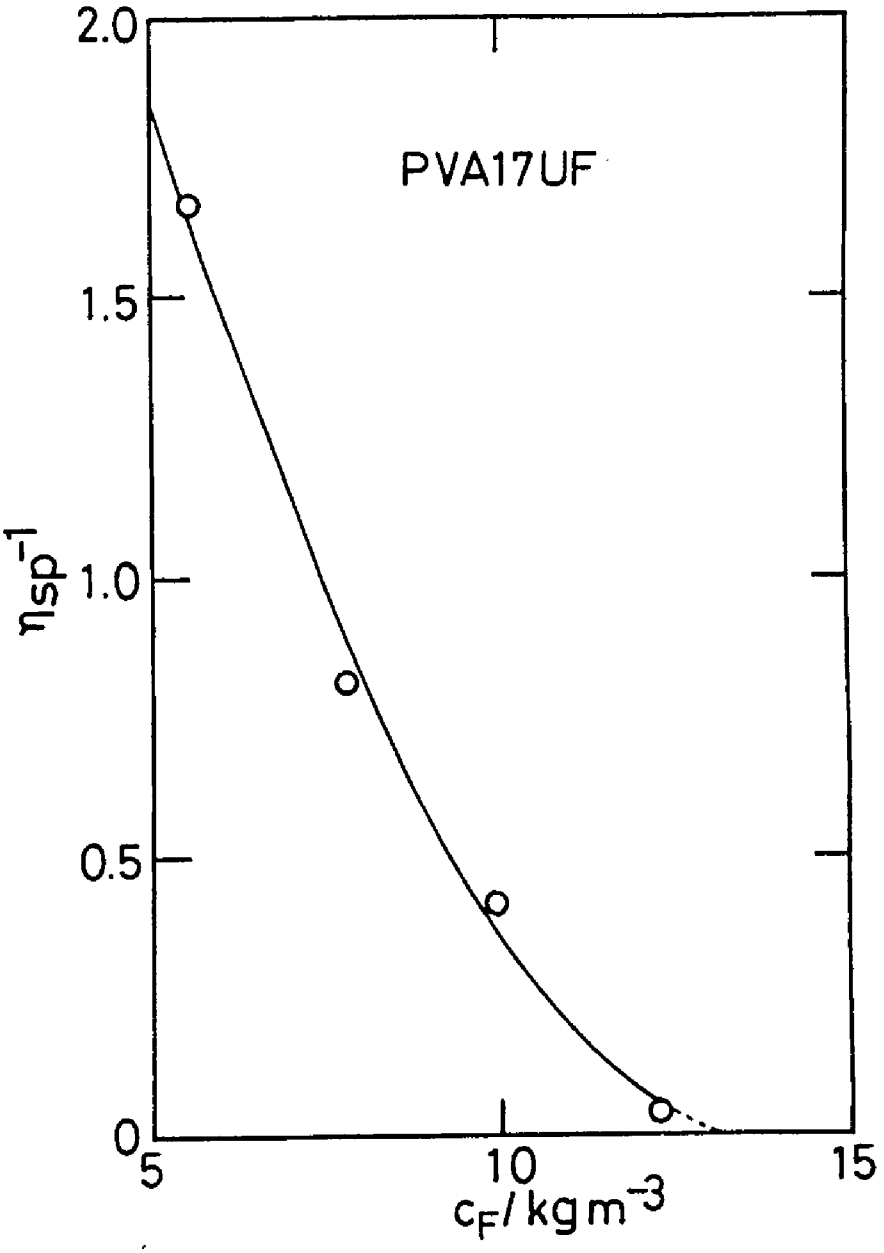

Figure 3-2. Plots of the inverse value of the specific viscosity (η_{sp}) vs. polymer concentration (c_F) for PVA17UF.

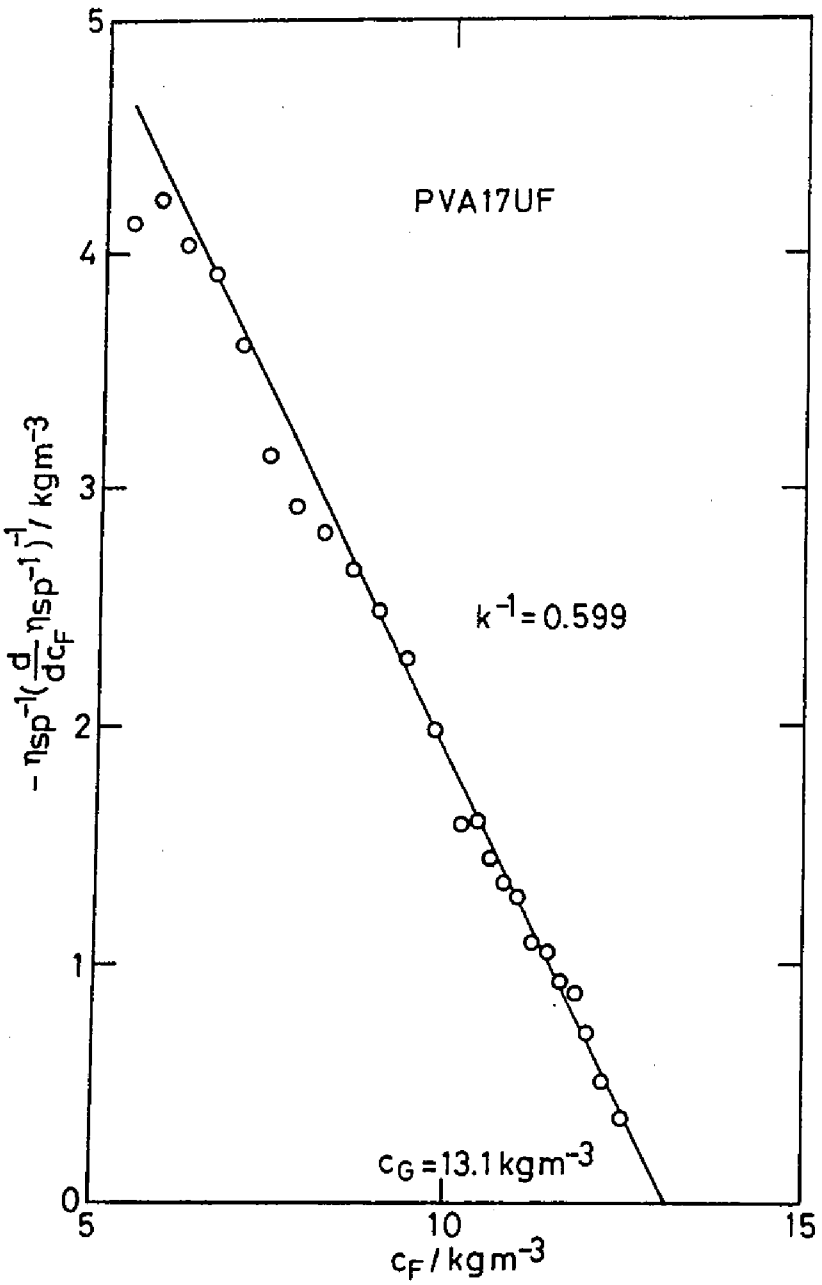

Figure 3-3. Plots of the quantity, $-\eta_{sp}^{-1}(d\eta_{sp}^{-1}/dc)^{-1}$ vs. polymer concentration (c_F) for PVA17UF.

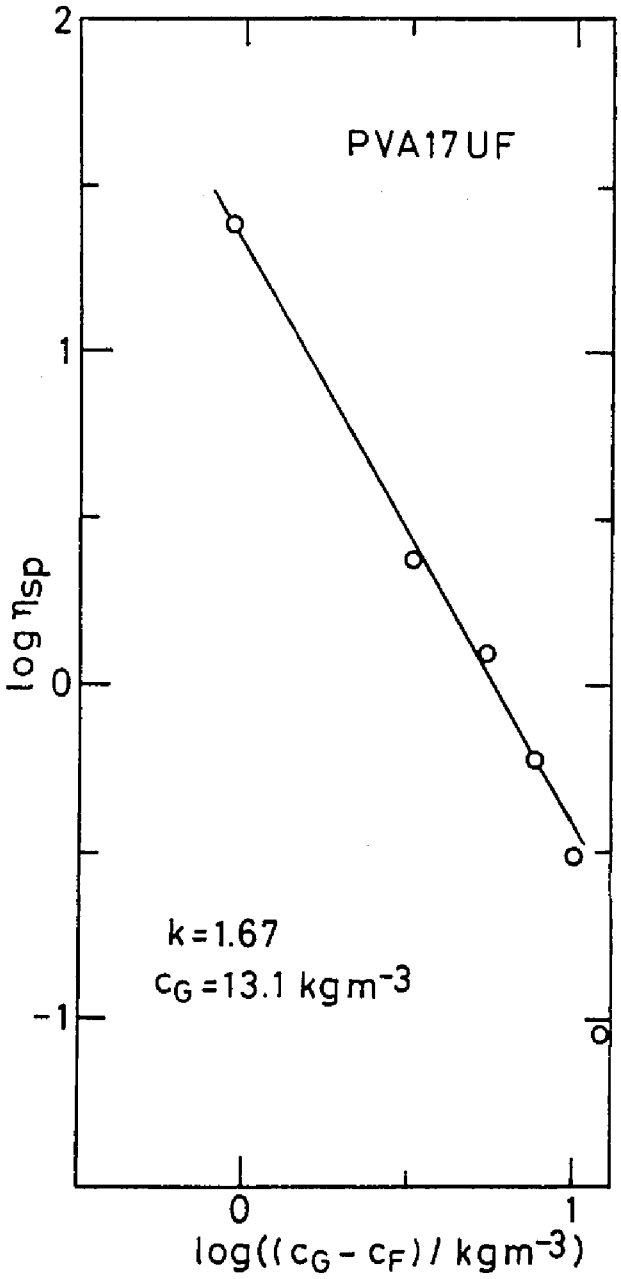

Figure 3-4. Double-logarithmic plots of the specific viscosity (η_{sp}) vs. the concentration difference (c_G-c_F).

value obtained here is different from their values. The reason for the enhanced value of k appears to be due to the shrinkage of molecules by the intramolecular hydrogen bonding. The shrinkage does not occur for the polymerization systems employed by Adam and coworkers.[6] Since the triple helical domains acts as cross-linking points for a gelatin gel, the clusters of gelatin molecules may occur by the formation of the triple helical domains even at concentrations lower than that of the gelation point. However, the triple helical domains can not be easily formed within a molecule. Hence, shrinkage of a molecule does not occur for gelatin solutions.

3-3-2 Divergence of Intrinsic Viscosity

In Figure 3-5, η_{sp}/c and $(\ln\eta_r)/c$ are plotted against c for the non-cooled PVA solution (PVA17U). Both the reduced and inherent viscosities show a linear relation to c. The intrinsic viscosity $[\eta]$, which corresponds to the intercept, and is identical for the two lines, is equal to $0.122 m^3/kg$. The constant k' of the Huggins equation is 0.43 for this system.

In order to determine $[\eta]$ of PVA17UF, we measured viscosity of diluted solutions. In this dilution process, the associated polymer chains (clusters) formed by inter-molecular hydrogen bonding may be eliminated. For PVA17UF, intra-molecular hydrogen bonding also exists, as will be discussed later. The intra-and inter-molecular hydrogen bonding is chemically equivalent. The effect of the dilution on $[\eta]$, if any, is the elimination of the intra-molecular hydrogen bonding as well as that of the inter-

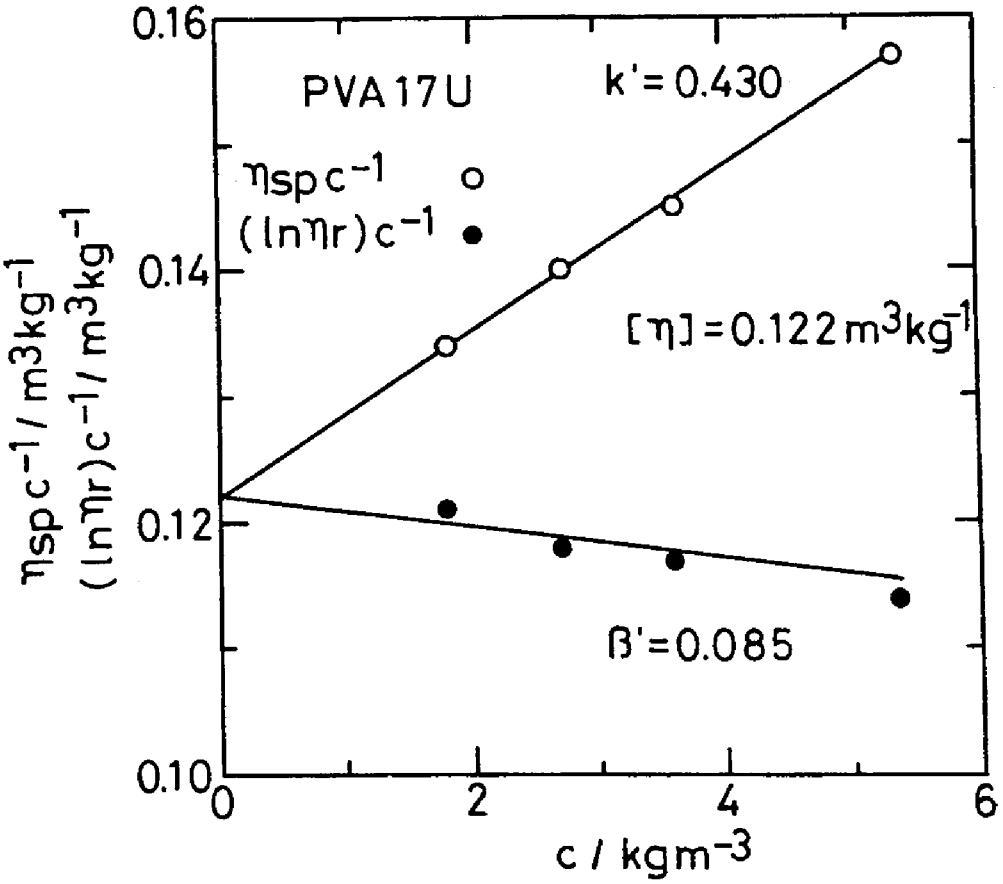

Figure 3-5. Plots of the reduced viscosity (η_{sp}/c) and the inherent viscosity ($(\ln\eta_r)/c$) vs. concentration (c) for PVA17U.

molecular hydrogen bonding. Although [η] of PVA17UF at c_F=12.2kg/m^3 was larger than that of PVA17U because of the increased formation of PVA clusters, the smaller [η] caused by the intra-molecular hydrogen bonding was definitely observed for PVA17UF at c_F<12.2kg/m^3, as is shown later. Then, we neglected the effect of the elimination of hydrogen bonding by dilution in obtaining k' and [η].

Figure 3-6 shows similar plots for a PVA17UF of c_F=9.90kg/m^3. As can be seen from the figure, a linear portion is observed for both η_{sp}/c and $(\ln\eta_r)/c$ vs. c plots at concentrations lower than approximately 4kg/m^3. The intercept, which corresponds to [η], is an identical 0.100m^3/kg for both lines. By comparing [η] of this sample with that of PVA17U in Figure 3-5, it was observed that [η] of PVA17UF at c_F=9.90kg/m^3 is smaller than that of PVA17U. At c_F much lower than the concentration for gelation, molecules have difficulty forming the clusters by the inter-molecular hydrogen bonding. However, the intra-molecular hydrogen bonding can be formed even at that concentration. The intra-molecular hydrogen bonding makes molecular conformation compact. Of course, both the compact conformation of molecules and the formation of PVA clusters by the inter-molecular hydrogen bonding occur simultaneously for this sample. However, this result implies that the reduction of [η] is more dominant for this sample than the increase of [η] by the formation of the clusters at c_F=9.90kg/m^3. On the other hand, k' of this sample is larger than that of PVA17U which was shown in Figure 3-5. The values of [η] and k' with probable errors for

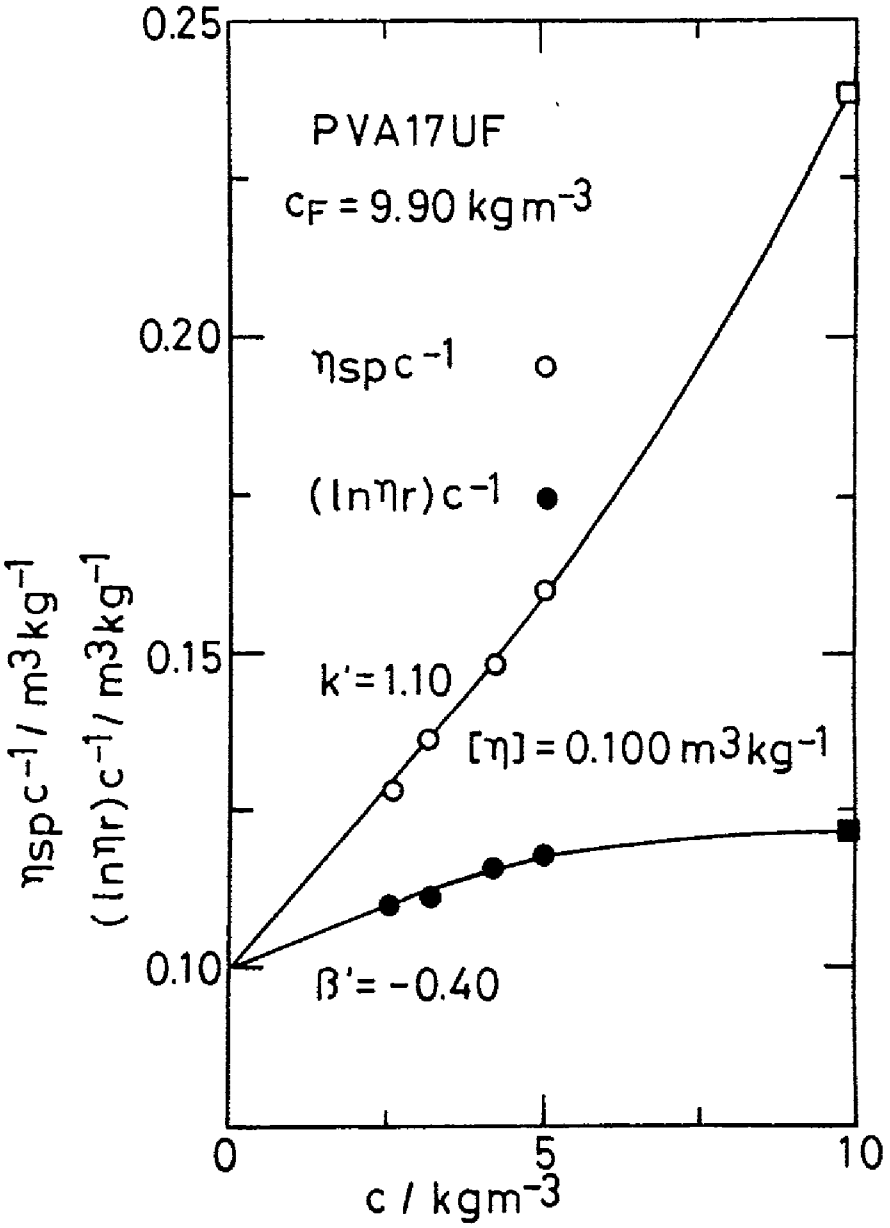

Figure 3-6. Plots of the reduced viscosity (η_{sp}/c) and the inherent viscosity ($(\ln\eta_r)/c$) vs. concentration (c) for PVA17UF. The polymer concentration (c_F) at which the solution was prepared, and cooled, is 9.9kg/m^3. The reduced and inherent viscosity for non-diluted solution at c_F are specified as (η_{sp}/c_F) and ($(\ln\eta_r)/c_F$), respectively. Square symbols indicate the data at $c=c_F$ (before dilution).

PVA17U and PVA17UF at various c_F, as well as η_{sp} and $ln\eta_r$ at each c are summarized in Table 3-1.

Figure 3-7 shows plots of k' vs. c_F for PVA17UF samples. The constant k' of PVA17U is also shown as an arrow in the figure. As can be seen from this figure, k' for PVA17UF at various c_F values examined in this study was larger than that for PVA17U. The value of k' is almost constant for PVA17UF at c_F equal to and lower than 7.72kg/m^3. Also k' increases with increasing c_F for PVA17UF samples at c_F higher than 7.72kg/m^3. The constant k' is a measure of polymer-polymer interaction,[12] and almost independent of molecular weight for linear polymers.[12] However, the clusters formed in PVA17UF solutions are considered to be branched polymers. Cragg et al.[13] have shown that k' increases with increasing molecular weight by branching for fractionated branched polymers. It has been shown[13] that polymers with broad molecular weight distribution have high value of k'. Molecular weight distribution of clusters becomes broader, as the system comes closer to the gelation point.[5,10] For the case where inter-molecular hydrogen bonding is dominant, the increased k' with increasing c_F values occurs because of the effects of both increased branching by the formation of clusters and broadening on molecular weight distribution of the clusters. No c_F dependence of k' at low c_F region in Figure 3-7 suggests that the effect of the formation of PVA clusters on the two-bodies interaction is still small in this c_F region. The reason why k' of PVA17UF in this c_F region is larger than that of PVA17U is not clear, but it may be closely related to the reduction in size of

Sample	c/kgm^{-3}	η_{sp}	$\ln\eta_r$	$[\eta]/m^3kg^{-1}$	k'
PVA17U	5.35	0.838	0.610	$(1.22\pm0.02)\times10^{-1}$	$(4.3\pm0.3)\times10^{-1}$
	3.57	0.517	0.419		
	2.67	0.373	0.315		
	1.78	0.239	0.215		
PVA17UF[a]	3.33	0.310	0.270	$(7.74\pm0.05)\times10^{-2}$	$(7.8\pm0.4)\times10^{-1}$
	2.78	0.252	0.223		
	2.23	0.196	0.182		
	1.67	0.142	0.131		
PVA17UF[b]	5.50	0.605	0.476	$(8.18\pm0.08)\times10^{-2}$	$(7.4\pm0.4)\times10^{-1}$
	3.68	0.368	0.315		
	2.76	0.263	0.231		
	1.84	0.166	0.157		
PVA17UF[c]	7.72	1.23	0.802	$(9.90\pm0.03)\times10^{-2}$	$(7.3\pm0.5)\times10^{-1}$
	5.18	0.722	0.543		
	3.89	0.495	0.402		
	2.59	0.304	0.265		
PVA17UF[d]	9.90	2.38	1.22	$(1.00\pm0.03)\times10^{-1}$	1.1 ± 0.1
	4.99	0.799	0.587		
	4.16	0.618	0.481		
	3.24	0.441	0.365		
	2.59	0.332	0.286		
PVA17UF[e]	12.2	23.9	3.21	$(1.32\pm0.04)\times10^{-1}$	1.8 ± 0.2
	4.73	1.45	0.897		
	3.64	0.867	0.625		
	3.15	0.676	0.516		
	2.37	0.435	0.361		
	1.58	0.270	0.239		

Table 3-1 Specific viscosity (η_{sp}), logarithm of relative viscosity ($\ln\eta_r$), intrinsic viscosity ($[\eta]$), and the constant of the Huggins equation for viscosity (k') for PVA17U and PVA17UF.
c_F for PVA17UF with superscript a, b, c, d and e is respectively 3.33, 5.50, 7.72, 9.90 and 12.2 in kg/m^3.

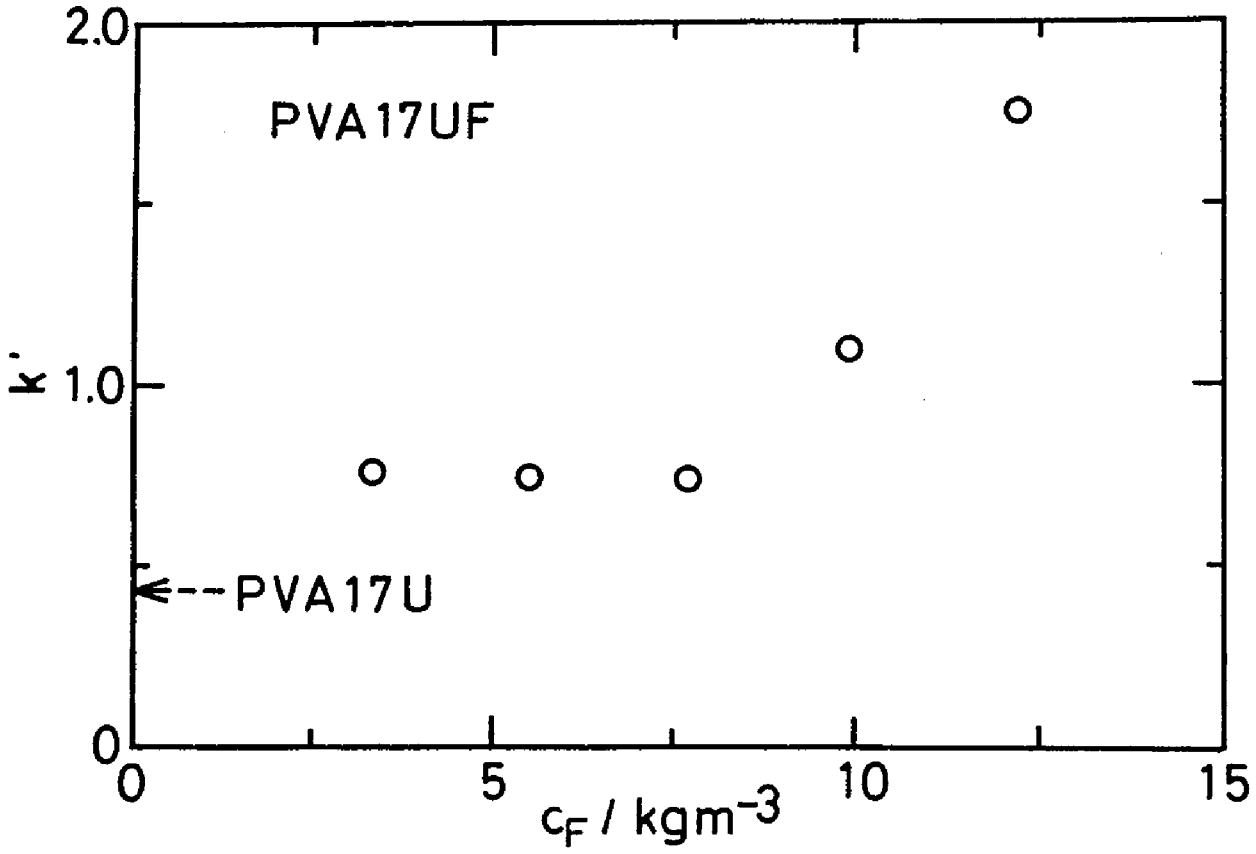

Figure 3-7. The plots of the constant of Huggins equation (k') vs. the polymer concentration (c_F) at which the solutions were prepared, and cooled.

clusters, which corresponds to the increase of monomer density in a molecule, by the intra-molecular hydrogen bonding. For PVA17UF at c_F>7.72kg/m^3, the increasing of k' with increasing c_F is due not only to the increased molecular weight by the formation of PVA clusters, but also to the broadening of molecular weight distribution of the systems.

Figure 3-8 shows plots of [η] vs. c_F for PVA17UF. The value for PVA17U is also shown by the arrow in this figure. The value of [η] of PVA17UF increases with increasing c_F. The value of [η] of PVA17UF at c_F less than or equal to 9.90kg/m^3 is smaller than that of PVA17U. Only one sample of c_F=12.2kg/m^3, that which is closest to the gelation point, shows larger [η] than that of PVA17U.

Figure 3-9 shows double-logarithmic plots of [η] vs. (c_G-c_F) for PVA17UF. The critical concentration used was c_G=13.1kg/m^3, as shown previously. As can be seen from this figure, the data fall on a line of slope -0.20±0.03. The intrinsic viscosity [η] is written by:

$$[\eta]\sim(c_G-c_F)^{-x} \quad (x=0.20\pm0.03) \qquad (3\text{-}9)$$

The uncertainty of c_G affects the value of x; the error in the estimation of c_G propagates the error of x. The error in the estimation of c_G was within 0.1kg/m^3, as mentioned above. We calculated the error of x propagated from the uncertainty of c_G. The error was within 0.01. This error range is narrow enough compared with that originated from the uncertainty in the plots

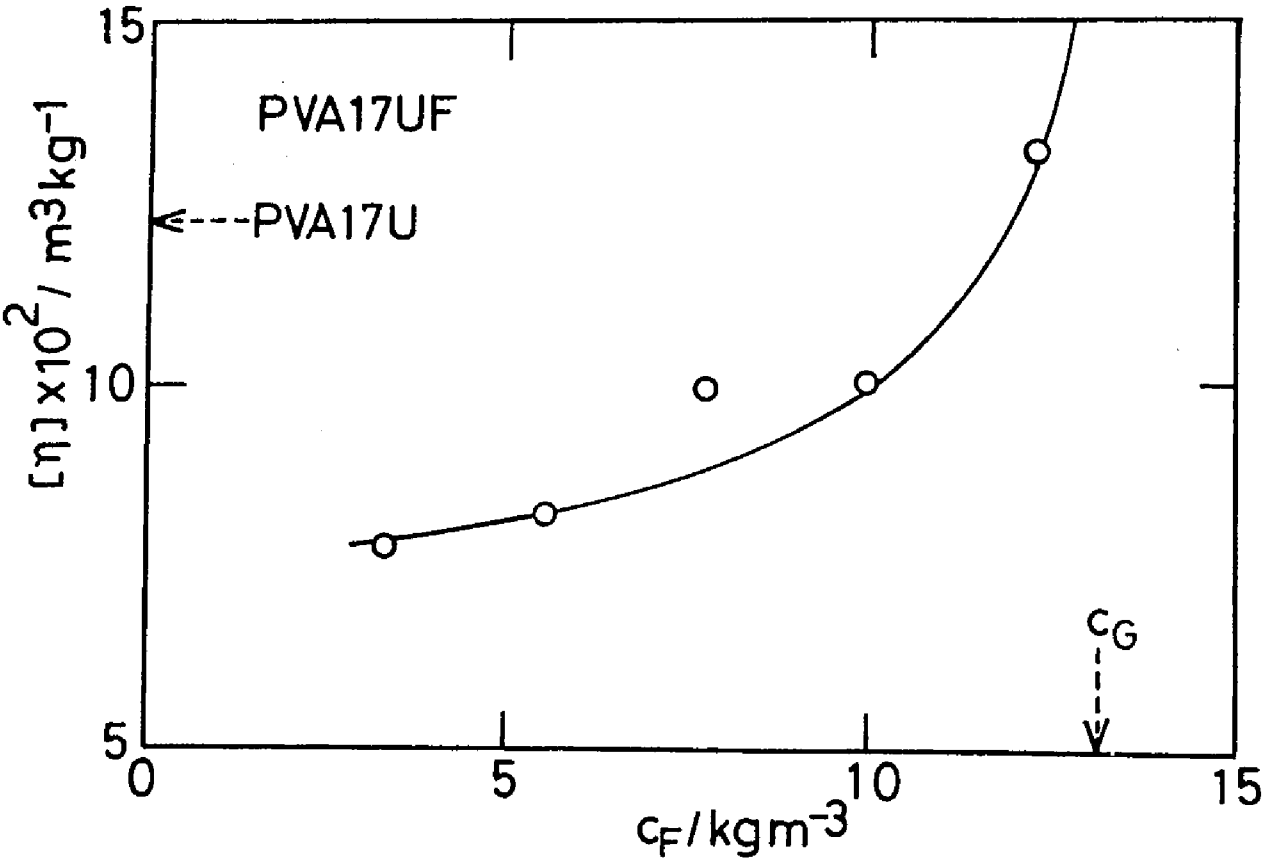

Figure 3-8. The intrinsic viscosity ([η]) plotted against the polymer concentration (c_F) at which the solutions were prepared, and cooled.

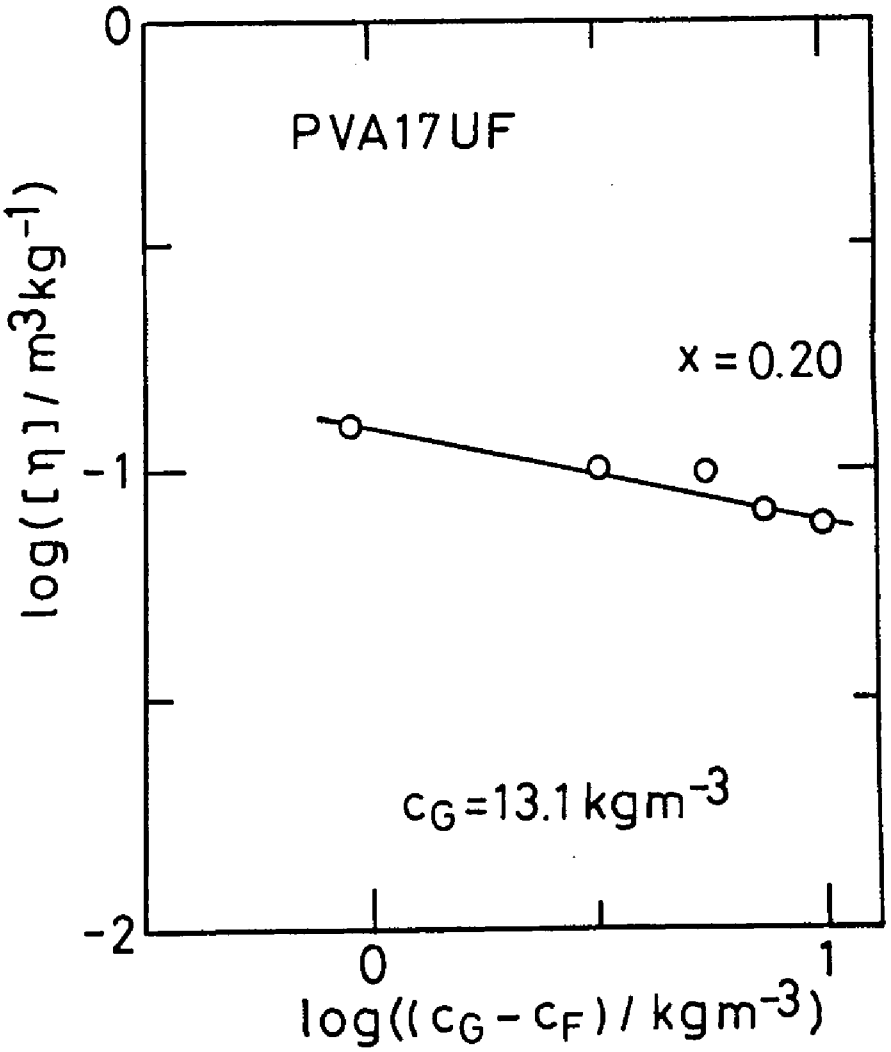

Figure 3-9. Double-logarithmic plots of the intrinsic viscosity ([η]) vs. the concentration difference (c_G-c_F). c_G stands for the concentration of the gelation, and c_F the polymer concentration at which the solutions were prepared, and cooled.

($\pm$0.03) in Figure 3-9.

According to a scaling theory,[5,10] x for Rouse clusters[10] is related to the other scaling exponents as:

$$x=-\beta+2\nu \qquad (3\text{-}10)$$

for cases where the hydrodynamic interaction is ignored in calculation of $[\eta]$. By the 3d percolation, exponents β and ν are 0.4 and 0.9, respectively.[10] This gives x=1.4. Since β and ν are 1.0 and 0.5 respectively, for the Bethe lattice,[5,10] x for Rouse clusters described by the classical theory of the Flory-Stockmeyer type should be 0. Even in this case, however, $[\eta]$ diverges logarithmically with increasing c_F. On the other hand, x for Zimm clusters,[10] for which the hydrodynamic interaction is taken into account in calculation of $[\eta]$, is expressed as:[5]

$$x=3\nu-\gamma-2\beta \qquad (3\text{-}11)$$

For the 3d percolation, x is identical to 0 if the hyperscaling law[5,10] is valid, and $[\eta]$ shows logarithmic divergence at the gelation point.[5] Sievers[8] has reported that x for Zimm clusters described by the classical theory is 0, and $[\eta]$ remains a finite value even at the gelation point. The value of x obtained by our experiment does not agree exactly with any of the exponents predicted by the 3d percolation and classical theories. The exponent x obtained in this study is considered to be affected by the reduced $[\eta]$ at c_F region below the gelation point, though we

do not know how the reduced [η] affects x at present. The effect of the reduced [η] may be characteristic of PVA system. The exponent x for PVA17UF is rather small and the divergence of [η] at the gelation point is weak. This means that the critical behavior of [η] for PVA17UF resembles that for Zimm clusters predicted by the 3d percolation theory, or that for Rouse clusters by the classical theory, in a sense of the weak divergence at the gelation point. Sievers[8] has shown that Zimm clusters are more preferable than Rouse clusters for the description of the critical behavior of [η] in the vicinity of the gelation point. The experimental results described above might suggest that the critical behavior of [η] of PVA solution should be considered to be close to that of Zimm clusters of the 3d percolation theory rather than that of Rouse clusters of the classical theory.

3-4 Conclusions

The critical exponents for the specific viscosity (η_{sp}) and intrinsic viscosity ([η]) were examined for poly(vinyl alcohol) (PVA) solutions. The critical exponent for η_{sp} was found to be 1.67. This value is larger than those reported previously for various polymerizing systems and for a gelatin system.

The constant in the Huggins equation for viscosity (k') for PVA clusters was higher than that of linear PVA, and the value of [η] for PVA clusters was smaller than that of linear PVA at lower polymer concentrations, at which PVA solutions were prepared and cooled. The critical exponent for [η] was 0.20. The

weak divergence of $[\eta]$ resembles the critical behavior of Zimm clusters predicted by 3d percolation theory, or that of Rouse clusters by the classical theory of Flory-Stockmeyer type. The critical behavior of $[\eta]$ of PVA solutions, however, may be considered to be close to Zimm clusters of the 3d percolation theory rather than that of Rouse clusters by the classical theory, because Zimm clusters are more preferable than Rouse clusters for the description of the critical behavior of $[\eta]$.

References

1. P. G. de-Gennes, *J. Phys. (Paris)*, **40**, L197 (1979)
2. B. Gauthier-Manuel and E. Guyon, *J. Phys. (Paris)*, **41**, L503 (1980)
3. M. Tokita, R. Niki and K. Hikichi, *J. Chem. Phys.*, **83**, 2583 (1985)
4. M. Tokita, K. Hikichi, *Phys. Rev.*, **A35**, 4329 (1987)
5. D. Stauffer, A. Coniglio and M. Adam, *Adv. Polym. Sci.*, **44**, 103 (1982)
6. M. Adam, M. Delsanti, D. Durand, G. Hild and J. P. Munch, *Pure Appl. Chem.*, **53**, 1489 (1981)
7. J. Dumas and J. -C. Bacri, *J. Phys. (Paris)*, **41** L279 (1980)
8. D. Sievers, *J. Phys. (Paris)*, **41**, L535 (1980)
9. R. S. Whitney and W. Burchard, *Makromol. Chem.*, **181**, 869 (1980)
10. D. Stauffer, "*Introduction to Percolation Theory*", Taylor and Francis, London and Philadelphia, 1985
11. F. W. Billmeyer, Jr., "*Textbook of Polymer Science, 3rd ed.*, John Wiely & sons, New york, N. Y., 1984
12. L. H. Cragg and R. H. Sones, *J. Polym. Sci.*, **9**, 585 (1952)
13. L. H. Cragg and G. R. H. Fern, *J. Polym. Sci.*, **10**, 185 (1953)

Chapter 4

Critical Behavior of Modulus of Poly(vinyl alcohol) Gels near the Gelation Point

4-1 Introduction

In the previous chapter, the critical behavior of the specific and intrinsic viscosities was described. The critical behavior of the other physical quantities has been investigated theoretically and experimentally by many research groups,[1-13] and the experimental data were analyzed by using the percolation theory, which is now closely related to the fractal theory.[14-19] More recently, much attention has been also paid to a dynamic scaling exponent for modulus; Cates[6] and Muthukumar[7] have proposed theories determining an exponent for the frequency dependence of modulus at the gelation point. Experimentally, Winter and coworkers[8] have extensively investigated the viscoelasticity of critical gels.

The critical behavior of modulus (E) is expressed by using a exponent (t) as[1,14]

$$E \sim \varepsilon^{t} \qquad (4\text{-}1)$$

Here, ε is the relative distance from the gelation point. When we use c as a variable, ε for E is defined by using c and c_G, the concentration at the gelation point, as

$$\varepsilon = (c - c_G)/c_G \qquad (4\text{-}2)$$

The elasticity has been considered to scale in the same way as conductivity.[1,12,14] The value of t was theoretically obtained from the analogy between conductivity and modulus, showing $t \cong 1.8$.[1,12,14] In this model, the effect of blobs on E of the critical gels was ignored. Martin et al.[15] have also shown that $t \cong 2.67$, which fundamentally corresponds to the critical exponent for steady-state compliance (J_e^0). Therefore, it is unclear whether their value is valid for E. On the other hand, classical theory[1,14,20,21] predicts exactly t=3. Experimental results on t have been also scattered;[2,3,9-11] thus the value of t seems to be still uncertain at present. In order to clarify the critical behavior of E, the value of t must be evaluated for various gel systems. For this purpose we evaluated the value of t for poly(vinyl alcohol) (PVA) gel systems. This chapter describes the results of the critical behavior of E. First, a new scaling relation for E is presented, and then the experimental results for t for PVA gels are described. The experimental results contain those for the preliminary study. The PVA gels focused here was very tenuous so that the preliminary study was conducted in order to check whether testing apparatus in our laboratory can be used for the elasticity measurement of such tenuous gels with enough accuracy.

4-2 Critical Behavior of Modulus

In order to explain the critical behavior of the exponent t for the gel systems, we introduce a scaling relation between E and ε near the gelation point on the basis of fractality of gels

near the gelation point. We introduce here the system size (L). L is of the order of a dimension of the reaction bath considered. We call the molecular weight of the gel simply the mass. For the gels far from the gelation point, the mass is proportional to L^d. Here, d is the space dimension. The gel considered here is, however, the critical gel, namely, the gel near the gelation point. The mass of the critical gel (m_f) scales as $m_f \sim L^{d_f}$ with L and the fractal dimension (d_f).[15-18] The backbone cluster is defined by cutting off the dangling ends from the gel.[15-18] The backbone is composed of singly connected bonds, and blobs where the bonds are multiply connected.[17,18] The mass of the backbone of the gel (m_B) is given a fractal dimension d_B by $m_B \sim L^{d_B}$, and is mostly dominated by the mass of blobs in the backbone.[17,18] The other fractal is the minimum (or chemical) path defined on the fractal objects.[17,18] The path length is measured by the number of connected units and therefore by a dimension of mass. The minimum path length (l) scales as[17,18] $l \sim L^{d_{min}}$. The exponent d_{min} is the fractal dimension for the minimum path. The connectivity of chains in the backbone is expressed by using a chemical dimension (d_{bc}) for the backbone, which is defined by $d_{bc}=d_B/d_{min}$. This gives the relation $m_B \sim l^{d_{bc}}$. Just above the gelation threshold, the structure of backbone has been approximated by the node-link-blob model[14,19] in the percolation theory. According to this model, the backbone forms the superlattice network of nodes. The connective strand between neighboring nodes is composed of links and blobs, and its Euclidian length is order of correlation length (ξ). The link is

a union of singly connected (or red) bonds, whose total mass (m_{red}) scales as[15,17,18] $m_{red} \sim L^{d_{red}}$. The strand composed of links and blobs can be regarded as the model of the backbone fractal near the threshold.

To determine the elastic properties of critical gels which can be regarded as the percolation clusters, we replace the bonds in the links and the blobs by springs. For polymer gels a bond corresponds to a polymer chain between crosslinks. We can also rearrange all the singly connected springs in series and all the multiply connected ones similarly, with keeping the original connectivity. After the replacement and rearrangement, the series of singly connected springs can be again replaced by a (long) spring. The series of multiply connected springs can also be considered to be a (large) blob composed of springs with various length, because there is no singly connected bond in the union. We assume that the elastic behavior of the spring is linear at microscopic strain magnitude (γ_m) smaller than a finite but small critical value (γ_0) and the spring is rigid at $\gamma_m > \gamma_0$. When macroscopic tensile strain with the magnitude of $\gamma(=\delta L/L)$ is applied to the backbone fractal, the origin of elasticity of the backbone is quite different depending on the value of γ. The spring model proposed above logically gives a critical macroscopic strain magnitude (γ_c), which is expressed by L and γ_0 as

$$\gamma_c \simeq \gamma_0 L^{(d_{red}/d_{min})-1} \qquad (4\text{-}3)$$

According to the finite size scaling,[15,18] L can be considered to be identical to the correlation length (ξ). The quantity ξ scales as $\xi \sim \varepsilon^{-\nu}$ with the exponent ν. γ_c is a critical quantity near the gelation point and it should be infinitesimal in a space of d lower than 6, because $d_{min} > d_{red}$ for the percolation clusters with ideally infinite L.[17,18] When d=6 (classical limit), however, it is expected that $\gamma_c \simeq \gamma_0$ because of no blob in the backbone of the percolation cluster. Namely, $d_B = d_{min} = 2$, and d_{red} is also two for d=6.[18]

These results imply that there are two distinct regimes depending on applied strain, $\gamma < \gamma_c$ and $\gamma_c < \gamma < \gamma_0$, in the elastic response of the percolated cluster in the gels. The macroscopic elastic properties of gels in the first regime ($\gamma < \gamma_c$) are dominated by the deformation of the link composed of singly connected bonds. The other regime ($\gamma_c < \gamma < \gamma_0$) is the case that the effect of the blob on elastic properties are fully considered. In other words, the singly connected bonds will contribute mainly to the macroscopic deformation at $\gamma < \gamma_c$. On the other hand, at $\gamma > \gamma_c$ the singly connected bonds behave as a rigid body as a whole because they are fully extended, and the bonds in blob mainly contribute to the macroscopic deformation. In the 3d space where actual gelation takes place, it is very difficult to satisfy the condition of $\gamma < \gamma_c$ experimentally: As the system approaches the gelation point ($\xi \longrightarrow \infty$), the mass of the backbone m_B is mostly dominated by the blob and $\gamma_c \longrightarrow 0$. We believe that all the experiments on E of critical gels have been carried out in the case $\gamma_c << \gamma < \gamma_0$, based on the model proposed above.

E of the clusters is proportional to the number of the active chains (N) in system volume.

$$E \sim N/L^{d} \tag{4-4}$$

We try to estimate the scaling form for N in the case that γ is small but finite at $\gamma<\gamma_0$. Although exact scaling law for N has not been obtained, N is assumed as $N \sim l^{h}$. In a space of d<6 where the large blob exists, N will be the number of different paths in the blob. As d increases, h decreases because the blob structure becomes tenuous. We expect h=0 for the limiting value for d=6. Taking above consideration into account, we write h with d_{bc} as a following form.

$$h=d_{bc}-1 \tag{4-5}$$

The relation between E and L is given by

$$E \sim L^{-(d+d_{min}-d_B)} \tag{4-6}$$

Then, E scales with ε as

$$E \sim \varepsilon^{(d+d_{min}-d_B)\nu} \tag{4-7}$$

which means $t=(d+d_{min}-d_B)\nu$. When d=6 (classical limit), t=3, because $d_B=d_{min}=2$ and $\nu=1/2$,[14,17,18] which recovers the value of t predicted by the classical theory.[1,14,20,21] For d=3, we

obtain t≅2.27 by using d_{min}≅1.33, d_B≅1.74 and ν≅0.875 for the percolation cluster.[18]

4-3 Experimental

PVA used in this study was supplied by Unitika, Co. The average degree of polymerization is 1700, and the average degree of saponification 99.5mol%. The solvent used in this study is a mixture of dimethylsulfoxide (DMSO) and water (W) (4:1 by weight), which is designated as D/W or DMSO/W. Details of the gel preparation is described in Chapter 2. Dynamic Young's modulus (E') of PVA gels was measured by means of a Rheometrics Solids Analyzer (RSAII) by a frequency (ω) sweep mode at 25°C. The range of ω was 10^{-1} to $10^{2}s^{-1}$. The initial Young's modulus (E_0) of the gels was measured by using a tensile tester (Orientec RTM 250) in tensile and compressional modes at 25°C. Prior to the dynamic mechanical and tensile testing of PVA gels, the preliminary experiments were carried out under the same experimental conditions.

4-4 Results and discussion

4-4-1 Preliminary Study

Figure 4-1 shows the frequency dependence of dynamic Young's modulus (E') of PVA gels. No variation with frequency is observed for any gel and E' increases with increasing polymer concentration. Figure 4-2 shows the polymer concentration, c, dependence of E' for PVA gels. In this figure, the dependence of E' on the concentration difference from the critical

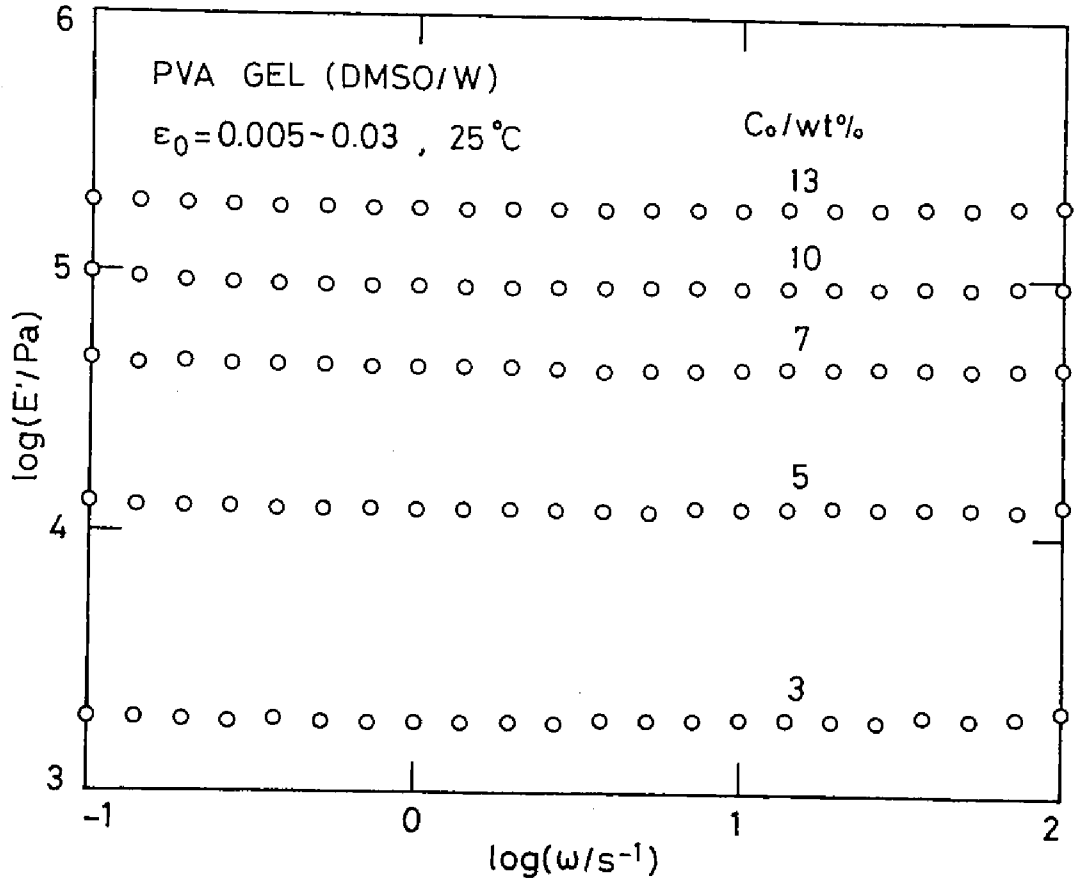

Figure 4-1. The frequency dependence of dynamic Young's modulus (E') of PVA gels.

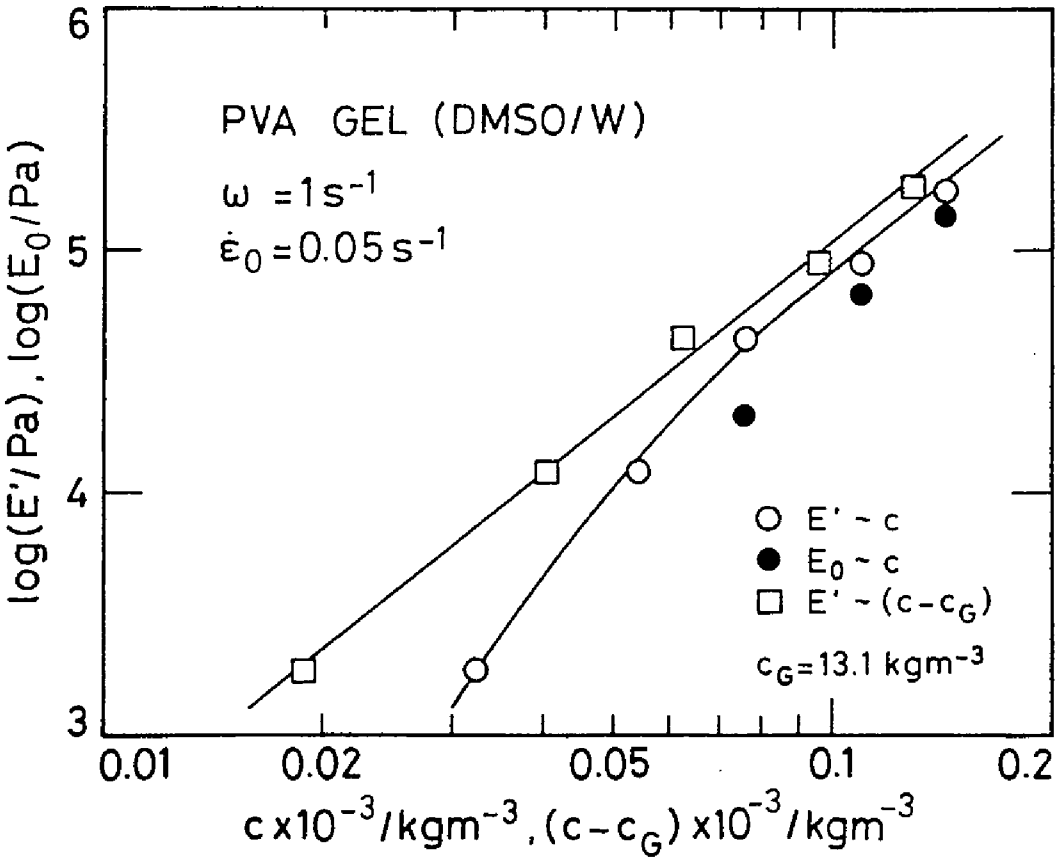

Figure 4-2. Double-logarithmic plots of dynamic Young's modulus (E') vs. polymer concentration (c), and vs. the concentration difference, $(c-c_G)$, from the critical concentration for gelation (c_G) of PVA gels.

concentration of gelation, c_G is also shown. Here, the value of E' used is that at a frequency of 1 s^{-1}. We used c_G=13.1kg/m^3, which was obtained by examining the critical behavior of the viscosity for the PVA solution systems as shown in the previous chapter. E' increases with increasing c, and the relation of E' vs. c is expressed by a curve. At c higher than 75kg/m^3, the curve is approximated by a straight line of slope 2.4. This dependence of E' of c in the high c region agrees fairly well with the result derived from so-called "c* theorem".[1] This agreement also shows that experimental data obtained here are reliable. The concentration dependence of E' is stronger in the region of lower c, but the linear relation between logE' and $\log(c-c_G)$ is observed over a concentration range examined. The exponent t is then estimated to be 2.4. The value of t obtained here is smaller than that of the classical theory,[1,14,20,21] but is slightly larger than those reported by previous researchers.[9,10,12,14] The exponent lies within the range of value reported by Adam et al.[11] The reported values of t are a little scattered; the value will depend on the system used for study. We think that the value of t obtained here is not erroneous but reliable, and the measurements were also made with enough accuracy even for the gels at low c.

The crossover behavior of t has been observed at about ε=2 for casein Michelle gels,[9] and at about ε=3 for agarose gels,[10] though the reason why ε of the crossover point depends on the type of gel is still unclear. If the crossover of t is a universal phenomenon for the sol-gel transition, the crossover

behavior should also be observed for PVA gels at almost the same region of ε, as for casein micelle gels and agarose gels. Hence, we expected that the crossover behavior for PVA gels was observed at ε=2-3, which corresponds to the region of $(c-c_G)$=39.3-52.4 kg/m^3. As can be seen from Figure 4-2, however, the crossover behavior of t is not observed for PVA gels. This implies that only one exponent describes the critical behavior of E' of PVA gels over a rather wide range of ε.

4-4-2 Critical Exponent of Modulus for PVA Gel

Figure 4-3 shows the c dependence of E' at ω=1s^{-1} and E_0 of PVA gels at 25°C. The figure involves the data obtained in the preliminary study. The absolute values of E' and E_0 obtained by the preliminary experiments are slightly lower than those in this study. This is due to the difference in the sample lot. The data obtained in this study fall on a single curve. In the high c region, the curve can be approximated by a straight line, but data points in the low c region, less than about 80 kgm^{-3}, show a stronger c dependence than those at high c. This strong c dependence at low c suggests the critical anomaly of E' of PVA gels. The plots of E' at ω=1s^{-1} and E_0 vs. ε using the value c_G=13.1kg/m^3 are shown for PVA gels in Figure 4-4. This also contains the data obtained by the preliminary experiments shown before. The critical exponent t should be evaluated from the plots of modulus against ε in the critical region of c. The critical region of ε extends to ε lower than about 5 which corresponds to c≅80kg/m^3. All data points within and out of the

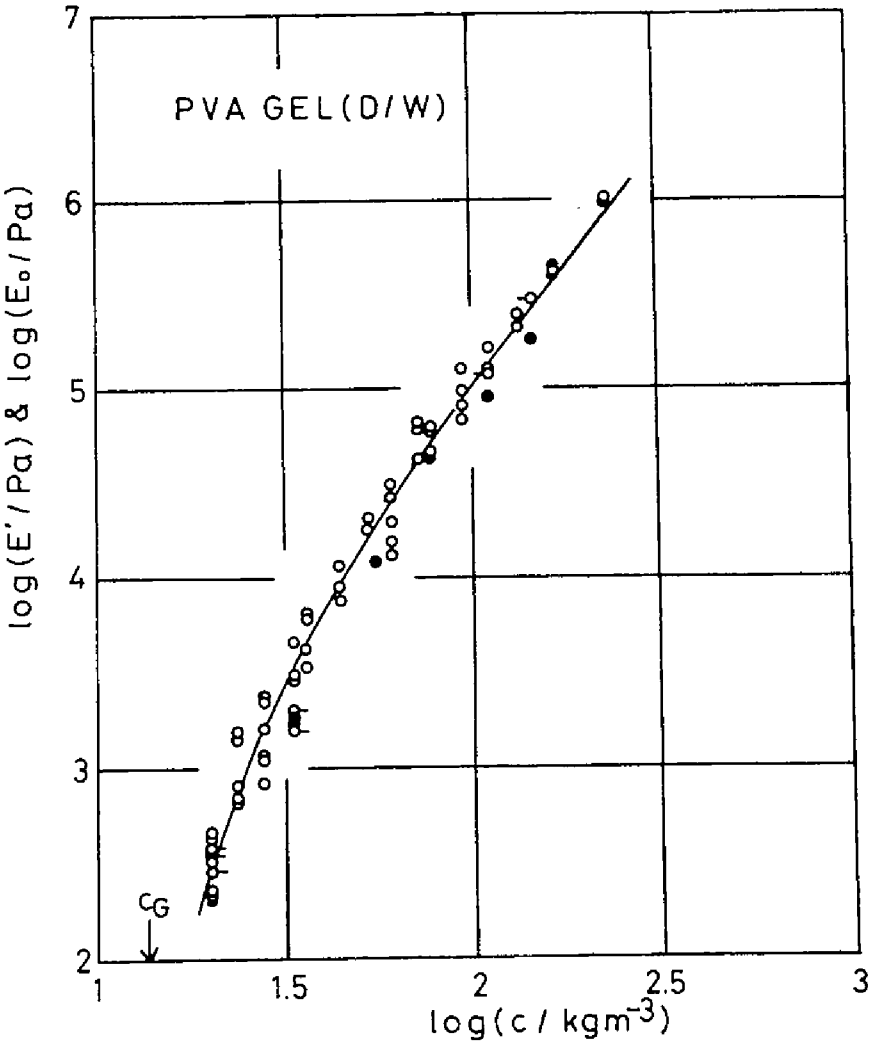

Figure 4-3. Concentration (c) dependence of dynamic Young's modulus (E') at frequency (ω) of $1s^{-1}$ and initial Young's modulus (E_0) of PVA gels: Symbols (○) for E'; (–○) for E_0 from tensile testing; (○–) for E_0 from ompression; (●) from preliminary study.

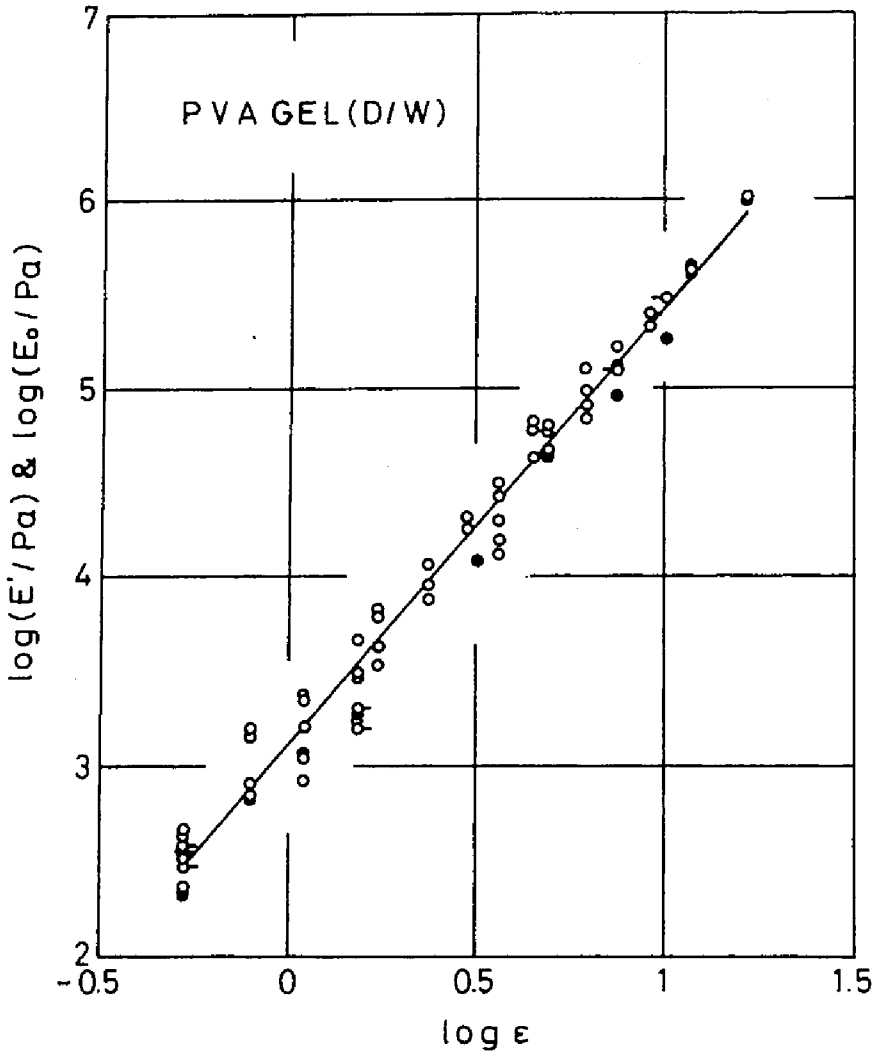

Figure 4-4. Plots of dynamic Young's modulus (E') at frequency (ω) of $1s^{-1}$ and initial Young's modulus (E_0) vs. ε. ε stands for the relative distance from the gelation point. Symbols are the same as Figure 4-3.

critical region obtained in this study fall on a single line. We determined t from the slope of the line by least-square method, showing $t=2.31\pm0.04$. The absolute values of E' and E_0 obtained in the preliminary study is slightly lower, but the value ($t=2.4$) is close to that ($t=2.31$) obtained in this study, suggesting that the value is reliable for PVA gels. Comparing the value with the prediction ($t\cong2.27$) of our model, the agreement is excellent. On the other hand, the experimental value of t is larger than that ($t\cong1.83$) predicted by the percolation theory from the electrical analogy[1,12,14] where it is assumed that only the singly connected bonds contribute to modulus. Finally, from the results obtained in this study, we can conclude that the elastic properties of gels measured experimentally near the critical point is definitely dominated by blobs rather than links.

4-5 Conclusions

The value of critical exponent for modulus (t) was estimated by using a model based on the percolation theory, and the value was experimentally determined for poly(vinyl alcohol) (PVA) gels. The model proposed has shown that there is a critical strain (γ_c), which distinguishes two regimes in the elastic response of the gel network near the gelation point. The theory has also shown that γ_c is infinitesimally small for a realistic gelation in the 3d space. The exponent t for $\gamma>\gamma_c$ scales as $(d+d_{min}+d_B)\nu\cong2.27$ with fractal dimensions, d_{min} and d_B, and the exponent ν for correlation length for gels near the gelation point. The value of t for PVA gels has been found to be 2.31 ± 0.04

and is close to the one predicted by the model proposed. The crossover behavior of modulus was not found for PVA gels investigated here.

References

1. P. G. de Gennes, "*Scaling Concept in Polymer Physics*", Cornell University Press, Ithaca and London, 1979
2. C. Pebiche-Covacs, S. Dev, M. Gordon, M. Judd and K. Kajiwara, in "*Polymer Networks*, A. Chompff and S. Newman, eds., Plenum Press, New York, 1971
3. B. Gauthier-Manuel and E. Guyon, *J. Phys. (Paris)*, **41**, L503 (1980)
4. J. Bauer, P. Lang, W. Burchard and M. Bauer, *Macromol.*, **24**, 2634 (1991)
5. M. Adam, M. Delsanti, J. P. Munch, D. Durand, *J. Phys. (Paris)*, **48**, 1809 (1987)
6. M. E. Cates, *J. Phys. (Paris)*, **46**, 1059 (1985)
7. M. Muthukumar, *J. Chem. Phys.*, **83**, 3161 (1985)
8. H. H. Winter and F. Chambon, *J. Rheol.*, **30**, 367 (1986): F. Chambon and H. H. Winter, *J. Rheol.*, **31**, 683 (1987): H. H. Winter, P. Morganelli and F. Chambon, *Macromol.*, **21**, 532 (1988): J. C. Scanlan and H. H. Winter, *Macromol.*, **24** 2422 (1991)
9. M. Tokita, R. Niki and K. Hikichi, *J. Chem. Phys.*, **83**, 2583 (1985)
10. M. Tokita and K. Hikichi, *Phys. Rev.*, **A35**,4329 (1987)
11. M. Adam, M. Delsanti, D. Durand, G. Hill and J. P. Munch, *Pure Appl. Chem.*, **53**, 1489 (1981)
12. P. G. de Gennes, *J. Phys. (Paris)*, **37**, L1 (1976)
13. J. E. Martin, D. Adolf, J. P. Wilcoxon, *Phys. Rev.*, **A39**, 1325 (1989)

14. D. Stauffer, A. Coniglio and M. Adam, *Adv. Polym. Sci.*, **44**, 103 (1982)

15. D. Stauffer, "*Introduction to Percolation Theory*", Taylor and Francis, London and Philadelphia, 1985

16. B. B. Mandelbrot, "*The Fractal Geometry of Nature*", W. H. Freeman and Company, New York, 1977

17. "*On Growth and Form*, H. E. Stanley and N.Ostrowsky, eds., Martinus Nijhoff publishers, Boston, Dordrecht and Lancaster, 1986

18. "*Fractals and Disordered Systems*",A. Bunde and S. Havlin, eds., Springer-Verlag, Berlin, Heidelberg and New York, 1991

19. H. E. Stanley, *J. Phys.*, **A10**, L211 (1977)

20. W. Stockmayer, *J. Chem. Phys.*, **11**, 45 (1943)

21. G. R. Dobson and M. Gordon, *J. Chem. Phys.*, **43**, 705 (1965)

Chapter 5

Theoretical Studies on Swelling and Stress Relaxation of Polymer Gels

5-1 Introduction

The equilibrium swelling behavior of gels has been investigated by many researchers.[1-6] However, the studies have concerned mostly the free swelling of polymer gels. The studies on swelling under deformation are only a few at present.[7,8] Concerning the mechanical properties of gels, there are many studies.[9-14] For example, stress-strain behavior has been examined for various kinds of gels.[11,15] The studies are limited to the properties at short times. The mechanical properties of gels at long times are still unclear because of only a few experimental and theoretical studies.[14,16] When a gel is stretched, the free energy of the gel system will change to attain a new equilibrium state under deformation. This may cause a volume change of the gel. Tanaka et al. have reported[17,18] that the relaxation time for swelling is determined by the diffusion constant and the sample size of freely swelling gel systems. The same concept may be applicable to the swelling of the stretched gel systems, that is, the swelling of the stretched gel also takes long time until reaching the equilibrium size. As can be easily imagined, the swelling behavior strongly affects mechanical properties of polymer gels. We have already reported the mechanical properties at short times, such as the stress-strain behavior and Poisson's ratio (μ) of poly(vinyl alcohol)

(PVA) gels.[19] The mechanical properties of the PVA gels could be regarded as that of a swollen rubber; μ was very close to 0.5 independently of the strain rates. This fact implies that μ of the gels is a "material constant", and happens because the reciprocal of the experimental strain rate, which can be considered as a time-scale of the experiment, is much shorter than the time required for the swelling and volume change. It is very important to investigate the coupling between swelling and the mechanical properties under deformation for understanding the properties of gels at long times. The equilibrium swelling behavior of gels under deformation, and the dynamics of swelling and stress relaxation under uniaxial elongation are treated theoretically in this chapter.

5-2 Swelling Behavior of Uniaxially Stretched Gels

We consider here uniaxial elongation process of isotropic gels from a freely swollen state, i.e., the state without external tension. The state is referred to as the reference state. Thermodynamics required for describing free swelling behavior of polymer gels is summarized in Chapter 1. In the present chapter swelling behavior under tension is focused but the thermodynamics employed is almost the same as that shown in Chapter 1 except that now the work done by the external force appears in free energy.

Using Flory-type expression,[1] the Gibbs free energy (F) of the uniaxially stretched gel in x-direction can be expressed as[20]

$$F=F_0+N_S k_B T[\ln(1-\phi)+\chi\phi]$$
$$+(N_C k_B T/2)[\lambda_x^2+\lambda_y^2+\lambda_z^2-3-\ln(\lambda_x\lambda_y\lambda_z/V_0)]$$
$$+\tilde{f}_x l_{x0}(\lambda_x-1) \qquad (5\text{-}1)$$

where F_0 is the free energy of pure polymer and solvent, N_C and N_S respectively the number of active chains and of solvent molecules in the reference state, V_0 the volume in the reference state, ϕ the polymer volume fraction, k_B the Boltzmann constant, T the absolute temperature, $\tilde{f}_x$ the external force, l_{x0} the initial length of the gel in x-direction, and χ the polymer-solvent interaction parameter. The quantity λ_i (i=x, y and z) is defined by

$$\lambda_i=l_i/l_{i0} \qquad (5\text{-}2)$$

where l_i is the sample dimension in the i-direction in the stretched state, l_{i0} that in the reference state, and $\lambda_x\lambda_y\lambda_z=V/V_0=\phi_0/\phi$, where V is the volume in the deformed state and ϕ_0 is the value of ϕ in the reference state. The shear modulus G_0 in the reference state is written by $G_0=N_C k_B T$. Without losing generality, we can set $l_{i0}=1$ and accordingly $V_0=1$. In this case, the quantity $\tilde{f}_x$ can be considered as the nominal stress acting in x-direction. Regarding F as a function of λ_i, Π_i (i,j,k=x, y and z) can be defined as

$$\Pi_i=-(1/\lambda_j\lambda_k)(\delta F/\delta\lambda_i) \qquad (5\text{-}3)$$

Π_i is the swelling stress (pressure) acting normally on the surface of the gel perpendicular to i-axis, and $\Pi_i=0$ in equilibrium, namely,

$$-\Pi_x=(k_BT/v_s)[\ln(1-\phi)+\phi+\chi\phi^2] +(N_Ck_BT/2\lambda_y\lambda_z)(2\lambda_x-\lambda_x^{-1})-\tilde{f}_x/\lambda_y\lambda_z=0 \qquad (5\text{-}4)$$

$$-\Pi_y=(k_BT/v_s)[\ln(1-\phi)+\phi+\chi\phi^2] +(N_Ck_BT/2\lambda_z\lambda_x)(2\lambda_y-\lambda_y^{-1})=0 \qquad (5\text{-}5)$$

$$-\Pi_z=(k_BT/v_s)[\ln(1-\phi)+\phi+\chi\phi^2] +(N_Ck_BT/2\lambda_x\lambda_y)(2\lambda_z-\lambda_z^{-1})=0 \qquad (5\text{-}6)$$

where v_s is the volume of a solvent molecule and is given by $v_s=(1-\phi)V/N_s$. The average swelling pressure (Π) is written by $\Pi=(1/3)\Sigma\Pi_i$, and $\Pi=0$ is also satisfied in equilibrium. The quantity $\tilde{\sigma}_{x\infty}$, the external stress exerted on the gel in x-direction in equilibrium, is expressed by

$$\tilde{\sigma}_{x\infty}=\tilde{f}_x/\lambda_y\lambda_z=(k_BT/v_s)[\ln(1-\phi)+\phi+\chi\phi^2] +(N_Ck_BT/2\lambda_y\lambda_z)(2\lambda_x-\lambda_x^{-1}) \qquad (5\text{-}7)$$

In the reference state, $\tilde{\sigma}_{x\infty}=0$ and also $\Pi_i=0$. Then, we obtain

$$N_C=-2[\ln(1-\phi_0)+\phi_0+\chi\phi_0^2]/v_s \qquad (5\text{-}8)$$

Hereafter, we deal with the gels with $\phi_0<<1$, and also $\phi<<1$.

When k<<1, ln(1-k) can be expanded as $-k-(1/2)k^2+O(k^3)$. Using the approximation, we try to obtain the expressions for μ, Π_i, and $\tilde{\sigma}_{x\infty}-\Pi_x$ in equilibrium. Since we consider the uniaxial elongation of isotropic gels in x-direction, $\alpha_y=\alpha_z$. Then, Equation 5-5 coincides with Equation 5-6, and is expressed by

$$-\Pi_y=(k_BT/2v_s)(2\chi-1)(\phi_0/V)^2 + (N_Ck_BT/2)(2\lambda_x^{-1}-V^{-1})=0 \qquad (5\text{-}9)$$

Equation 5-8 is also written by

$$N_C=(\phi_0^2/v_s)(1-2\chi) \qquad (5\text{-}10)$$

Combining Equation 5-9 with Equation 5-10, we have

$$(1/V)^2+(1/V)-(2/\lambda_x)=0 \qquad (5\text{-}11)$$

From this equation, α_y^2 and α_z^2 are given by

$$\lambda_y^2=\lambda_z^2=[\lambda_x+(\lambda_x^2+8\lambda_x)^{1/2}]/4\lambda_x \qquad (5\text{-}12)$$

Since the strain in i-direction (ε_i) for the gel is defined by

$$\varepsilon_i=\lambda_i-1 \qquad (5\text{-}13)$$

we can linearize Equation 5-12 using Equation 5-13 when the strain is small. At equilibrium ε_y and ε_z are written by

$$\varepsilon_y=\varepsilon_z=-\varepsilon_x/6 \tag{5-14}$$

Equation 5-14 shows that the value of Poisson's ratio μ at equilibrium (μ_∞) is 1/6. Using the value of μ_∞ and the relation $K_{os}=2(1+\mu_\infty)G_0/3(1-2\mu_\infty)$, the osmotic bulk modulus K_{os} is given by $K_{os}=(7/6)G_0$. The linearized expressions for $-\Pi_i$ ($i=y,z$) and $\tilde{\sigma}_{x\infty}-\Pi_x$ at fixed ε_x are given by

$$-\Pi_y=G_0\varepsilon_x/2+[3G_0(\varepsilon_y+\varepsilon_z)/2] \tag{5-15}$$

$$-\Pi_z=G_0\varepsilon_x/2+[3G_0(\varepsilon_y+\varepsilon_z)/2] \tag{5-16}$$

$$\tilde{\sigma}_{x\infty}-\Pi_x=(5G_0\varepsilon_x/2)+[G_0(\varepsilon_y+\varepsilon_z)/2] \tag{5-17}$$

In the equilibrium state under tension where $\Pi_x=0$, $\tilde{\sigma}_{x\infty}$ is given by

$$\tilde{\sigma}_{x\infty}=7G_0\varepsilon_x/3 \tag{5-18}$$

5-3 Swelling Dynamics of Gels after Elongation

After a tension in x-direction is applied to a gel, the gel system moves toward a new equilibrium state under tension by expanding in y- and z-direction. This accompanies a volume change of the gel. In order to describe the dynamics of the gel swelling, we set the size of the gel in y- and z-direction in the reference state (i.e., the state without tension) is a_r. The small volume element of the gel can be specified by the position

vector, $\mathbf{r}=(x,y,z)$ $(0\leq y,z\leq a_r)$ in the coordinate of the reference state. According to Tanaka et al.,[17,18] the equation, which governs the time (t) dependent motion of the small volume element (dxdydz) at the position of (x,y,z) after instantaneous elongation with ε_x at t=0, can be written by

$$\zeta(\delta\mathbf{v}/\delta t)=(K_{os}+G_0/3)\mathrm{grad}(\mathrm{div}\mathbf{v})+G_0\Delta\mathbf{v} \qquad (5\text{-}19)$$

Here, $\mathbf{v}(x,y,z,t)$ is the displacement vector specified in the reference frame, and ζ the friction coefficient between gel network and solvent molecules.

Since Equation 5-19 has a complicated form, we simplify the equation. The displacement vector ($\mathbf{v}$) can be generally written by using scalar potential ($\Phi/2G_0$) and vector potential ($\Psi/2G_0$) with $\mathrm{div}(\Psi/2G_0)=0$ as

$$\mathbf{v}=\mathrm{grad}(\Phi/2G_0)+\mathrm{rot}(\Psi/2G_0) \qquad (5\text{-}20)$$

From Equations 5-19 and 5-20, we obtain

$$(\delta\Delta\Phi/\delta t)=D_L\Delta(\Delta\Phi) \qquad (5\text{-}21)$$

$$(\delta\Delta\Psi/\delta t)=D_T\Delta(\Delta\Psi) \qquad (5\text{-}22)$$

Here, D_L and D_T are the diffusion constants given with $K_{os}=(7/6)G_0$ by

$$D_L=[K_{os}+(4/3)G_0]/\zeta=5G_0/2\zeta \quad (5\text{-}23)$$

$$D_T=G_0/\zeta \quad (5\text{-}24)$$

The diffusion constant, D_L, is identical to the collective diffusion constant introduced by Tanaka et al.[17,18] The quantities, $\Delta\Phi$ and $\Delta\Psi$ are given by

$$\Delta\Phi=2G_0 div\mathbf{v}=2G_0 tr(u_{ij}) \quad (5\text{-}25)$$

$$\Delta\Psi=-2G_0 rot\mathbf{v}=-4G_0\omega \quad (5\text{-}26)$$

where ω is the rotation vector, and u_{ij} is the ij component of strain tensor ($\mathbf{u}$) for the small volume element and is defined by i and j components of the displacement vector (v_i and v_j) as $u_{ij}=(1/2)(\delta v_i/\delta x_j+\delta v_j/\delta x_i)$.[21] Equation 5-21 corresponds to the longitudinal mode of the diffusion, and Equation 5-22 to the transverse mode. It should be noted that the diffusion of the gels is generally separated into two modes, and each mode can be described by the diffusion equation. The longitudinal mode of the diffusion accompanies the volume change, while the transverse mode does not accompany the volume change but determines the change of shape. We can see from Equations 5-23 and 5-24 that the diffusion constant for the longitudinal mode is 2.5 times larger than that of the transverse mode.

We deal here with the longitudinal mode of the diffusion for swelling behavior, since the quantity of interest is the degree

of swelling of gels determined by the longitudinal mode of the diffusion. The swelling after elongation can be assumed to occur in y- and z-direction, so that $v(x,y,z,t)$ is independent of x. This means that $u_{xy}=u_{yx}=u_{xz}=u_{zx}=0$, and u_{xx} is constant. We re-write Equation 5-21 by using $\Delta\Phi=2G_0 tr(u_{ij})$ in Equation 5-25 as

$$[\delta tr(u_{ij})/\delta t]=D_L \Delta tr(u_{ij}) \qquad (5\text{-}27)$$

It should be noted that this diffusion equation is defined in 2-dimensional (2d) space. The volume change (the change of the cross-sectional area in the 2d space) of the gels is determined by the above equation with the initial and boundary conditions given by

$$tr(u_{ij})=(\varepsilon_{y0}+\varepsilon_{z0}) \quad \text{at } t=0 \qquad (5\text{-}28)$$

$$tr(u_{ij})=-2\mu_\infty \varepsilon_x \quad \text{at boundaries} \qquad (5\text{-}29)$$

The quantities ε_{y0} and ε_{z0} are the initial values of strain imposed in y and z directions, and are respectively written by using a macroscopic strain in x direction (ε_x) and μ at short times (μ_0) by $\varepsilon_{y0}=-\mu_0\varepsilon_x$ and $\varepsilon_{z0}=-\mu_0\varepsilon_x$, where $\varepsilon_x=u_{xx}$. The value of μ_0 is ideally 1/2. Equation 5-28 means that the cross-section of the gel shrinks at t=0, and Equation 5-29 shows that the osmotic pressure acting on the small element at the boundaries relaxes at any $t(>0)$.

The solution of Equation 5-27 satisfying the above

conditions is

$$tr(u_{ij})=\Sigma A_{mn}\sin(m\pi y/a_r)\sin(n\pi z/a_r)\exp(-k_{mn}t) \\ -2\mu_\infty \varepsilon_x \qquad (5\text{-}30)$$

Here, the constants in the equation above are given by

$$A_{mn}=-32(\mu_0-\mu_\infty)\varepsilon_x/mn\pi^2 \qquad (5\text{-}31)$$

$$k_{mn}=D_L\pi^2(m^2+n^2)/a_r^2=(m^2+n^2)/2\tau_L \qquad (5\text{-}32)$$

and τ_L is the longest relaxation time for the longitudinal mode, and m and n are odd integers. The t dependence of the average width of the gel (a(t)) in the y- and z-direction is determined by

$$a(t)^2=a_r^2[1+\varepsilon_y(t)+\varepsilon_z(t)]=\int dS' \qquad (5\text{-}33)$$

where $dS'=dS(1+u_{yy}+u_{zz})$ with $dS=dydz$. The t dependence of ε_y (or ε_z) can be written by

$$\varepsilon_y(t)=\varepsilon_z(t)=[a(t)^2-a_r^2]/a_r^2 \\ =(1/2a_r^2)[\int dy \int dz \\ \times\{\Sigma A_{mn}\sin(m\pi y/a_r)\sin(n\pi z/a_r)\exp(-k_{mn}t) \\ -2\mu_\infty \varepsilon_x\}] \qquad (5\text{-}34)$$

5-4 Stress Relaxation

5-4-1 Zero-th Order Approximation

We consider the external stress for small volume element with $\mu_0=1/2$ ($\tilde{s}_x(x,y,z,t)$). When $\tilde{s}_x(x,y,z,t)$ is instantaneously released, the small volume element will shrink in x direction and expand in y- and z-direction. The recovered size in the three directions are identical, and is determined in order to keep the volume constant before and after the stress release. This means that $\tilde{s}_x$ is proportional to the difference in u_{xx} between the stretched state and the isotropically swollen state. Using an average strain magnitude, $(u_{xx}+u_{yy}+u_{zz})/3$, $\tilde{s}_x$ can be written by

$$\begin{aligned}\tilde{s}_x &= 3G_0[u_{xx}-(u_{xx}+u_{yy}+u_{zz})/3] \\ &= G_0(2u_{xx}-u_{yy}-u_{zz}) \end{aligned} \qquad (5\text{-}35)$$

It should be noted that the average strain magnitude characterizes the new reference state, and is measured from the original reference state, and u_{xx} is a constant ($=\varepsilon_x$). Finally, the t-dependent macroscopic stress, $\tilde{\sigma}_x(t)$, can be expressed by

$$\tilde{\sigma}_x(t) = \int dS' s_x(t) / \int dS' \cong \int dS s_x(t) / \int dS$$

$$= (G_0/a_r^2) \int dy \int dz [2(1+\mu_\infty)\varepsilon_x - \Sigma A_{mn} \sin(m\pi y/a_r) \sin(n\pi z/a_r) \exp(-k_{mn}t) \qquad (5\text{-}36)$$

This agrees with Equation 5-18 at long t limit because $\mu_\infty=1/6$.

5-4-2 First-Order Approximation

In order to describe the stress relaxation in detail, the constitutive equation and the equation of motion are required. For deformed gel in solvent, the stress acting on small volume element of the gel ($\mathbf{s}$) can be written by the sum of the osmotic stress ($\mathbf{s}'$) and the external stress ($\tilde{\mathbf{s}}$) as

$$\mathbf{s}=\mathbf{s}'+\tilde{\mathbf{s}} \tag{5-37}$$

and the total strain ($\mathbf{u}$) is also given by

$$\mathbf{u}=\mathbf{u}'+\tilde{\mathbf{u}} \tag{5-38}$$

where $\mathbf{u}'$ and $\tilde{\mathbf{u}}$ are the osmotic and external strains, respectively. The quantity $\mathbf{s}'$ is given by[17,18]

$$\mathbf{s}'=2G_0[\mathbf{u}'-(1/3)\mathrm{tr}(\mathbf{u})\mathbf{I}]+K_{os}\mathrm{tr}(\mathbf{u}'-\mathbf{u}'_{\infty})\mathbf{I} \tag{5-39}$$

and depending on μ_0, $\tilde{\mathbf{s}}$ can be written by

$$\tilde{\mathbf{s}}=2G_0\tilde{\mathbf{u}}+p\mathbf{I} \qquad (\mu_0=1/2) \tag{5-40}$$

or

$$\tilde{\mathbf{s}}=2G_0+[K-(2/3)G_0]\mathrm{tr}(\tilde{\mathbf{u}})\mathbf{I} \quad (\mu_0\neq 1/2) \tag{5-41}$$

Here, $\mathbf{I}$ is the unit tensor, p the internal pressure, and $\mathbf{u}'_{\infty}$

being **u'** at equilibrium. The quantity K is the bulk modulus as a material constant. The value of p is determined by the condition that $\tilde{s}_{ii}$ (i=y,z) is zero for uniaxial elongation. The quantity K is assumed to be constant independently of the polymer concentration of the gel. We deal here also with the case of $\mu_0=1/2$ for simplicity. As can be seen from Equations 5-37 and 5-38, the total stress and strain are separated into two deformation modes. The displacement vector related to **u'**(**v'**) must obey the same type of equation of motion because the origin of the driving force for them is equally the diffusion. Then, we can also impose the following condition on **v'**.

$$\zeta(\delta \mathbf{v}'/\delta t)=\mathrm{div}\mathbf{s}' \qquad (5\text{-}42)$$

This equation means that the reference state for the external stress changes with increasing t after deformation. The physical picture of this equation is natural because the reference state changes with t only by swelling. For swelling after uniaxial defromation of the rectangular gel, the following relations are obtained.

$$v'_x=u'_{xx}(y,z,t)x \qquad (5\text{-}43)$$

$$v'_y=v'_y(y,z,t) \qquad (5\text{-}44)$$

$$v'_z=v'_z(y,z,t) \qquad (5\text{-}45)$$

From Equations 5-42 to 5-45 we can obtain

$$(\delta u'_{xx}/\delta t)=D_T\Delta u'_{xx} \qquad (5\text{-}46)$$

It is clear that Equation 5-46 corresponds to the transverse mode of diffusion. For swelling of a rectangular gel after uniaxial (x-directional) elongation, u_{xx}=constant and the swelling occurs in 2d, namely, y and z directions, but u'_{xx} as well as u'_{ii} (i=y,z) is t-dependent due to the existence of the transverse mode of diffusion.

In order to obtain the t dependence of $\tilde{s}$ for the small volume element, the solution of Equation 5-46 is required. The initial and boundary conditions for Equation 5-46 are given by

$$u'_{xx}=0 \qquad \text{at } t=0 \qquad (5\text{-}47)$$

$$u'_{xx}=(V_\infty - V_0)/3V_0$$
$$=2(\mu_0-\mu_\infty)\varepsilon_x/2 \qquad \text{at boundaries} \qquad (5\text{-}48)$$

Here, V_0 and V_∞ are the initial and final volumes of the element. The value of μ_∞ is 1/6, as shown previously. The solution of Equation 5-46 under the above initial and boundary conditions is

$$u'_{xx}=[(V_\infty - V_0)/3V_0]\{\Sigma B_{mn}\sin(m\pi y/a_r)\sin(n\pi z/a_r)$$
$$\times\exp(-k'_{mn}t)+1] \qquad (5\text{-}49)$$

Here, B_{mn} and k'_{mn} are

$$B_{mn}=-16/mn\pi^2 \tag{5-50}$$

$$k'_{mn}=(m^2+n^2)/2\tau_T \tag{5-51}$$

The quantity τ_T is the longest relaxation time of the transverse diffusion mode and is given by

$$\tau_T=a_r^2/2D_T\pi^2 \tag{5-52}$$

Finally, the t dependence of the stress acting on the whole gel ($\tilde{\sigma}_x$) is given by using $\mu_0=1/2$ and $\mu_\infty=1/6$ as

$$\tilde{\sigma}_x=(G_0\varepsilon_x/3a_r^2)\int dy \int dz[7-2\Sigma B_{mn} \times\sin(m\pi y/a_r)\sin(n\pi z/a_r)\exp(-k'_{mn}t)] \tag{5-53}$$

This implies that stress relaxation based on this approximation is governed by the transverse mode of the diffusion.

5-5 Conclusions

The swelling ratio and the stress value ($\tilde{\sigma}_{x\infty}$) in equilibrium after uniaxial elongation were evaluated, employing the Flory-type of Gibbs free energy formula. Poisson's ratio in equilibrium (μ_∞), which determines the degree of swelling under deformation, was estimated to be 1/6 so far as the applied strain is not large. The expression for $\sigma_{x\infty}$ was also derived by the

free energy. Swelling dynamics, which describes the volume change of the gels after uniaxial elongation, and stress relaxation were also formulated.

References

1 P. J. Flory, "Principles of Polymer Chemistry", Cornell University Press, Ithaca, 1953

2 R. W. Brotzman and B. E. Eichinger, *Macromolecules*, **14**, 1445 (1981)

3 R. W. Brotzman and B. E. Eichinger, *Macromolecules*, **16**, 1131 (1983)

4 N. A. Neuburger and B. E. Eichinger, *Macromolecules*, **21**, 3060 (1988)

5 F. Horkay, *Macromolecules*, **22**, 2007 (1989)

6 F. Horkay, A. -M. Hecht, and E. Geissler, *J. Chem. Phys.*, **91** 2706 (1989)

7 A. -M. Hecht, F. Horkay, E. Geissler, and M. Zrinyi, *Polym. Commun.*, **31**, 53 (1990)

8 Y. Rabin and E. T. Samulski, *Macromolecules*, **25**, 2985 (1992)

9 S. Daoudi, *J. Phys. (Paris)*, **38**, 1301 (1977)

10 E. Geissler and A. -M. Hecht, *Macromolecules*, **13**, 1276 (1980)

11 K. Nishinari, M. Watase, K. Ogino, and M. Nambu, *Polym. Commun.*, **24**, 345 (1983)

12 E. Geissler and A. -M. Hecht, *Macromolecules*, **14**, 185 (1981)

13 E. Geissler, A. -M. Hecht, F. Horkay, and M. Zrinyi, *Macromolecules*, **21**, 2594 (1988)

14 M. Watase and K. Nishinari, *Polym. J.*, **21**, 567 (1989)

15 S. -H. Hyon, W. I. Cha, and Y. Ikada, *Kobunshironbunshu*,

46, 673 (1989)

16 S. Alexander and Y. Rabin, *J. Phys.: Condens. Matter*, **2**, SA313 (1990)

17 T. Tanaka, L. Hocker, and G. Benedek, *J. Chem. Phys.*, **59**, 5151 (1973)

18 T. Tanaka and D. J. Fillmore, *J. Chem. Phys.*, **70**, 1214 (1979)

19 K. Urayama, T. Takigawa, T. Masuda, *Macromolecules*, **26**, 3092 (1993)

20 S. Hirotsu and A. Onuki, *J. Phys. Soc. Jpn.*, **58**, 1508 (1989)

21 L. D. Landau and E. M. Lifshitz, "Theory of Elasticity", Nauka, Moscow, 1987

Chapter 6

Experimental Studies of Swelling and Stress Relaxation of Poly(acrylamide) Gels

6-1 Introduction

In Chapter 5, equilibrium Poisson's ratio and stress under uniaxial deformation (μ_∞ and $\tilde{\sigma}_{x\infty}$, respectively) were evaluated based on the Flory-type free energy, and the swelling dynamics and stress relaxation behavior were also discussed theoretically. The main aim of this chapter is to compare the theoretical predictions with experimental results for poly(acrylamide) (PAAm) gels. The values of μ_0 for PAAm gels swollen with water are also shown in this chapter.

6-2 Experimental

PAAm gels used were prepared by employing a radical polymerization technique. Acrylamide (AAm), methylene bis(acrylamide) (MBA; crosslinker) and ammonium persulfate (initiator) were dissolved in distilled water at room temperature. The molar ratio of MBA to AAm and that of initiator to AAm were 0.002 and 0.006, respectively. The solution was cast into metal mold in order to obtain rectangular gels. Gelation was performed at 33^{o}C, and gels were kept in the mold for 3 days for curing. Gels were removed from the mold, and transferred in a large amount of water. Gels were maintained at 33^{o}C for about 10 days to achieve the equilibrium swelling. The water was exchanged everyday.

Measurements were carried out by using an Orientec RTM-250 tensile tester with a water bath at a constant crosshead speed (v). The temperature was kept at 25°C. The extension ratio in i-direction λ_i was calculated by $\lambda_i=l_i/l_{i0}$, where l_i is the sample dimension in the i direction and λ_{i0} being that at rest. Here, elongated direction was assigned as x-direction. We assumed here $l_z=l_y$ and $l_{z0}=l_{y0}$, which gives consequently $\lambda_z=\lambda_y$. The quantity l_x as well as l_{x0} corresponded to the distance of the two marked points at the center of the gel and was measured by using a magnified picture on the video monitor, and l_y (as well as that at rest, l_{y0}) was the width in the central region of the gel specimen near the marked points. For x-directional deformation, extension ratio (or strain) was also calculated by using the crosshead distance (L_x) and that at rest (L_{x0}). The extension ratio (strain) calculated by the combination of l_x and l_{x0} is called hereafter the extension ratio (strain) at local level, and the other the extension ratio (strain) at global level. Basically, the local quantities were used for calculation of μ_0 and μ_∞, while the global ones were used for calculation of the initial Young's modulus (E_0) and the initial strain rate ($\dot{\varepsilon}_0$) defined by $\dot{\varepsilon}_0=v/L_{x0}$. The applied force $\tilde{f}_x$ in x-direction was monitored by recorder. The quantity, μ_0, was calculated by $\mu_0=-\ln\lambda_y/\ln\lambda_x$.[1] For the swelling and stress relaxation under deformation, the gel samples were kept under the elongated state after the application of elongational strain. The time t=0 for swelling and stress relaxation was taken as the time when the elongation was stopped. The global strain initially applied to

the gel samples was fixed to be 10%. The width (l_y) as well as applied force ($\tilde{f}_x$) was measured as a function of time (t). The strains ε_x and ε_y were calculated by $\varepsilon_x=\lambda_x-1$, and $\varepsilon_y=\lambda_y-1$. The stress at time t ($\tilde{\sigma}_x(t)$) was calculated by $\tilde{\sigma}_x(t)=\tilde{f}_x(t)/S(t)$ where $\tilde{f}_x(t)$ is the force and S(t) is the cross-sectional area of the gels at time t. Actually $\tilde{\sigma}_x$ was almost identical to the engineering stress because the applied strain was small. S(t) was assumed to be $l_y(t)^2$.

6-3 Results and Discussion

6-3-1 Initial Poisson's Ratio

As stated in the experimental section, we elongated the gel uniaxially (in x-direction) and measured the extension ratio for the small central region of the sample as well as that for the whole gel. The former is λ_x in the local level and the latter that in the global level. The extension ratio in experiments was controlled globally. The extension ratio in the local level ranged from 78.6% to 107% of the extension ratio in the global level for the samples, showing that the extension ratio in the local level is almost identical to that in the global one.

Eight gel samples sample-coded as PAAm27P1 to PAAm27P8 were used to evaluate the value of μ_0 for PAAm gels. L_{x0}, E_0 and μ_0 are summarized in Table 6-1 together with the code name. The initial polymer concentration (c_0) for the samples was 270kg/m^3. Figure 6-1 shows typical plots of $-\ln\lambda_y$ against $\ln\lambda_x$, as an example, for the sample PAAm27P3. The data points can be well described by a straight line and the slope gives μ_0. The line was

sample	L_{x0}(mm)	v(mm/min)	E_0(kPa)	μ_0
PAAm27P1	32.4	0.5	34.5	0.464
PAAm27P2	36.6	3.0	34.0	0.467
PAAm27P3	35.0	3.0	37.0	0.442
PAAm27P4	34.0	3.0	36.0	0.442
PAAm27P5	41.8	3.0	35.5	0.472
PAAm27P6	46.7	3.0	36.0	0.454
PAAm27P7	29.0	30.0	48.0	0.461
PAAm27P8	33.5	300.0	44.0	0.456

Table 6-1. Sample code, the initial length (L_{x0}), the crosshead speed (v), the initial Young's modulus (E_0) and the initial Poisson's ratio (μ_0) of poly(acrylamide) (PAAm) gels.

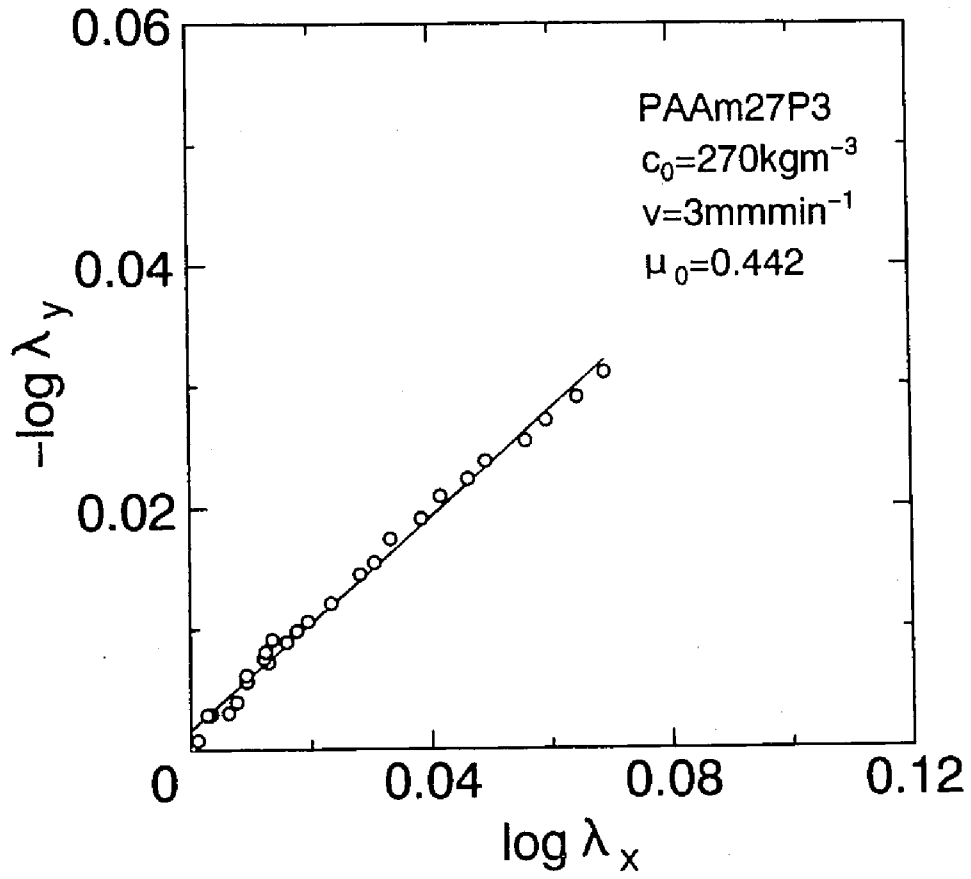

Figure 6-1. Double-logarithmic plots of $-\ln\lambda_y$ vs. $\ln\lambda_x$ for PAAm27P3.

determined by the least square method. The intercept in the figure originates from the experimental errors in determining λ_x and λ_y. For PAAm27P3, we have μ_0=0.442. The other samples also showed almost the same linearity as PAAm27P3, although we do not show here.

Figure 6-2 shows the dependence of μ_0 on $\dot{\varepsilon}_0$. As can be seen from this figure, μ_0 is independent of $\dot{\varepsilon}_0$. For PVA gels swollen in the mixed solvent composed of DMSO and water, μ_0 was independent of $\dot{\varepsilon}_0$.[1] Table 6-1 summarized the value of μ_0 for all specimens examined in this study. The average value of μ_0 with standard deviation (SD) is 0.457 ± 0.011. Although SD is a little large, the average is closer to that for PVA gels swollen in the mixture of DMSO and water than that for PVA hydrogels ($\mu_0\cong0.46$ for PVA gels in the mixed solvent and $\mu_0\cong0.43$ for PVA hydrogels). Since water is considered to be a good solvent for PAAm,[2] a PAAm chain is as flexible as PVA chain in the mixed solvent or water when the chain ends are free. The PAAm chains in the gel are anchored at both ends by the crosslinks if we ignore the dangling chains. For such chains, the mobility of the network chain is mainly governed by the size of the crosslink region; the large crosslink domains restrict much the mobility of the polymer chains in the gel. Then, the fact that μ_0 for PAAm gels is closer to that for the PVA gels swollen in the mixed solvent than μ_0 of PVA hydrogel originates from the small crosslink domains for PAAm gels and PVA gels in the mixed solvent compared with the crosslink domains for PVA hydrogels.

The size of the crosslink region for PAAm gels will be

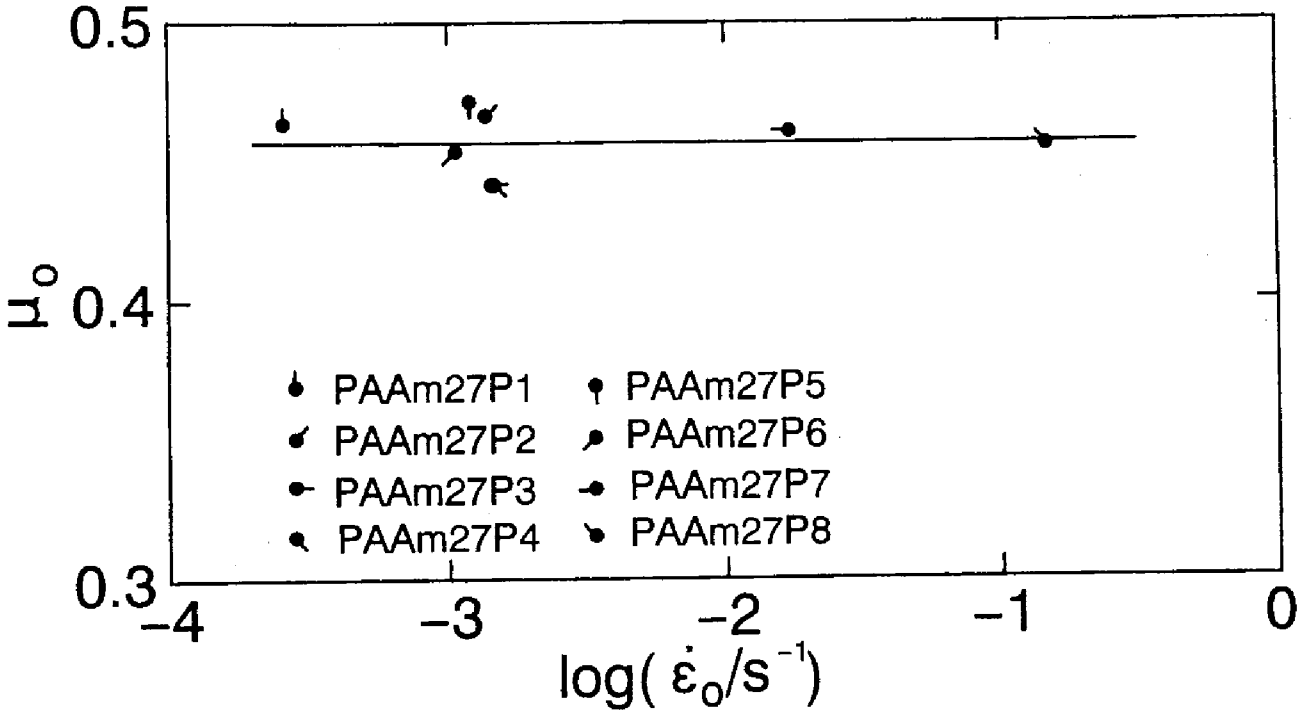

Figure 6-2. μ_0 vs. $\dot{\varepsilon}_0$ plots for PAAm gels.

smaller than that for the PVA gels in the mixed solvent, because the former is chemically crosslinked and the latter is formed by physical crosslinks. This may indicate that μ_0 of PAAm gel is larger than that of the PVA gels in the mixed solvent. The difference in μ_0 between PAAm gels and PVA gels in the mixed solvent is order of magnitude of 0.01, which is well within the experimental error. Polymer gels with highly mobile network chains may have the limiting value of μ_0 around 0.47. The limiting value of μ_0 is smaller compared with the value of the incompressible limit (1/2). Although the domain size for PAAm gels and PVA gels in the mixture is different, the size is too small to affect the mobility of the network chains, which governs the value of μ_0, for both gels.

6-3-2 Equilibrium Poisson's Ratio

The experimental results on the values of μ_∞ and $(\tilde{\sigma}_{x0}-\tilde{\sigma}_{x\infty})/\tilde{\sigma}_{x0}$ for PAAm gels are summarized in Table 6-2. The values of E_0 for PAAm271 to PAAm278 were a little scattered, although we tried to prepare the gels with almost the same E_0 by fixing the concentration of the reagents as well as the conditions for gelation. Comparing the E_0 values for specimens differing in c_0, E_0 becomes higher with increasing c_0. The plots of μ_∞ against E_0 are shown in Figure 6-3. The data points are a little scattered but they appear to be independent of E_0. The average value with SD is 0.149 ± 0.030. Figure 6-4 shows the plots of $(\tilde{\sigma}_{x0}-\tilde{\sigma}_{x\infty})/\tilde{\sigma}_{x0}$ against E_0. The data points are also independent of E_0 in this region of E_0. The average value of

sample	c_0/kgm^{-3}	l_{y0}/mm	E_0(kPa)[a]	μ_∞	$(\tilde{\sigma}_{x0}-\tilde{\sigma}_{x\infty})/\tilde{\sigma}_{x0}$
PAAm271	270	9.5	22.9	----	0.271
PAAm272	270	9.0	41.0	0.130	0.164
PAAm273	270	9.5	38.2	0.116	0.173
PAAm274	270	9.0	35.0	0.128	0.282
PAAm275	270	6.2	49.5	0.141	0.215
PAAm276	270	6.8	30.0	0.202	0.199
PAAm277	270	3.2	43.0	----	0.194
PAAm278	270	3.1	31.0	----	0.138
PAAm191	190	8.9	9.6	----	0.242
PAAm201	200	9.0	12.5	0.136	0.149
PAAm331	330	9.3	78.0	0.155	0.216
PAAm401	400	9.0	100	0.187	0.146

Table 6-2. Sample code, initial concentration (c_0), width in the reference state (l_{y0}), initial Young's Modulus (E_0), equilibrium Poisson's ratio (μ_∞), and relative stress reduction ($(\tilde{\sigma}_{x0}-\tilde{\sigma}_{x\infty})/\tilde{\sigma}_{x0}$) for poly(acrylamide) (PAAm) gels.

a calculated by using global strain.

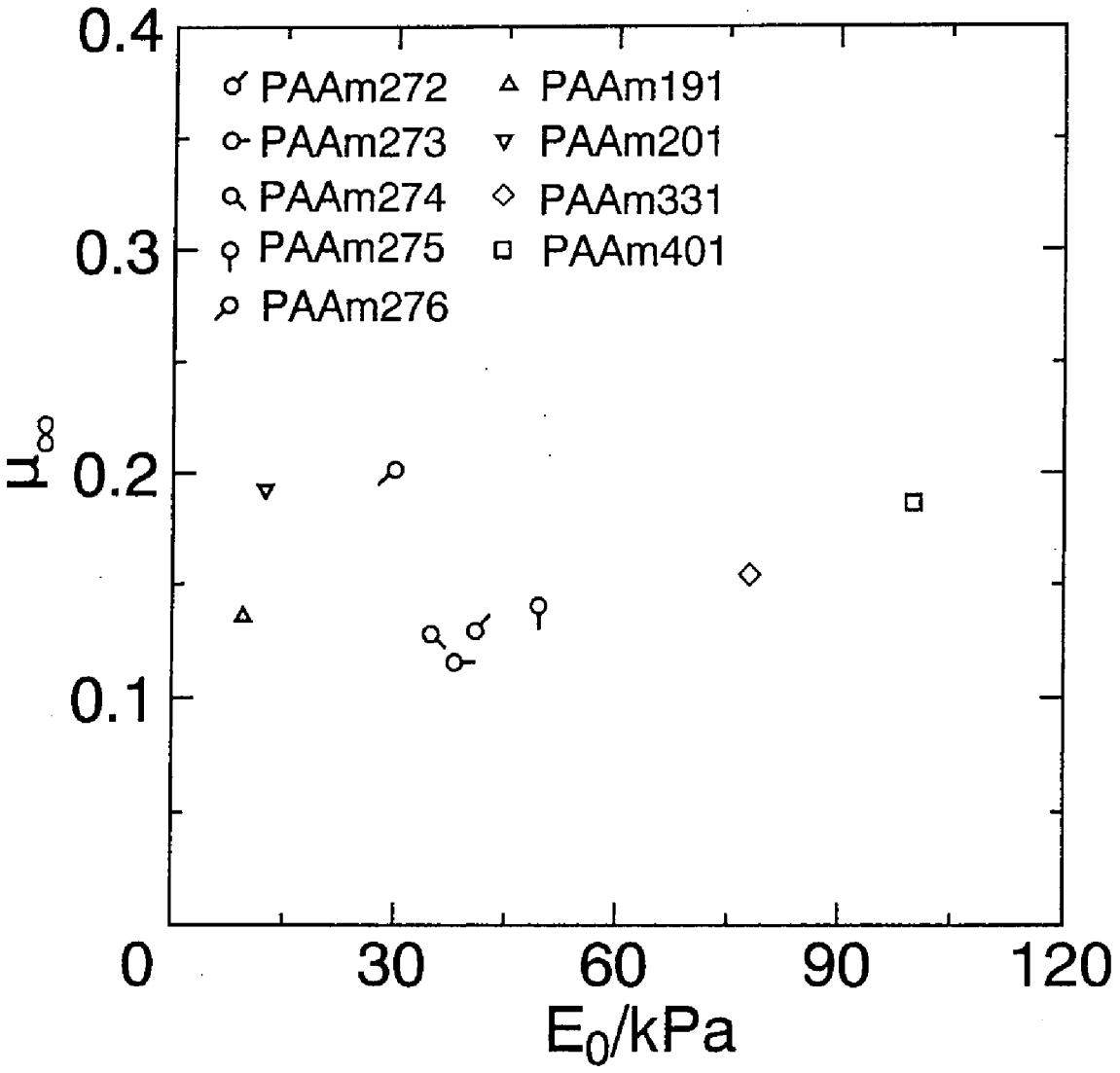

Figure 6-3. The E_0 dependence of μ_∞ for PAAm gels.

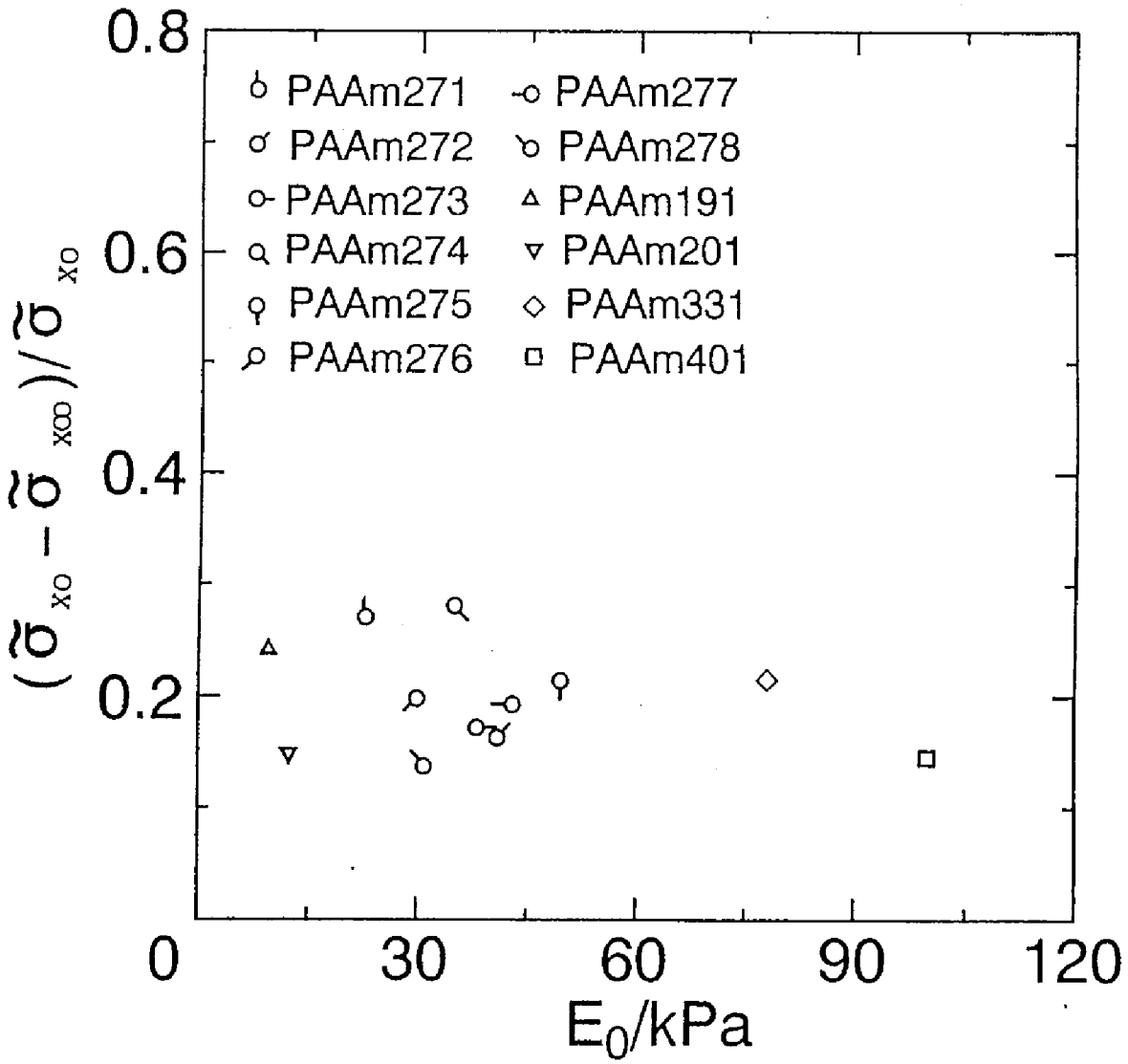

Figure 6-4. The E_0 dependence of the stress reduction, $(\tilde{\sigma}_{x0}-\tilde{\sigma}_{x\infty})/\tilde{\sigma}_{x0}$ for PAAm gels.

$(\tilde{\sigma}_{x0}-\tilde{\sigma}_{x\infty})/\tilde{\sigma}_{x0}$ is 0.199±0.048 with SD.

As can be seen from Equation 5-14 in the previous chapter that the theoretical value of μ_∞ is 1/6. The average value of μ_∞ for PAAm gels experimentally obtained in this study (=0.149) is close to the theoretical prediction (μ_∞=1/6≅0.167). Geissler et al.[2-4] have reported values of μ_∞, and μ_∞=0.275±0.011 has been obtained for PAAm gel in their latest work.[3] The values are higher compared with those obtained in this study. The difference might be due to the different methods to obtain μ_∞. Geissler et al. have estimated μ_∞ from the combination of two different moduli, and we measured the values directly from the dimensional change of the sample in solvent under uniaxial deformation.

The equilibrium stress can be calculated by using Equation 5-18 as $\tilde{\sigma}_{x\infty}=(7/3)G_0\varepsilon_x$ with shear modulus G_0. The initial stress, $\tilde{\sigma}_{x0}$, is given by $3G_0\varepsilon_x$ when the gel is incompressible as assumed basically in the theory in Chapter 5. In this case, $(\tilde{\sigma}_{x0}-\tilde{\sigma}_{x\infty})/\tilde{\sigma}_{x0}$ gives the value of 2/9≅0.222. The average value of $(\tilde{\sigma}_{x0}-\tilde{\sigma}_{x\infty})/\tilde{\sigma}_{x0}$ for PAAm gels shown here was 0.199. The difference in $(\tilde{\sigma}_{x0}-\tilde{\sigma}_{x\infty})/\tilde{\sigma}_{x0}$ between experiment and theory is not so large.

By using the value of $(\tilde{\sigma}_{x0}-\tilde{\sigma}_{x\infty})/\tilde{\sigma}_{x0}$, we can also estimate μ_∞ for PAAm gels by experiment when μ_0 is known, since $\tilde{\sigma}_{x0}=(1+\mu_0)G_0\varepsilon_x$ and $\tilde{\sigma}_{x\infty}=(1+\mu_\infty)G_0\varepsilon_x$. For PAAm gels examined here, we have $(\mu_0-\mu_\infty)/(1+\mu_0)$=0.199. As stated before, the PAAm gels were not actually incompressible and μ_0 of the gels was about 0.46, which gives μ_∞=0.17. This is close to the value

(μ_{∞}=0.149) obtained directly by the ratio ($-\varepsilon_y/\varepsilon_x$) at long t limit, indicating that the two values of μ_{∞} obtained independently by experiment are consistent with each other.

6-3-3 Swelling Dynamics and Stress Relaxation

The width determined by experiments is considered to be affected by the transverse mode of the diffusion. This means the boundaries of the gels are actually curvilinear. However, since the change of $l_y(t)$ with t was very small and then the boundary can be approximated by the plane, we assumed that the t dependent change of $l_y(t)$ originated only from the volume change.

Four kinds of PAAm gels (PAAm271 to PAAm274) were used for swelling and stress relaxation experiments. E_0 of the gels is almost identical to each other for the PAAm gels (see, Table 6-2), although the value of PAAm271 is a little smaller compared with those for the others. The longest relaxation time (τ_1) determined by swelling and stress relaxation are tabulated in Table 6-3 and the ratio of the width in the reference state (l_{y0}) to final one ($l_{y\infty}$), is also shown in the table. The ratio is almost constant for the four gel samples. The value of τ_1 for the gels was obtained by the two different ways; one is obtained from the plots of $\log(-\mu_{\infty}\varepsilon_x-\varepsilon_y(t))$ vs. t in the long t region, and the other from the plots of $\log(\tilde{\sigma}_x(t)-\tilde{\sigma}_{x\infty})$ vs. t in the same t range. The values of τ_1 obtained by the different ways are almost identical to each other for all the gels. This implies that the stress relaxation is induced by the swelling of the gels. The two values for PAAm271 are larger than those for

the other samples. This may be due to the low value of E_0 for PAAm271. The diffusion constant (D) was calculated by $D=l_{y0}^2/(2\pi^2\tau_1)$ using the values of l_{y0} and τ_1 obtained by the stress relaxation experiments. Based on the theoretical consideration presented in the previous chapter, D is the diffusion constant for the transverse mode under the first order approximation, but corresponds to the diffusion constant of the longitudinal mode under the zero-th order approximation. The value of D obtained by experiments, which is tabulated in Table 6-3, ranges from 2.5×10^{-7} to $7.4\times10^{-7}cm^2s^{-1}$. Although we can also calculate D by using τ_1 obtained by swelling, which corresponds to that for the longitudinal mode of diffusion, the value is very close to the calculated ones because τ_1 for the two cases are almost identical, as stated previously. The calculated value for PAAm271 is slightly smaller than those for the other samples, but their order of magnitude agrees well with the values of D for the PAAm gels reported for the free swelling.[5-7]

The value of ε_y for PAAm274 is plotted against the reduced time (t/τ_1) in Figure 6-5. It is clear that the absolute value of ε_y decreases with increasing t; the width increases as t increases. A maximum is observed at about $\log(t/\tau_1)=-1.1$ in the figure. Since the experimental error for ε_y is about 0.002, the maximum may only be apparent. The leveling-off at long times indicates that the gel under a fixed strain reaches the new swelling equilibrium state. The solid curve in Figure 6-5 shows the theoretical results calculated based on Equation 5-34 with $\mu_0=1/2$ and $\mu=1/6$. Here, l_{y0} is used for a_r in the equation. The

Sample	$l_{y\infty}/l_{y0}$	$\tau_1/10^4$s		$D/10^{-7}cm^2s^{-1}$
PAAm271	0.973	15[a]	18[b]	2.5
PAAm272	0.979	6.0[a]	7.5[b]	5.5
PAAm273	0.986	6.6[a]	6.2[b]	7.4
PAAm274	0.984	9.4[a]	9.1[b]	4.5

Table 6-3. The ratio of sample width in the final state to that in the reference state ($l_{y\infty}/l_{y0}$) using the values, the longest relaxation time (τ_1), and the diffusion constant (D) for poly(acrylamide) (PAAm) gels.

a measured by swelling experiment

b measured by stress relaxation

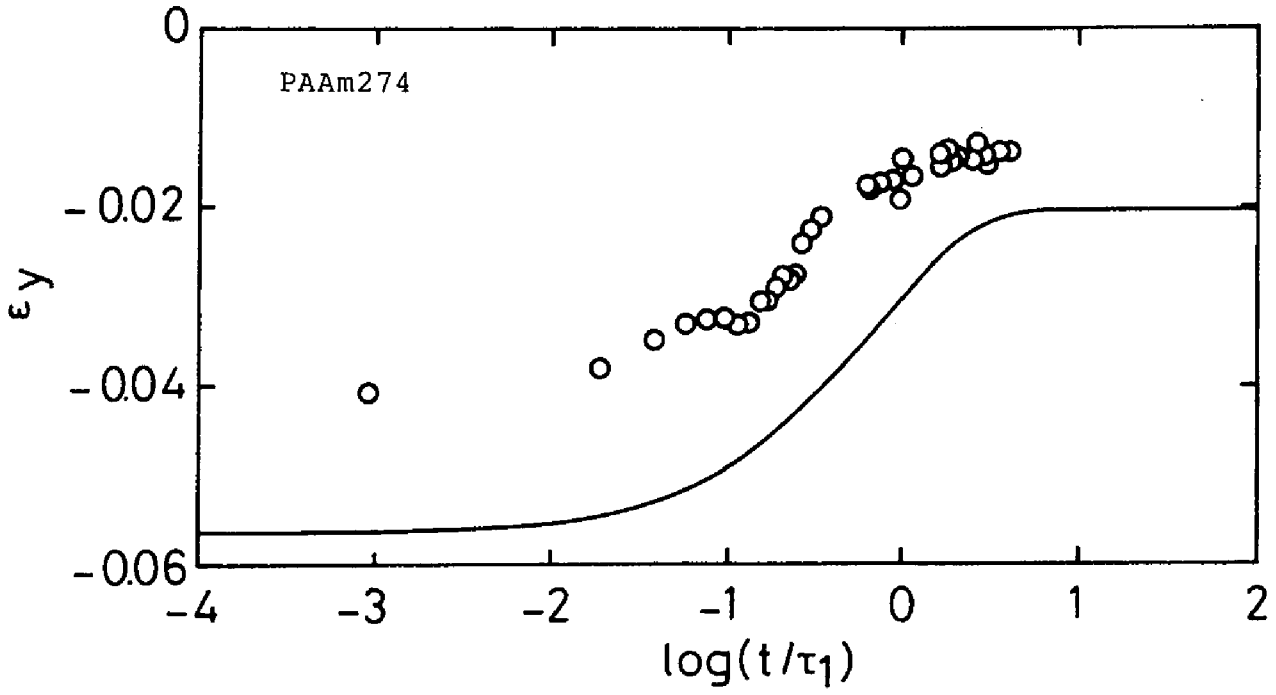

Figure 6-5. The time dependence of strain perpendicular to the stretched direction (ε_y) for PAAm274.

value of ε_x in local level was employed for the calculation of ε_y, because the strain in y direction obtained by experiment corresponded to that in the central region of the gels. The value of μ_0 was 0.41 and μ_∞=0.128 (Table 6-2) for PAAm274, which are not so far from the ideal values of μ_0=1/2 and μ_∞ =1/6. Therefore, we limited the theoretical calculation to the ideal case and no curve fitting for the experimental data was made here. Although the ε_y values on the theoretical curve are small compared with the experimental data, the t dependence of the strain is described fairly well by the theory. The difference of the absolute value between the experimental data and calculated curve originates from the fact that the absolute value of ε_y obtained by calculation at short times is rather sensitive to μ_0, and that in the long time region also sensitive to μ_∞.

Figure 6-6 shows the double-logarithmic plots of $\Delta\varepsilon_y/\Delta\varepsilon_{y0}$ vs. t/τ_1 for PAAm271 to PAAm274. Here,

$$\Delta\varepsilon_y=-\mu_\infty\,\varepsilon_x-\varepsilon_y(t) \qquad (6\text{-}1)$$

$$\Delta\varepsilon_{y0}=(\mu_0-\mu_\infty)\varepsilon_x \qquad (6\text{-}2)$$

The values of local ε_x were used for the theoretical calculation of ε_y in Equation 5-34. The curve in the figure is independent of values of μ_0 and μ_∞. Only the t dependence of the strain function appears in the figure. The experimental data points for each gel sample are scattered, but the t dependence seems to be rather well described by the theory.

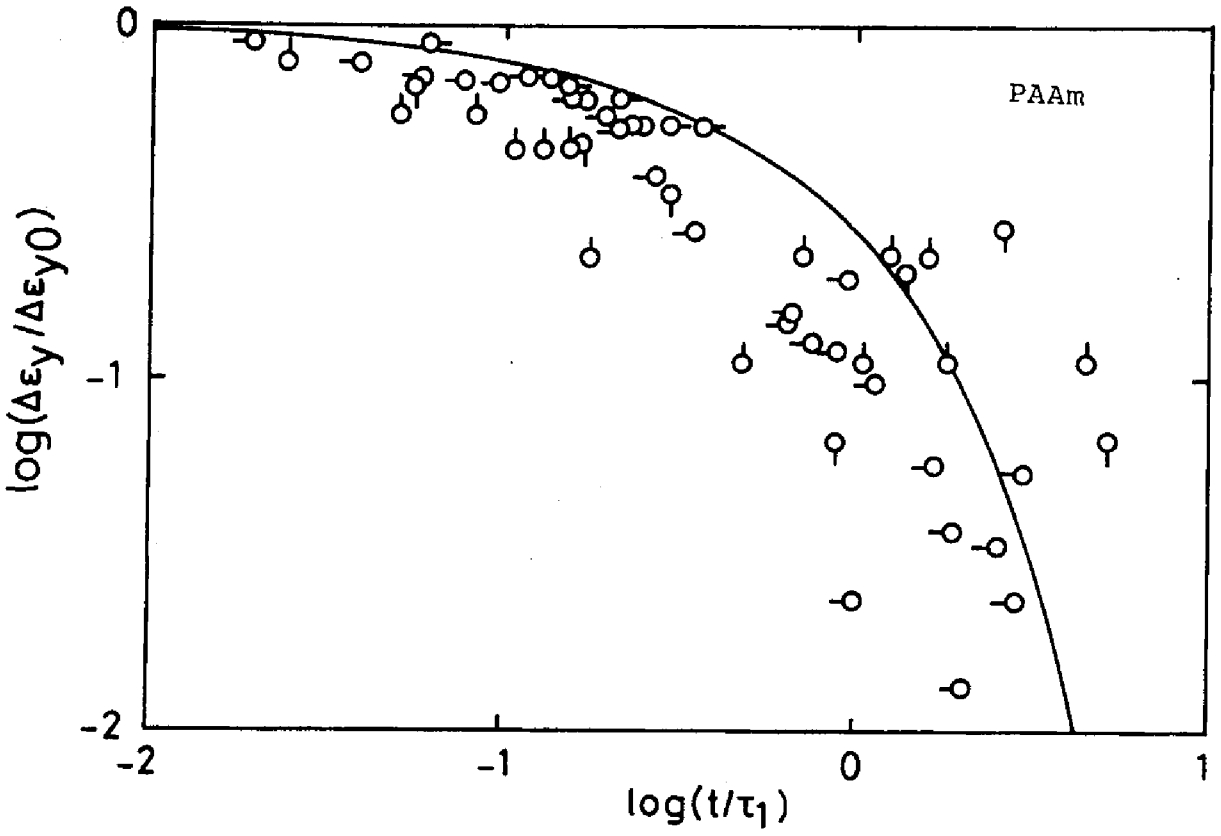

Figure 6-6. The time dependence of the reduced strain difference in the direction perpendicular to the stretched direction ($\Delta\varepsilon_y/\Delta\varepsilon_{y0}$). The symbols are : PAAm271 (○), PAAm272 (○–), PAAm273 (○), PAAm274 (–○).

Figure 6-7 shows the double-logarithmic plots of $\tilde{\sigma}_x(t)$ vs. t/τ_1 for PAAm274. The curve in the figure was calculated from Equation 5-36 by regarding $E_0=3.5\times10^4$Pa as $3G_0$, which means that $\mu_0=1/2$ is assumed. In addition, $\mu_\infty=1/6$ is also assumed in the calculation. Since the stress relaxation behavior obtained by experiment is basically determined by the whole gel nature, we used the macroscopic value of ε_x for the calculation, ignoring the non-uniform elongation. The theoretical curve seems not to coincide with the experimental data concerning the stress values, but the curve and the plots are very similar to each other concerning the t dependence of $\tilde{\sigma}_x$. Although the difference of $\tilde{\sigma}_x$ between theory and experiment mainly originates from the difference of μ_0 and μ_∞, as in the case of the absolute value of ε_y, the difference at short times, if we see it in the value of E_0, is about 25%, and that in the long time region is smaller. The value of $\tilde{\sigma}_x$ in the long time region agrees rather well with the expected value in equilibrium (the leveled-off value at long times in the figure).

Figure 6-8 shows the double-logarithmic plots of $\Delta\tilde{\sigma}_x/\Delta\tilde{\sigma}_{x0}$ vs. t/τ_1 for PAAm271 to PAAm274. $\Delta\tilde{\sigma}_x$ and $\Delta\tilde{\sigma}_{x0}$ are

$$\Delta\tilde{\sigma}_x=\tilde{\sigma}_x(t)-\tilde{\sigma}_{x\infty} \qquad (6\text{-}3)$$

$$\Delta\tilde{\sigma}_{x0}=\tilde{\sigma}_{x0}-\tilde{\sigma}_{x\infty} \qquad (6\text{-}4)$$

Only the t dependence of the stress function is observed in the reduced plots shown here. The solid curve in the figure was

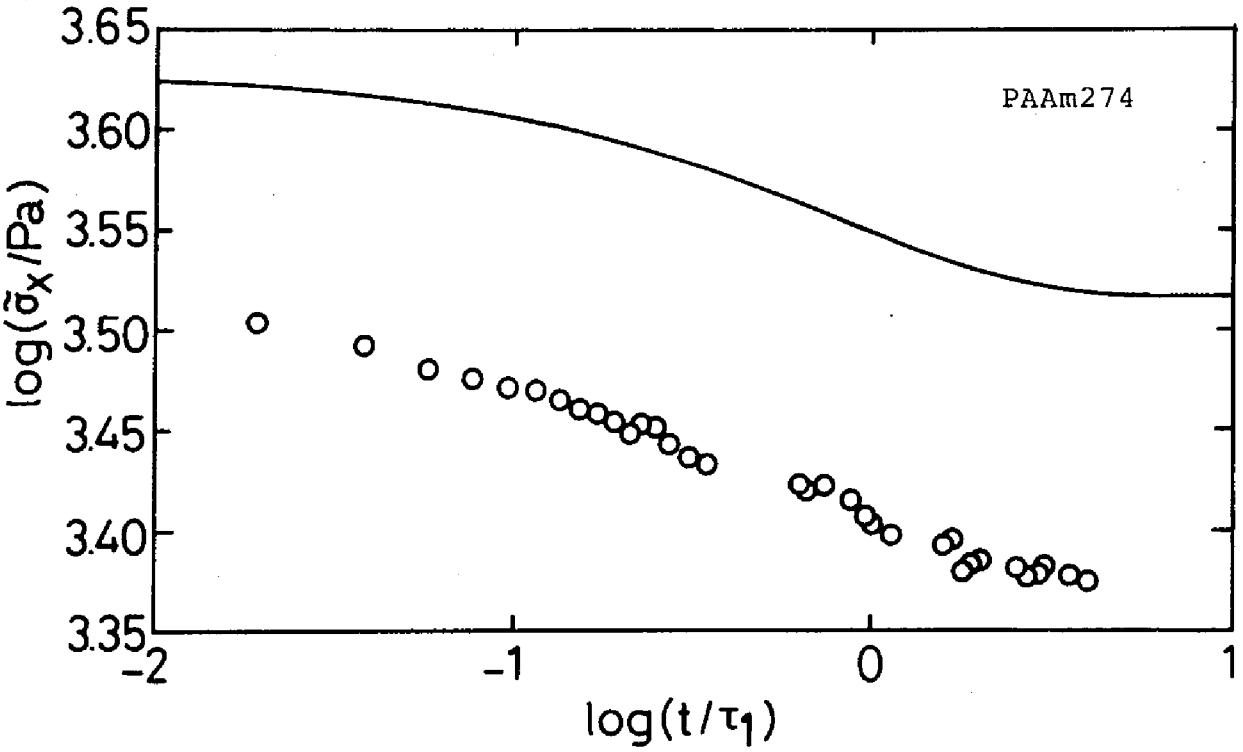

Figure 6-7. The time dependence of stress in stretched direction ($\tilde{\sigma}_{x0}$) for PAAm274.

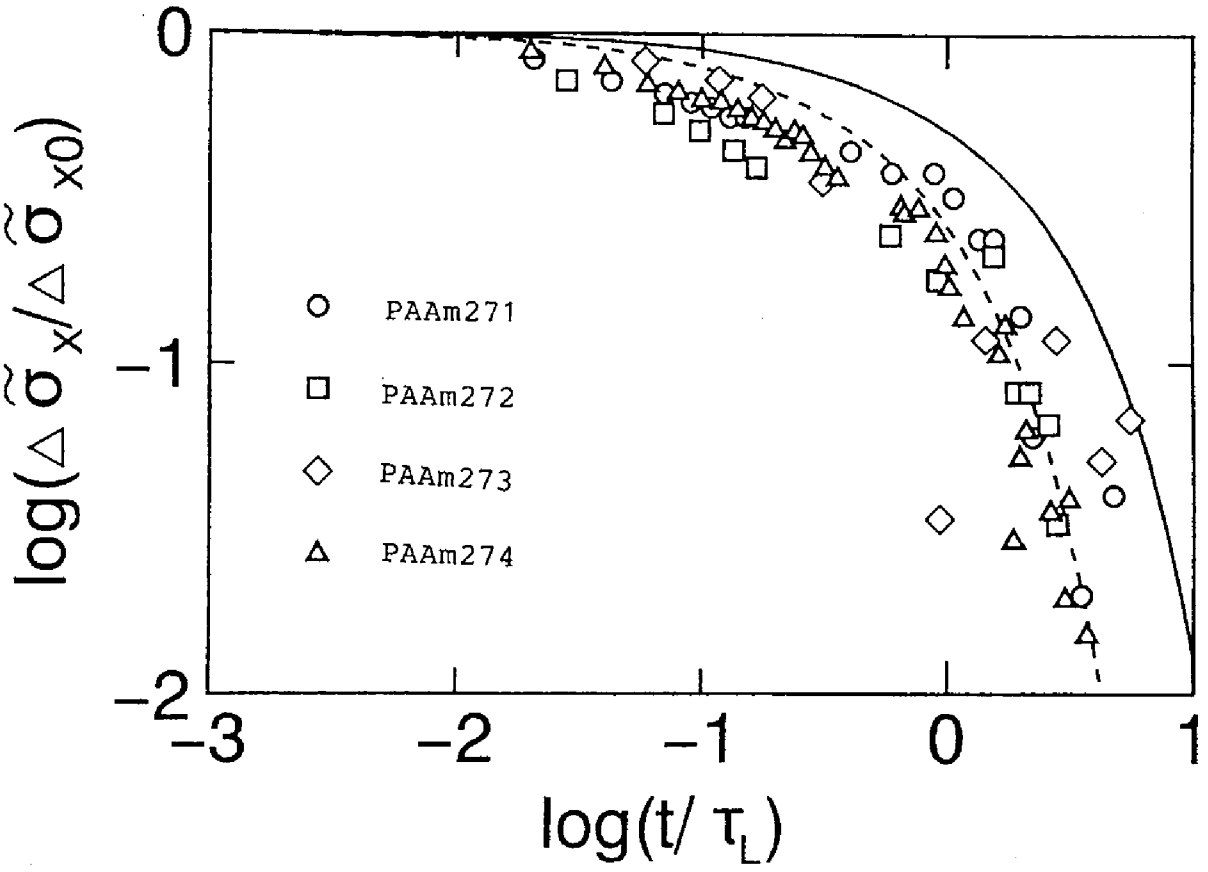

Figure 6-8 The time dependence of the reduced stress difference in the stretched direction ($\Delta\tilde{\sigma}_x/\Delta\tilde{\sigma}_{x0}$).

calculated using the expression of $\tilde{\sigma}_x(t)$ in Equation 5-53, and dashed curve was drawn based on Equation 5-36. Here, we also used l_{y0} for a_r in calculation. The former corresponds to transverse mode of diffusion and the latter to the longitudinal mode. Here, the relaxation times for transverse and longitudinal modes (τ_T and τ_L, respectively) were assumed to be $\tau_T=(5/2)\tau_L$, as shown in Chapter 5 and τ_1 obtained by swelling experiment was taken as τ_L. In calculation, the macroscopic values of ε_x were employed. The curve for the transverse mode is slightly shifted towards the longer time side, but the shapes of these curves are similar to each other. The two curves agree well with each other in the short time region. The data points are located downward compared with the two curves, suggesting that the stress relaxation of the gel network only occurs in this time region. The stress relaxation at short times is the same as that observed for crosslinked rubber.[8] On the other hand, data points at long times lie more closely around the dashed curve. This may show that the stress relaxation in this time region is described better by the longitudinal mode than the transverse mode. However, since the data points scattered, we can not say definitely at present which mode of diffusion is better for describing the experimental data of the stress relaxation at long times. More precise data are required for the evaluation.

6-4 Conclusions

The initial and equilibrium Poisson ratios (μ_0 and μ_∞, respectively) of poly(acrylamide) (PAAm) gels were examined. The

value of μ_0 was found to be 0.457, and μ_0 was independent of the strain rate. The value of μ_∞ and the relative stress reduction $((\tilde{\sigma}_{x0}-\tilde{\sigma}_{x\infty})/\tilde{\sigma}_{x0})$ were respectively 0.149 and 0.199, which are rather close to the theoretical predictions shown in Chapter 5. The swelling dynamics for PAAm gels could be described fairly well by the theory. The stress relaxation of PAAm gels agreed better with the longitudinal mode of diffusion than with the transverse mode.

References

1. K. Urayama, T. Takigawa, and T. Masuda, *Macromol.*, **26**, 3092 (1993)
2. E. Geissler, A. M. Hecht, *Macromol.*, **13**, 1276 (1980)
3. E. Geissler, A. M. Hecht, F. Horkay and M. Zrinyi, *Macromol.*, **21**, 2594 (1988)
4. E. Geissler and A. M. Hecht, *Macromol.*, **14**, 185 (1981)
5. T. Tanaka, L. Hocker, and G. Benedek, *J. Chem. Phys.*, **59**, 5151 (1973)
6. A. Peters and S. J. Candau, *Macromolecules*, **19**, 1952 (1986)
7. Peters and S. J. Candau, *Macromolecules*, **21**, 2278 (1988)
8. S. Kawabata, M. Matsuda and H. Kawai, *Macromol.*, **14**, 154 (1981)

Summary

Chapter 1 described the historical background and motivation for this study; to what extent properties of polymer gels have become clear at present and what are the problems to be clarified. The theoretical background for this study was also reviewed briefly in this chapter. The percolation and fractal theories, now used widely for analysis for critical behavior of polymer gels, were introduced. The classical (mean-field) theory for gelation was also described in comparison with the percolation theory. Fundamentals in thermodynamics used for describing the swelling behavior of non-critical gels, i.e., the gels far from the gelation point were also summarized.

In Chapter 2, preparation, and swelling and mechanical properties of poly(vinyl alcohol) (PVA) hydrogels, and PVA gels obtained by swelling precursors in various solvents were investigated. On the basis of the experimental results, the structure of the gels in various solvents was estimated. Stress-strain curves of PVA gels in the mixture of dimethylsufoxide (DMSO) and water did not show a shoulder. It was estimated that the PVA gels had a uniform structure with flexible PVA chains and that the crosslink domains for the gels were estimated to be rather small. On the other hand, the gels swollen in methanol, ethanol and formamide showed a shoulder on the stress-strain curve. Based on the solvent power for PVA, it was concluded that the gels had a two-phase structure composed of PVA-rich and solvent rich phases. The PVA chains in the PVA-rich phase are

crosslinked by hydrogen bonding. The shoulder originated from the breakdown of the PVA-rich phase. The degree of swelling of PVA hydrogels depended on annealing temperature, but was almost independent of the initial polymer concentration. Mechanical properties of the hydrogels were also influenced by the degree of swelling. A shoulder was observed in double-logarithmic plots of stress vs. strain for the hydrogels, and became clearer as annealing temperature increased. This shoulder was closely related to the breakdown of the microcrystalline domains acting as crosslinks. Also, the shape of stress-strain curves plotted double-logarithmically for the hydrogels changed with the extension rate.

The critical exponents for the specific viscosity (η_{sp}) and intrinsic viscosity ([η]) were examined for poly(vinyl alcohol) (PVA) solutions in Chapter 3. A new plot was proposed to determine the critical exponent for the specific viscosity (η_{sp}) and gelation threshold (c_G). The value of the exponent (k) was found to be 1.67. This value was larger than those reported previously for various polymerizing systems and for a gelatin system. The constant of the Huggins equation for viscosity (k') for PVA clusters (i.e, sol of PVA) was higher than that of linear PVA, and the value of [η] for PVA clusters was smaller than that of linear PVA at lower polymer concentrations, at which PVA solutions were prepared and cooled. The critical exponent for [η] was 0.20, which implied that the divergence behavior was rather weak. This weak divergence of [η] resembles the critical behavior of Zimm clusters predicted by 3d percolation theory, or

that of Rouse clusters by the classical theory of Flory-Stockmeyer type. The critical behavior of [η] of PVA solutions, however, might be considered to be close to Zimm clusters of the 3d percolation theory rather than that of Rouse clusters by the classical theory, because Zimm clusters are more preferable than Rouse clusters for the description of the critical behavior of [η].

The value of critical exponent for modulus (t) was estimated by using a model based on the percolation theory, and the value was experimentally determined for poly(vinyl alcohol) (PVA) gels in Chapter 4. The model proposed was based on the multi-fractality of the gel at and near the gelation point. Three kinds of fractal dimensions, dimensions of red bonds, minimum path and backbone, were used for modeling together with the usual fractal dimension. It was also assumed that the effects of backbone was dominant for the critical behavior of modulus of polymer gels. According to the model, there was a critical strain (γ_c), which distinguishes two regimes in the elastic response of the gel network near the gelation point. The theory also showed that γ_c was infinitesimally small for a realistic gelation in the 3d space. The exponent t for $\gamma>\gamma_c$ scaled as $(d+d_{min}+d_B)\nu\cong 2.27$ with fractal dimensions, d_{min} and d_B, and the exponent ν for correlation length for gels near the gelation point. The value of t for PVA gels was found to be 2.31 ± 0.04 and was close to the one predicted the model proposed. The crossover behavior of modulus was not found for PVA gels investigated here.

In Chapter 5, the swelling ratio and the stress value

($\tilde{\sigma}_{x\infty}$) in equilibrium after uniaxial elongation were evaluated, employing the Flory-type of Gibbs free energy formula. Poisson's ratio in equilibrium (μ_∞), which determines the degree of swelling under deformation, was estimated to be 1/6 so far as the applied strain was not large. The expression for $\tilde{\sigma}_{x\infty}$ was also derived as $7G_0\varepsilon_x/3$ with the shear modulus (G_0) and the applied strain (ε_x) from the free energy. Swelling dynamics, which describes the volume change of the gels after uniaxial elongation, and stress relaxation were also formulated. It was shown that there were two kinds of diffusion modes; one was called the longitudinal mode of diffusion which determined the change of volume, and the other the transverse mode of diffusion determining the change of shape of the gels. The volume change (or, equivalently, the change of degree of swelling) was found to be determined by the longitudinal mode of diffusion. The stress relaxation was analyzed by two methods: zero-th order and first order approximations. The results showed that the stress relaxation obeyed the longitudinal mode according to the zero-th order approximation, while it was determined by the transverse mode based on the first order approximation.

Chapter 6 described the initial and equilibrium Poisson ratios (μ_0 and μ_∞, respectively) of poly(acrylamide) (PAAm) gels. The value of μ_0 was found to be 0.457 and was independent of the strain rate. The value of μ_∞ and the relative stress reduction $((\tilde{\sigma}_{x0}-\tilde{\sigma}_{x\infty})/\tilde{\sigma}_{x0})$ were respectively 0.149 and 0.199, which were rather close to the theoretical predictions shown in Chapter 5. The swelling dynamics for PAAm

gels was also investigated here and was found to be described fairly well by the theory. The stress relaxation of PAAm gels agreed better with the longitudinal mode of diffusion than with the transverse mode.

List of Publications

[I] Papers Related to the Present Dissertation

1. "Critical Behavior of Modulus of Poly(vinyl alcohol) Gels near the Gelation Point", T. Takigawa, H. Kashihara, K. Urayama and T. Masuda, *J. Phys. Soc. Jpn.*, **59**, 2598 (1990)

2. "Critical Behavior of the Specific Viscosity of Poly(vinyl alcohol) Solutions near the Gelation Threshold", T. Takigawa, K. Urayama and T. Masuda, *Chem. Phys. Lett.*, **174**, 259 (1990)

3. "Critical Behavior of the Intrinsic Viscosity of Poly(vinyl alcohol) Solutions near the Gelation Point", T. Takigawa, K. Urayama and T. Masuda, *J. Chem. Phys.*, **93**, 7310 (1990)

4. "Swelling and Mechanical Properties of Polyvinylalcohol Hydrogels", T. Takigawa, H. Kashihara and T. Masuda, *Polym. Bull.*, **24**, 613 (1990)

5. "Structure and Mechanical Properties of Poly(vinyl alcohol) Gels Swollen by Various Solvents", T. Takigawa, H. Kashihara, K. Urayama and T. Masuda, *Polymer*, **33**, 2334 (1992)

6. "Comparison of Model Prediction with Experiment for Concentration-Dependent Modulus of Poly(vinyl alcohol) Gels near the Gelation Point", T. Takigawa, M. Takahashi, K. Urayama and T. Masuda, *Chem. Phys. Lett.*, **195**, 509 (1992)

7. "Simultaneous Swelling and Stress Relaxation Behavior of Uniaxially Stretched Polymer Gels", T. Takigawa, K. Urayama and T. Masuda, *Polym. J.*, **25**, 929 (1993)

8. "Theoretical Studies on the Stress Relaxation of Polymer Gels under Uniaxial Elongation", T. Takigawa, K. Urayama and T. Masuda, *Polymer Gels and Networks*, **2**, 59 (1994)

9. Poisson's Ratio of Polyacrylamide (PAAm) Gels submitted to *Polymer Gels and Networks*

10. Osmotic Poisson's Ratio and Equilibrium Stress of Polyacrylamide (PAAm) Gels in Water to be submitted

[II] Other Papers

Originals

1. "Rheological Properties of Concentrated Solutions of Styrene-Butadiene Radial Block Copolymers" (in Japanese), T. Masuda, Y. Ohta, A. Morikawa and T. Takigawa, *J. Soc. Rheol. Jpn.*, **15**, 40 (1987)

2. "Viscoelastic Properties of Styrene-Butadiene Radial Block Copolymers in a Selective Solvent" (in Japanese), Y. Ohta, A. Morikawa, T. Takigawa and T. Masuda, *J. Soc. Rheol. Jpn.*, **15**, 141 (1987)

3. "Effect of Strain Amplitude on Viscoelastic Properties of Concentrated Solutions of Styrene-Butadiene Radial Block Copolymers", Y. Ohta, T. Kojima, T. Takigawa and T. Masuda, *J. Rheol.*, **31**, 711 (1987)

4. "Morphology and Viscoelastic Properties of Star-Shaped Styrene-Butadiene Radial Block Copolymers", T. Takigawa, Y. Ohta, S. Ichikawa, T. Kojima and T. Masuda, *Polym. J.*, **20**, 293 (1988)

5. "Rheology and Phase Transition in 30% Solutions of Styrene-Butadiene Radial Block Copolymers", T. Masuda, T. Takigawa, T. Kojima and Y. Ohta, *J. Rheol.*, **33**, 469 (1989)

6. "Synthsis and Swelling Behavior of Polyurethane-Polyacrylamide IPN's" (in Japanese), T. Takigawa, Y. Tominaga and T. Masuda, *Kobunshi Ronbunshu*, **47**, 433 (1990)

7. "The Effects of Aging and Solvent-Vapor Treatments on the Viscoelastic Properties of Star-Shaped Styrene-Butadiene Radial Block Copolymers", T. Takigawa, Y. Ohta and T. Masuda, *Polym. J.*, **22**, 447 (1990)

8. "The Long Time Relaxation of the Microheterogeneous Polymer Liquids. 1. General Model", T. Takigawa and T. Masuda, *J. Soc. Rheol. Jpn.*, **18**, 129 (1990)

9. "Comparison between Uniaxial and Biaxial Elongational Flow Behavior of Viscoelastic Fluids as Predicted by Differential Constitutive Equations", T. Isaki, M. Takahashi, T. Takigawa and T. Masuda, *Rheologica Acta*, **30**, 530 (1991)

10. "Uniaxial and Biaxial Elongational Flow of Low Density Polyethylene/Polystyrene Blends" (in Japanese), T. Hattori, T. Takigawa and T. Masuda, *J. Soc. Rheol. Jpn.*, **20**, 141 (1992)

11. "Fatigue Behavior of Segmented Polyurethanes under Repeated Strains", T. Masuda, T. Takigawa and M. Oodate, *Bull. Inst. Chem. Res. Kyoto Univ.*, **70**, 169 (1992)

12. "The Effects of Water on Stress-Strain Relationship in Human Hair" (in Japanese), C. Atsuta, Y. Ota, M. Awamura, T. Takigawa and T. Masuda, *J. Jpn. Soc. Biorheol.*, **7**, 31 (1993)

13. "Poisson's Ratio of Poly(vinyl alcohol) Gels", K. Urayama, T. Takigawa and T. Masuda, *Macromol.*, **26**, 3092 (1993)

14. "Simulation of Melt Spinning of Pitches" (in Japanese), T. Takigawa, M. Takahashi, Y. Higuchi and T. Masuda, *J. Soc. Rheol. Jpn.*, **21**, 91 (1993)

15. "Measurement of Biaxial and Uniaxial Extensional Flow Behavior of Polymer Melts at Constant Strain Rates", M. Takahashi, T. Isaki, T. Takigawa and T. Masuda, *J. Rheol.*, **37**, 827 (1993)

16. "Time Dependent Poisson's Ratio of Polymer Gels in Solvent", T. Takigawa, K. Urayama and T. Masuda, *Polym. J.*, **26**, 225 (1994)

17. "Stress Relaxation and Creep of Polymer Gels in Solvent under Uniaxial and Biaxial Deformations", K. Urayama, T. Takigawa and T. Masuda, *Rheologica Acta*, **33**, 89 (1994)

18. "Dynamic Viscoelasticity and Critical Exponents in Sol-Gel Transition of an End-Linking Polymer", M. Takahashi, K. Yokoyama, T. Takigawa and T. Masuda, *J. Chem. Phys.*, **101**, 798 (1994)

Reviews

1. "Divergence and Crossover in Concentration Dependent Compliance of Polymer Network Systems", T. Masuda, T. Takigawa, M. Takahashi, K. Urayama, in *"Theoretical and Applied Rheology I"*, P. Moldenaers and R. Keunig, Eds., Elsevier, Amsterdam, 1992

2. "Swelling and Mechanical Properties of Polymer Gels" (in Japanese), T. Takigawa and T. Masuda, *Kobunshi*, **43**, 554 (1994)

Acknowledgements

This dissertation has been written based on research carried out at the Research Center for Biomedical Engineering, Kyoto University under the guidance of Professor Toshiro Masuda. The author wishes to his sincere gratitude to Professor Toshiro Masuda for his continuous guidance and encouragement, and for valuable discussions.

The author is very grateful to Dr. Masaoki Takahashi for valuable suggestions and comments throughout this study. Thanks are also due to all of the members, past and current, of the laboratory including Messrs. Hisahiko Kashihara, Kenji Urayama and Yoshiro Morino for their kind help during the study. He would also thank Professors Kunihiro Osaki and Sadami Tsutsumi for their careful reading and corrections to this dissertation.

Toshikazu Takigawa

Kyoto, Japan

February, 1995